Development of Sustainable Pavements: An Experimental and Finite Element Analysis Study

Mr Kiran Sapkota

BEng (Hons),

Student ID: s4576946

Thesis submitted in fulfilment of the requirements for the degree of Master of Research

Principal Supervisor: Dr Ehsan Yaghoubi

Associate Supervisors: Dr Rudi van Staden and Dr Wasantha Liyanage

Institute of Sustainable Industries and Liveable Cities

College of Engineering and Science

Victoria University, Melbourne, Australia

Date: 28/01/2023

Abstract

The potential of using recycled aggregates, such as construction and demolition waste, and glass waste, has been considered in the asphalt industry in recent decades. However, only a low percentage of these materials have been used in the mixtures as permitted by relevant standards and guidelines. With the predicted increase in the population and industrial activities, not only the generation of waste is expected to rise, but also the demand for construction materials in transportation infrastructures is increasing, resulting in the depletion of natural resources. This research investigates the feasibility of increasing the percentage of recycled aggregates to 100% in hot mix asphalt (HMA). Recycled concrete aggregate (RCA), recycled glass (RG), and reclaimed asphalt pavement (RAP) were used to develop an HMA suitable for light to medium traffic roads. First, the properties of recycled aggregates were determined, and potential mix designs were proposed using an innovative approach that considered the industry's needs. Next, the mechanical and volumetric properties of the proposed mixtures were determined together with those of mixtures made of natural aggregates for validation. The resilient modulus response of the mixtures was determined under different temperature conditions. In general, the proposed HMA exhibited advanced mechanical and resilient modulus performances, i.e., a 45 to 145% increase in stiffness and up to 99% increase in Marshall stability when compared to conventional HMA. Experimental results showed that the newly developed mixtures have superior strength, resilient modulus and moisture susceptibility performances compared to conventional mixtures. The experimental outcomes were translated into material properties as design input that were next used for simulating four different flexible pavements using the CIRCLY7.0 software. The four pavement profiles included three flexible pavement systems that had 100% recycled material aggregates in the surface course at different

proportions and one pavement profile that had 100% natural aggregate. The designed pavement profiles were also modelled using finite element analysis (FEA) softwares, ABAQUS and Strand7, (SIMULIA, 2011; Strand7, 2010) for further evaluation of the performance and comparison of the stress-strain responses due to vehicle loadings. The findings of this research provide the industry with evidence-based insights into the performance of HMA with increased quantities of recycled materials, thereby promoting green pavement construction materials.

Keywords: Green asphalt, Recycled aggregates, Indirect Tensile Modulus; Moisture sensitivity; Finite Element Analysis, Sustainable pavements.

Acknowledgement

Declaration

I, Kiran Sapkota, declare that the Master of Research thesis entitled "Development of Sustainable Pavements: An Experimental and Finite Element Analysis Study" is no more than 50,000 words in length, including quotes and exclusive of tables, figures, appendices, bibliography, references, and footnotes. This thesis contains no material that has been submitted previously, in whole or in part, for the award of any other academic degree or diploma. Except where otherwise indicated, this thesis is my own work.

I have conducted my research in alignment with the Australian Code for the Responsible Conduct of Research and Victoria University's Higher Degree by Research Policy and Procedures.

Ethics Declaration

There was no ethics approval required for the research conducted.

"All research procedures reported in this thesis were approved by the Institute for Sustainable Industries and Liveable Cities Deputy Director, Dr Elmira Jamei, on 4 November 2022."

Signature: Date: 28/01/2023

Contents

List of Tables

List of Figures

Abbreviations

%HV	Average percentage of heavy vehicles
10NA	Sized 10 natural aggregate asphalt mix
10RCA 55	Sized 10 asphalt mix consisting of 55% RCA, 35% RAP, and 10% RG
10RCA 65	Sized 10 asphalt mix consisting of 65% RCA, 25% RAP, and 10% RG
10RCA 75	Sized 10 asphalt mix consisting of 75% RCA, 15% RAP, and 10% RG
20NA	Sized 20 natural aggregate asphalt mix
20RCA 55	Sized 20 asphalt mix consisting of 55% RCA, 35% RAP, and 10% RG
20RCA 65	Sized 20 asphalt mix consisting of 65% RCA, 25% RAP, and 10% RG
20RCA 75	Sized 20 asphalt mix consisting of 75% RCA, 15% RAP, and 10% RG
AADT	Average Annual Daily Traffic
AASTHO	American Association of State Highway and Transportation Officials
AS	Australian Standard
C&D waste	Construction and Demolition waste
CB	Crushed Brick
DGA	Dense Graded Asphalt
FEA	Finite Element Analysis
FEM	Finite Element Method
FI	Flakiness Index, %
G_{mm}	Maximum theoretical density, g/cm^3
HMA	Hot Mix Asphalt
HVAG	Heavy Vehicle Axle Group
IDT	Indirect Tensile Modulus, MPa

L.A. abrasion loss	Los Angeles Abrasion loss
N_{DT}	Design traffic in cumulative heavy vehicle axle group
OBC	Optimum Binder Content, %
OHS	Occupational Health and Safety
RAP	Reclaimed Asphalt Pavement
RCA	Recycled Concrete Aggregate
RG	Recycled Glass
V	Traffic speed, km/hr
VU	Victoria University
WMAPT	Weighted Mean Annual Pavement Temperature
ρ_{bulk}	Bulk density of the test specimen, g/cm^3
ρ_w	Density of water, g/cm^3

1 Introduction

Pavements enable a country's economy by connecting communities and industries, which makes them crucial for the development of a country. A pavement system aims to sustain repeated traffic loads and prevent several failures, such as rutting and cracking (Vicky, 2020). Depending on the type of pavement, different materials are used in distinct amounts. There are mainly two types of pavements: flexible pavements and rigid pavements. A flexible pavement consists of unbound granular materials as the base course and subbase course and an asphalt mixture as the surface layer. The asphalt mixture typically consists of binder and coarse and fine aggregates. A rigid pavement consists of cement concrete or reinforced concrete slabs as its surface course. A typical flexible pavement, which is the focus of this research, consists of 4 structural layers: treated subgrade, subbase, base, and surface course layers (Kieran Sharp, 2009). Pavement layers have a various material composition of specific properties. For example, the subbase and base courses comprise unbound granular materials, whereas the surface course (wearing and structural course) consists of a mixture of aggregates, filler, and binder. The surface course is at the top of a pavement structure to directly contact the vehicle tyre load and pressure as demonstrated in Figure 1.
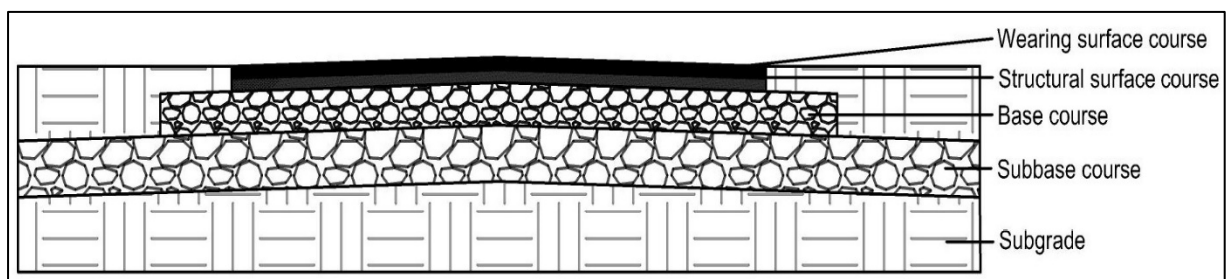
Figure 1. Typical structural layers of a flexible pavements.

Pavement industries work around six phases: raw material production, mixing, transportation, laying of materials, compaction and finally curing phase. Out of mentioned phases, the highest amount of greenhouse gas emission is produced from the mixing phase, followed by the raw material production phase (Ma et al., 2016). The raw material production phase includes sourcing aggregates, and the binder required for the asphalt production. This research investigates the possibility of using recycled aggregate in the asphalt mixture to produce green pavements.

Hot Mix Asphalt (HMA) typically consists of mineral aggregates and binder, where, mineral aggregates occupy 90 to 95% of the asphalt mixture by weight and 75 to 85% by volume (T.F. Fwa 2006). The physical composition of the mineral aggregate determines its hardness, durability, and stripping potential. The surface layer aggregates play an essential role in the asphalt mixture's performance over a particular time as the asphalt mixture consists of 90 to 95% mineral aggregate by weight. Simultaneously, bitumen is a highly viscous liquid that plays a vital role in firmly binding the aggregate of different sizes (Debnath, 2018). The properties of aggregates determine the quality and performance of a pavement (Aragao, 2007). The aggregate used in an asphalt mixture for the wearing course (or surface course), and intermediate course (or binder course) are preferred to exhibit low flakiness index, low water absorption, low Los Angeles (LA) abrasion loss, and higher strength to achieve the cost-effective and high-quality dense graded asphalt mixture. These properties play a vital role in determining pavement performance and quality.

The natural aggregate extraction process increases the aggregate cost; however, natural aggregates are typically used in the pavement industry as they are traditionally known to have overall better-desired attributes. With the significant improvement in the performance of recycling facilities compared to a decade ago, some produced recycled aggregates have properties comparable or even superior to those of natural aggregates (Arulrajah et al., 2014;

2

Yaghoubi et al., 2021). According to Mohr-Coulomb's theory, the higher internal friction of an aggregate represents higher shear strength, that eventually results in a greater capacity of the aggregate to sustain traffic load (T.F. Fwa 2006). The physical characteristics and mechanical behaviour of aggregates have critical controls on the performances of the HMA layer. Aggregates having higher flaky particles generally compact tightly, resulting in a reduced binder content requirement in the mixture. However, a large proportion of flaky particles are not desired in the pavements, especially in the surface course, because they are more prone to crushing under subsequent loading (Austroads-5.3.2, 2022). The water absorption characteristic of aggregates is another factor that changes the effective binder content, eventually influencing the optimum binder content of the asphalt mix. Therefore, recycled aggregates with similar or enhanced properties in terms of their internal friction, flakiness index, abrasion loss, water absorption, and particle density compared to a natural aggregate may be suitable alternatives to natural aggregates for producing asphalt.

The voluminous generation of various wastes, depletion of natural resources leading to a shortage of construction materials, and the ever-increasing transportation cost of natural aggregates are all current challenges. The use of a higher percentage of recycled materials in pavements can contribute to alleviating such challenges without compromising the required structural performance of the pavement system. For this aim, the aggregate's properties need to be experimentally tested, and after passing the required quality control measures, they could be incorporated in the mix design of asphalts mixtures for further laboratory experimentations.

Design for the pavement thickness consists of two main approaches, namely empirical and mechanistic procedure. The empirical procedure for pavement design is a common method based on the experimental test results carried out on different pavement layers. In other words, it is based on the response of pavement structural layers under traffic loads and climatic conditions and is dependent on the material composition. An example of the empirical

approach is the design charts provided in the Austroads-Part2 (2017). The empirical method is a very simple and user-friendly approach of pavement design. However, this method pays less attention to stress, strain, and deformation under traffic loading. In addition, the design charts are based on test results on specific conventional aggregates and do not apply to innovative pavement materials, such as recycled construction and demolition aggregates (Huang, 2003). This method underestimates distresses under vehicle loads which results in the overdesign of the pavement layer thickness, additionally, the empirical procedure cannot provide designs for pavement structures having asphalt surface course thicknesses of more than 40mm (Pavement_Science, 2022b).

The mechanistic procedure approach to pavement design allows designing of a wide range of pavement types for a broad range of loading conditions and configurations. This procedure consists of a few design steps. The first step is selecting input parameters such as the type of material, traffic, and environmental conditions. The second step is selecting a trial pavement to determine the allowable traffic and then comparing it with the design traffic. The final step is accepting or rejecting the trial pavement. The advantage of mechanistic procedure is that this procedure looks at the performance criteria, such as the fatigue life and rutting responses (Austroads-Part2, 2017). Furthermore, since mechanistic procedure takes the materials' mechanical characteristics into account, it applies to non-conventional pavement aggregates, the characteristics of which can be determined through laboratory testing.

The pavement design software, CIRCLY7.0, has been used regularly in Australia and worldwide for more than two decades (Pavement_Science, 2022a). The software uses a combination of mechanistic and empirical methods, namely, mechanistic–empirical method, for pavement design. The mechanistic part looks at the performance criteria to distresses, such as fatigue failure or rutting, while the empirical calibration factor is needed to relate the performance criteria to lab results. CIRCLY7.0 calculates the cumulative damage factor

(CDF), which indicates each layer's performance over the design period at the selected pavement layers, traffic load distribution, design traffic, and project reliability. CIRCLY7.0 allows pavement designers to perform hit and trail analysis on the selected thickness of each layer of pavement and calculate the CDF. This helps designers to select a pavement without overdesigning and suitable for the design period and predicted traffic loading conditions (Pavement_Science, 2022b).

The Finite Element Method (FEM) in pavement design is about the pavement's performance analysis over its design period. The FEM for pavement design involves the mathematical approach to solve complex geometric engineering problems by evaluating the stress, strain, and deformation of mechanical materials under dynamic traffic loading (Huang, 2003). It produces a result of high accuracy and helps in the pavement's performance over the design period of the pavement from the stress, strain, and deflection data at the critical locations of the pavement. The Finite Element Analysis (FEA) software used in this research were ABAQUS and Strand7. FEM can be used to analyse the pavement's performance and to predict the pavement responses due to the dynamic traffic loading. This study will investigate the performance of new material as an aggregate of the pavement structural layers using numerical modelling software. Overall, numerical pavement modelling saves time, funds, and the cost of physically testing a new aggregate in pavement layers.

Table 1 shows the location within the depth of the pavement together with the purpose and expected results in numerical modelling. Typically, a non-linear analysis solution gives stress and strain dependant displacements and strains in the pavement. The pavement performance can be analysed by computing the deflection, stress, or strain at different pavement structural layers under a vehicle wheel load. In this research, ABAQUS was used to prepare the pavement models and check against all of the numerical result mentioned in Table 1 to evaluate the pavement's performance (SIMULIA, 2011).

Table 1 Pavement analysis in FEA software (Interactive, 2021).

Purpose	Location	Numerical Result
To define load restriction during spring thaw and overlay design	Pavement surface	Deflection
To predict fatigue failure in the HMA	Bottom of HMA layer	Horizontal Tensile Strain
To predict the rutting failure in the base or subbase	Top of the base or subbase course	Vertical Compressive Strain
To predict rutting failure in the subgrade	Top of Subgrade	Vertical Compressive Strain

1.1 Objectives

The proposed research addresses the following research questions:

1) What is the best composition of recycled aggregates that has the potential to have performance comparable to conventional asphalt mixture?

2) What is the difference in the optimum binder content (OBC) of asphalt mixtures made of recycled materials compared to conventional asphalt?

3) Will the asphalt mixtures made of 100% recycled material satisfy the Indirect Tensile Modulus and Moisture sensitivity performance requirements mentioned in VicRoads-RC500.01 (2021)?

4) What is the stress-strain response of pavements consisting of recycled materials under dynamic loadings of vehicles?

In response to the above questions, the aim of the research is to analyse the feasibility of using 100% recycled aggregates in the surface course of a flexible pavement system and provide a comparison of the properties and performance against a conventional asphalt mixture. This research will hence seek the following objectives:

1) To select an appropriate composition of recycled aggregates to produce six different asphalt mixtures (two different sizes, 10 and 20mm) with a performance comparable to conventional asphalt,

2) To determine the OBC of the natural aggregate asphalt mixture and mixtures made of recycled aggregates,

3) To undertake experiments such as Indirect Tensile Modulus (IDT) test and moisture sensitivity testing of all asphalt mixtures to check the performance against the requirements mentioned in VicRoads-RC500.01 (2021).

4) To design four flexible pavement systems using a pavement design software commonly used by the industry, i.e., CIRCLY7.0, and to analyse and compare the pavement response (vertical stress, vertical strain, horizontal strain, vertical deflection and surface deflection) of the designed flexible pavement systems in response to vehicular wheel loadings using FEA software, ABAQUS and Strand7.

The secondary objective of this research is to support the United Nations' Sustainable Development Goals: SDG9, SDG11 and SDG12, being "Industry, Innovation, and Infrastructure", "Sustainable Cities and Communities", and "Responsible Consumption and Production", respectively.

1.2 Significance and novelty

The increased demand for the use of pavements made of reclaimed asphalt pavement (RAP), recycled glass (RG) and recycled concrete aggregate (RCA) will lead to significant environmental benefits worldwide against the ever-increasing anthropogenic wastes (Ai Jen Lim, 2020). Currently, sand and gravel are being extracted worldwide at a rate higher than their natural renewal rate (Board, 2021), while recycled materials are being used in the pavement industry at a limited amount. This proposed research aims to reduce the industry's dependency on natural aggregates such as sand and gravel. This research aims to pave the way to producing

green and sustainable HMA made of novel recycled aggregate blends. The optimised mix design in this study aims to address some of the drawbacks associated with the use of recycled aggregates in high percentages, such as durability, stability, and resilient modulus behaviour. Previous studies have either used a limited proportion of recycled/waste aggregates or have not discussed the real-life applications or translation of the experimental results into actual pavement design input to be used by the transport industry. The finite element models developed in this study will be the first to realistically model flexible pavements with wearing and structural course entirely made of recycled materials (RAP, RG and RCA).

This research will help reduce greenhouse gas emissions by utilising local waste, such as glass and construction and demolition (C&D) waste. The demand for these wastes must rise in the market to prioritise their recycling. The allowance of these recycled wastes in pavement structural layers has already increased its demand in the market. The hauling distance to transport aggregates from one site to another will also reduce when these local recycled wastes supplied by recycling facilities located near urban settings are consumed, rather than extracting natural aggregate mines located kilometres away from the urban areas. The decrease in hauling distance decreases the time for construction and results in less carbon emission due to the transportation of the materials.

1.3 Research Design

The proposed research used a quantitative methodological approach to meet the research aims. More specifically, it used experimental research to analyse recycled materials' properties and performance in a dense graded asphalt mixture to be used for the pavement surface layer of a flexible pavement. Recycled materials blend consisting of RG, RCA, and RAP at different proportions were designed using the "Marshall Mix design" method. The 10mm HMA in this research were developed as a type "N" HMA, and size 20mm asphalt mixture were prepared as a type "SI" HMA, following "VicRoads – Selection and Design of Pavements and surfacing"

code of practice (VicRoads-RC500.22, 2018). According to VicRoads-RC500.22 (2018), type "N" DGA is a 10mm wearing course suitable for light to medium traffic roads, and the type "SI" DGA is a multipurpose 20mm structural mixture for an intermediate course in heavy-duty pavements or an asphalt base course in medium duty pavements. Experimental tests such as maximum theoretical density testing, bulk density, stability and flow analysis, Indirect Tensile Modulus testing and Moisture sensitivity testings were carried out on the recycled materials asphalt mixtures to derive their property and later be compared with the conventional asphalt mixture.

This research selected RCA, RG and RAP as the three recycled materials that were used to prepare a dense-graded asphalt mixture. The literature review on recycled material showed RCA to have higher strength, and higher water absorption. In case of RAP, it consists of binder coated around the aggregate which in asphalt mixture helps to decrease the optimum binder content. Similarly, the RG in an asphalt mixture decreases the optimum binder content, as studied in the literature review. Alhassan et al. (2018) mentioned the fine RG to have engineering properties similar to sand. RCA is stronger than natural aggregates, but the optimum binder content could be higher because of a higher water absorption percentage. To balance this high demand for binder from RCA, other recycled materials with lower absorption potential were needed. RAP and RG have lower strength than natural aggregate, but they reduce the optimum binder content in an asphalt mixture as studied in the literature. Therefore, RCA, which were known to increase the optimum binder content, and RAP and RG, which were reported to reduce the optimum binder content, were selected to prepare asphalt mixtures in this research.

This research had deductive research questions which were analysed using multi-method of experimentation and numerical modelling. Similar research in the pavement research area used the same methodological approach as the post-positivism worldview. Experiments are based

9

on realistic and etic epistemology, as the process is meant to objectively find accurate data (Creswell, 2018). The performance and possibility of using 100% recycled material blends in an asphalt mixture were tested using the quantitative methodological and method steps (Anne-Marie, 2021). The layers of the research onion metaphor were used to illustrate the proposed research approach clearly:

1) Philosophies: Post-positivism worldview
2) Approach: Deductive approach
3) Strategy: Experiment and Numerical analysis
4) Choice: Multi-method
5) Techniques and Procedure: Data collection and Data analysis

Australian standards and guidelines suggested the method to carry out geotechnical and pavement experiments on the individual aggregate and asphalt mixtures. Furthermore, the guidelines and standards also provided the acceptance criteria of an asphalt mixture to be considered suitable for the surface course of the pavement.

Following above explanations, the laboratory tests on the aggregate and the DGA's in this research are listed below:

1) Particle Size Distribution (PSD),
2) Particle density and water absorption,
3) Flakiness index test,
4) Marshall Mix Design,
5) Indirect Tensile Modulus (IDT) test, and
6) Moisture sensitivity test.

The PSD, particle density, and water absorption tests were performed on aggregates to understand the aggregate's particle size gradation and mass required to achieve a particular volume and water holding capacity. These fundamental properties of the aggregate helped in making the selection for the percentage of each aggregate required to prepare asphalt mixtures of gradation within the upper and lower limits, as mentioned in VicRoads-RC500.01 (2021).

The percentage of aggregates selected for each asphalt mixture is presented in the "9.1 Proposed asphalt mixtures" section of this report.

Marshall Mix Design method analysed the OBC of all eight asphalt mixtures along with the volumetric and mechanical properties such as Marshall stability, air voids, voids filled with mineral aggregate (VMA), voids filled with asphalt (VFA), unit weight and flow value. Finally, to evaluate the performance of the asphalt mixture, this research conducted IDT and moisture sensitivity tests.

The test results obtained from the laboratory experiment were converted into design modulus, for later be used for four pavement thickness designs using CIRCLY7.0 software. One of the pavement profiles were designed using the natural aggregates as a benchmark and three other pavement profiles were designed using three different proportions of recycled materials. The pavement thickness determined using CIRCLY7.0 were used to draw pavement models in two different finite element analysis (FEA) softwares. ABAQUS and Strand7 are the two FEA softwares considered for this research. Both ABAQUS and Strand7 can generate precise pavement structure analysis results. The purpose of using two different softwares is to analyse and confirm the pavement's response under the dynamic vehicle wheel load. The method of drawing the pavement module in ABAQUS and Strand7 is distinct. The use of two softwares allowed cross comparison of their results which improved the confidence in the outcomes.

Figure 2 demonstrates the general methodological steps involved in this research. The methodological steps involved in this research has been described as follows:

1) Research proposal background study: A comprehensive study on the flexible pavements, finite element analysis software, aggregates, common types for failures, and tests and methods that could be done on the aggregate and asphalt mixes.

2) Literature review: A comprehensive review of the literature to understand the properties of recycled material aggregates as an individual aggregate and as a replacement of natural aggregate in the asphalt mixtures. This phase helped in selecting the recycled materials to be experimentally tested in this research.

3) Borrowing required aggregates and bitumen: The selected aggregates and bitumen were requested to be provided from local recycling industries such as Boral Asphalt, and Delta Group. This phase included arranging meetings, time for material pickup, ordering necessary equipment, organising transportation, and carrying out OHS safety risk assessments for safely picking up and bringing the required materials from the collection site to the geotechnical and pavement laboratory location (Victoria University, Footscray Park campus).

4) Experiments: Laboratory experiments using relevant Australian standard were carried out to determine the properties of individual aggregate and the recycled materials entirely replacing natural aggregates in an asphalt mixture. Particle Size Distribution (PSD), Particle density, water absorption, and Flakiness Index (FI) tests were conducted for individual aggregates. Next, the Marshall Mix Design method was used to design eight asphalt mixtures, then, Indirect Tensile Modulus (IDT), and Moisture sensitivity tests were undertaken to get performance results for all asphalt mixtures.

5) Pavement structural design: The resilient modulus test result obtained from Indirect Tensile Modulus (IDT) for all asphalt mixtures was converted to design modulus using relevant Australian Standard method. The design modulus of the asphalt mixtures was then used to design four flexible pavement using CIRCLY7.0.

6) FEA: The four designed pavements and experimental data were used as an input parameter to develop finite element model (FEM) models in finite element analysis

software's (both ABAQUS and Strand7). Finite element software helped compare the potential fatigue and rutting performance of four different pavement models.
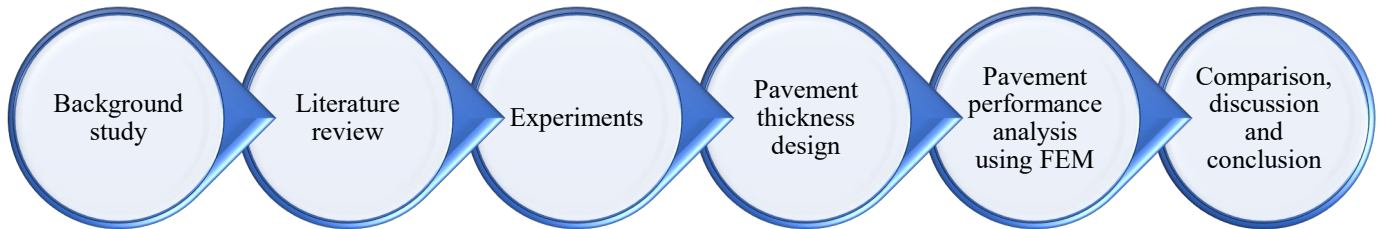
Figure 2 General methodological steps undertaken in this research.

1.4 Thesis Structure

This thesis contains six chapters and an appendix. A brief description of each chapter is presented below:

Chapter 1: Introduction

This chapter presents an overview of a flexible pavement with the idea of replacing the natural aggregates with recycled aggregates. This chapter also discusses the experimental tasks to be carried out on individual aggregates and asphalt mixtures, and numerical modellings on flexible pavement, which are the ways to demonstrate and compare recycled asphalt mixture's property against a conventional asphalt mixture. Additionally, objectives, significance, and novelty of this research are presented which were in response to the waste generation related problems, and the potential of using recycled aggregates at a higher proportion in asphalt mixtures.

Chapter 2: Literature review

In Chapter 2, first, the individual aggregate's engineering properties of RCA, RAP, and RG according to the literature, and later, the volumetric properties and performance of asphalt mixtures when the selected recycled materials were used in an asphalt mixture are reported. This chapter also presents the current limitations for using recycled materials in different states within Australia. Moreover, the aggregate volume imported into Australia and the C&D waste generated during the same period are also presented.

Chapter 3: Materials and research methodology

The material collected, types of material used, flexible pavement design, numerical modelling, as well as aggregates and asphalt mixture's volumetric and performance testing are detailed in Chapter 3. The proposed composition of the selected recycled aggregates has also been explained in this chapter.

Chapter 4: Experimental results and discussions

This chapter presents the experimental result obtained from laboratory tests. The chapter first reports on the properties of individual materials and next analyses and compares the properties and performance of the conventional asphalt mixtures with the proposed 100% recycled aggregate asphalt mixtures.

Chapter 5: Numerical Modelling

Chapter 5 discusses the result for converting laboratory-tested Indirect Tensile Modulus values of eight different mixes into field modulus, which were next used by the flexible pavement design software to design pavement thickness. In the end, the analysis outcomes of the developed FEM models are presented and discussed in this chapter.

Chapter 6: Conclusions and recommendations

Chapter 6 summarises the research findings based on the experimental test results and numerical modelling. Finally, this chapter makes recommendations for future research in this area.

Appendix

The appendix section provides plots of Marshall method charts for the seven different asphalt mixtures, while the eighth asphalt mixture's (10NA) plot has been mentioned in Chapter 4. Additionally, this section consists of figures comparing the horizontal and vertical microstrains between CIRCLY7.0 (Pavement_Science, 2022b) and ABAQUS (SIMULIA, 2011).

2 Literature review

This chapter provides discussions on previous research outcomes on the application of recycled materials in pavements, as well as potential environmental impacts and numerical modellings undertaken on pavements made of recycled materials.

2.1 Engineering properties of recycled aggregates

Recycled aggregates used in this study included RG and Construction and Demolition (C&D) materials. Generally, C&D wastes include aggregates such as RCA, RAP, Waste Rock (WR) and Crushed Brick (CB). However, in the current study, RCA and RAP were used. Selected research outcomes on recycled materials are summarised in Table 2 with their respective engineering properties and potential improvements.

Table 2 Summary of selected investigations on recycled materials in pavement applications.

Recycled material	Year of Publication	Research title	Methodology	Findings
RG	2020	Strength improvement of expansive soil by utilising waste glass powder (Blayi et al., 2020)	Experimental analysis	1) Improvement in shear strength of the expansive soil sample.
RCA	2019	Sustainable factors in pavement materials, design, and preservation strategies: A literature review (Plati, 2019)	Systematic literature review	1) Increase in stiffness and modulus. 2) RCA shows a similar mechanical property compared to conventional natural aggregates (50% of RCA can be a sustainable option).
RG	2019	Sustainable factors in pavement materials, design, and preservation strategies: A literature review (Plati, 2019)	Systematic literature review	1) Enhancement in strength and durability (15% strongly recommended for subbase and base layers).
RCA, CB and WR.	2021	Stress-strain response analysis of demolition waste as an aggregate base course of pavements (Yaghoubi et al., 2021)	Experimentation (RLT test, PSD) and Numerical modelling	1) The mean value of the resilient modulus suggested that RCA has the most significant resilient modulus, followed by CB and WR.

Table 3 summarises the engineering properties of recycled C&D waste in Australia in comparison with those of quarry materials.

Table 3 Engineering properties of Recycled materials (Arulrajah et al., 2013).

Geotechnical Parameters	RCA	RAP	Fine RG (<4.75 mm)	Typical Quarry Material
USCS classification	GW	GW	SW	-
Gravel content (%)	50.7	48.0	0.0	-
Sand content (%)	45.7	46.0	94.6	-
Fines content (%)	3.6	6.0	5.4	<10
Particle density – Coarse fraction (kN/m^2)	27.1	23.5	24.4	>19.62
Particle density – Fine fraction (kN/m^3)	26.0	23.4	24.3	>19.62
Water absorption – Coarse fraction (%)	4.7	2.2	1.0	<10
Water absorption – Fine fraction (%)	9.8	2.4	1.8	<10
Maximum Density (kN/m^3) – modified compaction	19.13	19.98	17.40	>17.5
Optimum moisture content (%) – modified compaction	11.0	8.0	10.5	8 to 15
Flakiness index (%)	11	23	-	<35
L.A. abrasion loss (%)	28	42	25	<40
CBR (%)	118-160	30-35	42-46	>80
Triaxial test (CD): Apparent cohesion (kPa)	44	53	0	>35
Triaxial test (CD): Frictional angle (degree)	49	37	37	>35
Resilient modulus: Target 90% of the OMC (kPa)	239-357	-	-	125 to 300

2.1.1 Recycled Concrete Aggregate

Recycled Concrete Aggregate (RCA) is typically the by-product of the demolition activities of concrete structures and buildings. Arulrajah et al. (2012) mentions that in Victoria, Australia, RCA is predominantly obtained from building demolition activities.

Based on the results presented in Table 3, due to the higher frictional angle and cohesion for RCA, the HMA mixture with RCA could be predicted to be more stable in rutting resistance than the typical quarry material. The CBR value of RCA is higher compared to typical quarry materials. The higher CBR value also represents the less thickness required for the pavement layer. This reduces the quantity of materials needed during the design and construction. RCA has a higher resilient modulus and stiffness than the typical quarry material representing minor deformation in the pavement structure under similar traffic loading conditions. However, the higher LA abrasion loss and lower frost resistance coefficient properties of RCA indicate the natural aggregates to be of higher quality with a better performance than the RCA aggregate (Arulrajah et al., 2013).

Sanchez-Cotte et al. (2020) conducted research using RCA in an asphalt mixture, where, the RCA was taken from two different concrete sources: one from the building demolition and another from the rehabilitation of a Portland cement concrete pavement. Their asphalt mixture was designed and compared, as shown in Tables 4 and 5. RCAP stands for recycled concrete aggregate from a Portland cement concrete pavement. In contrast, RCAB stands for recycled concrete aggregate obtained and processed from a building. Table 4 demonstrates the difference in engineering properties of an RCA depending on its source. The properties of RCAB were superior compared to RCAP in terms of particle density, water absorption and LA abrasion loss.

Table 4 Engineering properties of the obtained RCA aggregate samples (Sanchez-Cotte et al., 2020).

Method	ASTM C127 – 15	ASTM C128-07a	ASTM C127-15	ASTM C131-06
Mix	Bulk specific gravity (g/cm^3)	Absorption of fine aggregate (%)	Absorption of coarse aggregate (%)	L.A. abrasion test (%)
RCAP	2.32	7.14	6.17	31.6
RCAB	2.24	6.59	5.28	27.3
Natural aggregate	2.59	1.91	1.16	21.5

Table 5 illustrates the optimum binder content of the mixture consisting of different percentages of RCA. Despite having a higher water absorption, the RCAP asphalt mixture has lower optimum binder content (OBC) compared to RCAB as can be seen in Table 5. 45% of RCAB and Natural aggregate has a difference of 1% in terms of OBC. Bitumen is considered as an expensive material being used in the pavement design and construction. With the OBC being higher, the pavement construction cost using RCAB mixture will be higher than natural aggregate asphalt mixture. Nevertheless, the cost for the volume of aggregate required for pavement construction will be less by using RCAB asphalt mixture, as the RCAB asphalt mixture has a lower bulk density than natural aggregate asphalt mixture.

Table 5 Optimum binder content of RCA in different percentages in the mixture (Sanchez-Cotte et al., 2020).

Mix	OBC (%)	Air voids (%)	Bulk density (g/cm3)
Natural aggregate	4.4	4.3	2.366
RCAP 15%	4.5	4.8	2.31
RCAP 30%	4.8	4.8	2.305
RCAP 45%	5.2	4.8	2.289
RCAB 15%	4.9	4.3	2.349
RCAB 30%	5.1	4.0	2.336
RCAB 45%	5.4	4.4	2.304

Sanchez-Cotte et al. (2020) stated that laboratory results of RCA-modified mixtures had similar behaviour to conventional HMA mixture and had more significant environmental benefits. The higher amount of adhered mortar content in RCA aggregate causes the RCA to have higher water absorption, lower specific gravity, and higher porosity than the natural aggregate (Khayat andSadati, 2020).

2.1.2 Recycled Glass

Crushed glasses are typically produced from container glass cullet. The contaminants are removed for crushed glass in pavement application, and the glass is crushed to a specific size. The recycled glass limit can differ when used as supplementary material in pavement application, depending on the location used within the pavement structure.

Disfani et al. (2011) demonstrated reasonable evidence of medium and fine-sized recycled glass having geotechnical engineering properties suitable to replace natural aggregates. The recycled glass was divided into three groups based on its particle size: Fine Recycled Glass (FRG), Medium Recycled Glass (MRG) and Coarse Recycled Glass (CRG). FRG, MRG and CRG had particle sizes smaller than 0.075mm, between 0.075 – 2.36 mm, and greater than 2.36mm, respectively. Table 6 demonstrates the engineering properties of recycled glass of three different particle sizes. The LA abrasion loss percentage for CRG is more than FRG and MRG. Due to the lack of cohesion between the glass particles, Disfani et al. (2011) reported that Repeated Load Triaxial (RLT) test could not be performed with the recycled glass. The internal frictional angle of the different sized RG is also presented in Table 6, which shows MRG has internal friction slightly over FRG.

Table 6 Geotechnical engineering properties of the recycled glass (Disfani et al., 2011).

Geotechnical parameter	FRG	MRG	CRG
Specific gravity (g/cm3)	2.48	2.5	2.5
Flakiness index (%)	-	85.4	94.7
Maximum density – standard proctor (kN/m3)	16.7	18	-
Optimum moisture content – Standard proctor (%)	12.5	9	-
Maximum density – modified proctor (kN/m3)	17.5	19.5	-
Water absorption – modified proctor (%)	10	8.8	-
LA abrasion value (%)	24.8	25.4	27.7
CBR (%) – Standard compaction	18-24	31.32	-
CBR (%) – Modified compaction	42-46	73-76	-
Triaxial shear test – Angle of internal friction (degrees) (60 – 240 kPa stress)	42-43	50-51	-
Direct shear test – Angle of internal friction (degrees) (60 – 240 kPa stress)	38	41	-

Hughes (1990) conducted research to evaluate the feasibility of using graded RG at 95% of the particle passing through 9.5mm sieve, 58% passing through 4.75mm sieve, and 39% passing through 2.36mm sieve in an asphalt mixture. The author mentioned the addition of RG from 0 to 15% RG in the asphalt mixture showed a declining trend in the Marshall stability value (from around 9.9kN to 9.5kN); all of them satisfying the Marshall stability requirement. Furthermore, the addition of up to 15% RG didn't adversely affect neither the resilient modulus nor the tensile strengths. Therefore, the author considers the use of up to 15% RG in the asphalt mixture to be technically feasible.

2.1.3 Reclaimed Asphalt Pavement

RAP is a reprocessed pavement consisting of both asphalt and aggregate. RAP can be reused as an aggregate in dense-graded asphalt. Research shows that addition of RAP to the mixture

can enhance fatigue life compared to a typical natural aggregate asphalt mixtures (Su et al., 2009). Al-Qadi et al. (2012) prepared HMA using 0, 30, 40, and 50% RAP, and conducted asphalt mixture's performance testing such as beam fatigue, and wheel tracking. An increase of RAP from 0 to 30% showed approximately 22% increase in flexural modulus. In terms of rutting depth evaluated through wheel tracking test, mixtures with 30% RAP showed rutting depth around 30% lower than conventional asphalt mixture. Similarly, the increase in RAP in the mixture from 30 to 50% showed declining trend in the depth value, which was down to 50% than conventional mixture.

Table 7 demonstrates the obtained engineering property results of the 40% and 70% RAP when mixed with natural aggregate for the surface course for an airport pavement (Su et al., 2009). The OBC for asphalt mixtures with 40% and 70% RAP content is 5.4 and 5.3%, respectively. This OBC is close to the virgin aggregate asphalt mixture. Additionally, Table 7 demonstrates that OBC decreases with increased RAP content in HMA.

Table 7 RAP engineering properties (Su et al., 2009).

Mixture	Bulk specific gravity (g/cm3)	Air voids (%)	Stability (kN)	Flow (1/10mm)	Optimum Asphalt Content (%)
Virgin	2.408	2.8	13.6	26	5.4
RAP 40%	2.401	3.0	16.1	30	5.4
RAP 70%	2.409	2.9	15.4	29	5.3

2.2 Literatures Review: Recycled C&D Materials in HMA

Su et al. (2009) conducted research using 40% and 70% of RAP combined with natural aggregates in an asphalt mixture and observed the Optimum Binder Content (OBC) to be 5.4% and 5.3%, respectively. Similarly, Sanchez-Cotte et al. (2020) worked with different percentages of RCA combined with natural aggregate, and demonstrated that using 45% RCA led to 0.8 to 1% higher OBC than the conventional asphalt mixture depending on the source of the RCA. In their study, asphalt mixtures made of RCA were observed to have lower bulk density compared to conventional mixtures. Su and Chen (2002) worked with RG and demonstrated that the rise in the RG percentage of an asphalt mixture decreased the OBC of an asphalt mixture due to the lower moisture absorption potential of crushed glass. Yaghoubi et al. (2013) used up to 10% rejuvenating agents for preparing HMA made of RAP and carried out Marshal stability test and dynamic creep tests to compare the properties of mixtures with conventional asphalt. Their results showed that while none of the mixtures made of RAP exhibited greater stability and indirect tensile resilient modulus, or lower permanent deformation compared to the conventional asphalt, adding 10% rejuvenator to RAP developed HMA that met the requirements of the Iran's Highway Asphalt Paving Code. More findings based on the previous research on the performance and properties of asphalt mixtures that incorporated RG, RAP, and RCA are outlined in Table 8.

Table 8 A summary of research outcomes on the incorporation of recycled materials in the asphalt mixtures.

Recycled material type	Reference	Percentages of recycled content	Types of tests	Some key findings
RG	Su and Chen (2002)	0, 5, 10, and 15%	Marshall stability, moisture sensitivity, skid resistance, light reflection, & permeability	• The experimental pavement test section with 10% of RG showed acceptable performance even after a year of observation. • The Marshall stability values of 5 to 15% of RG were within the limits specified. Additionally, the increase in lime in the mixture showed improved stability values.
RG	Alhassan et al. (2018)	5, 6, 7, 8, 9, and 10%	Marshall Stability, flow, bulk density, & air voids	• Asphalt produced with an 8% RG were suitable to be used as wearing course material. • The fine-sized RG cullet from waste glass bottles showed similar behaviour to natural aggregate. • The result of the Marshal Stability, flow, bulk density, and air voids test showed the HMA that incorporated 5 to 10% RG contents were desirable.
RG	Lachance-Tremblay et al. (2016)	5, 10, 15, 20, and 25%	Laboratorie des Chaussees (LC) mix design method, thermal stress restrained specimen test, complex modulus test, & stripping resistance test.	• The use of crushed RG increased mixture workability and decreased the rutting resistance. • The addition of RG eventually increased the effective binder content by reducing the volume of binder absorbed. • The stripping resistance of the mixture consisting of 10% RG was lower than that of the conventional mixture.
RAP	Su et al. (2009)	0, 40, and 70%	Marshall Mix Design, wheel tracking, & three-point bending test	• 40% RAP showed similar properties compared to the control HMA mixture without RAP, except for moisture susceptibility. • RAP (40% and 70%) showed similar evenness and bearing capacity as the HMA control mixture without RAP after three years of service life. • The 40% RAP mixture showed similar fatigue properties to that of the controlled HMA mixture without RAP, whereas the 70% RAP mixture showed poor fatigue properties. • The use of 40% RAP reduced the cost by almost 38% compared to the HMA mixture without RAP per ton.
RCA	Cho et al. (2011)	1) 100% RCA 2) 100% coarse RCA mixed with fine natural aggregate 3) 100% fine RCA mixed with coarse natural aggregate	Marshall mix design, Indirect Tensile Test (IDT), wheel tracking test, and tensile strength ratio (TSR) test.	• Mixtures made of natural coarse aggregate with fine recycled concrete aggregate had the highest resistance to rutting. • Coarse RCA with fine natural aggregate and natural coarse aggregate with fine RCA showed comparable performance in indirect tensile strength ratio, deformation strength, and rut depth. • RCA with fine recycled coarse aggregate showed the lowest resistance to tensile stress and shear flow. Thus, the proposed mix was not recommended to be used as a base layer aggregate.
RCA	Bhusal et al. (2011)	20, 40, 60, 80, and 100 %	HMA Superpave Mix Design (OBC, VMA, bulk and maximum theoretical density)	• The cement paste in RCA increased the water absorption rate and decreased the particle density. • The OBC of the asphalt mixture increased from 6.8 to 9.2% with the increase of RCA from 20 to 100%.

2.3 Recycled Materials Content Limitations

Technical notes of different states and countries have different limitations on recycled materials' content in pavement structural layers. All technical notes have expressed the possibility that the allowable limit of recycled material might increase in the future.

According to VicRoads Section 407 – Hot Mix Asphalt, RG shall be limited to intermediate and base course layers. In contrast, the Queensland government of Australia allows up to 10% recycled crushed glass in dense-graded asphalt other than surfacing and 2.5% in dense-graded asphalt surfacing. The 'Section 407- Hot Mix Asphalt' of VicRoads is the standard and guideline for dense-graded asphalt in Victoria, Australia. The RAP has different limitations for its use on dense-graded asphalt. The limitation of using RAP in Victoria, Australia, depending on the traffic volume of the target road is presented in Table 9. However, the limitation of recycled glass and concrete in the HMA mixture is not explicit in the VicRoads standards and guidelines.

Table 9 RAP allowable limit in Victoria, Australia.

Pavement type	Allowable limit
Light duty size 7 or 10 wearing course for use in lightly trafficked pavements	Up to 20% by mass
Light to medium size 7,10 or 14 wearing course or regulating course for use in light to moderately trafficked pavements–	Up to 15% by mass
Heavy-duty size 7, 10 or 14 asphalt wearing course or regulating course for use in the most heavily trafficked pavement –	Up to 10% by mass
A multi-purpose size 14 or 20 structural asphalt for an intermediate course in heavy-duty pavements or base course in medium-duty pavements	Up to 20% by mass
A fatigue-resistant size 20 structural base course asphalt for heavy-duty asphalt pavements	Up to 30% by mass

In Queensland, Australia, fine RG can be used within 10% in dense-graded asphalt layers and 2.5% in asphalt surfacing. There is no evidence for the limit of RCA in dense-graded asphalt. Table 10 demonstrates the maximum limit of RAP in an asphalt mixture in Queensland.

Table 10 Limitation of RAP in Queensland, Australia.

Asphalt mixture	Base, Intermediate and corrector courses				Surface course	
RAP approval level	1	2	3	4	1S	2S
Allowable percentage of RAP in mixture (%)	15	25	30	40	15	20

2.4 Environmental impact

The pavement industry is one of the primary greenhouse gas emission sources. Recycled materials consumption in the pavement structural layer will benefit the environment, at least by reducing the rate of extraction of natural aggregates from aggregate mines or mountains.

According to the UNEP (United Nations Environment Programme) global environmental alert services 2014, the annual global aggregate extraction such as sand, gravel and other aggregate materials extracted from the Earth is between 47,000 and 59,000 megatons (Hall, 2020; Programme, 2014). During 2008 - 2009, 19 megatons of construction and demolition waste (CDW) were generated in Australia, where 55% was recovered while the rest was disposed of in landfills (Hyder-consulting, 2011). At around the same time, i.e. in 2008, Australia imported 200 megatons of construction materials (Wiedmann et al., 2015). The national waste report 2018, prepared by collecting data from Environment Protection Agencies (EPA) across Australia, stated that, in 2017, Australia generated 20.4 megatons of CDW, where only 66.9% were recycled, and the remaining were disposed of at landfills, in addition, approximately 1.1 megatons of glass waste was generated from 2016 to 2017, where, 57% was recycled (Joe Pickin, 2018). In contrast, 1.29 megatons of glass waste were produced in the 2017 -2018

financial year, where the recycling rate of glass decreased to 46%. Additionally, the glass packaging, which is the largest market for glass consumption, is reported by industry to slowly continuing to lose market share to plastic packaging (Allan, 2019).

The voluminous generation of various wastes, depletion of natural resources, leading to shortage of construction materials, and the ever-increasing transportation cost of natural aggregates are all challenges that the use of a higher percentage of recycled materials in pavements can contribute to alleviating without compromising the required structural performance of the pavement system.

2.5 Numerical Modelling

FEM enables analysis of the stress, strains, or deflections at different points from the applied tyre load. Such analysis is not usually possible to be undertaken by pavement design software such as CIRCLY7.0. The layered elastic theory assumes that each layer is homogeneous with the same properties throughout the layer (Huang, 2003). This assumption makes it difficult to analyse pavement systems composed of non-linear materials, such as granular bases and subbases.

The two major failures of flexible pavement are rutting and fatigue cracking. Rutting is the permanent deformation along the wheel paths. Huang (2003) discussed the two design methods to control rutting, one by limiting the vertical compressive strain on top of the subgrade, and the other by limiting the rutting to a tolerable limit, typically 13mm. The first method requires a failure criterion based on correlations with road tests or the field performance. In contrast, the second method can be based on empirical correlation with road tests or on theoretical computations from the permanent deformation parameters of each component layer. The fatigue cracking of flexible pavements is based on the horizontal tensile strain at the bottom of

HMA (Yaghoubi et al., 2021). The failure criterion relates the allowable number of load repetitions to the tensile strain through the laboratory fatigue test on HMA specimens.

The linear FEA assumes that the model only undergoes small deformation and deflection based on the applied force, and it does not experience any plastic deformation or creep due to loading (Scott, 2021). The stress-strain response is a vital parameter in analysing the pavement's performance. Non-linear FEA provides a more realistic approach to simulation as it assumes material nonlinearity, such as the plasticity of the model or creep within the material (Scott, 2021). The finite element analysis of pavement structures using linear material properties may also provide accurate analysis (Duncan et al., 1968). Although not completely realistic, it can be a suitable basis for comparison of the behaviour of innovative HMA with the conventional HMA. Sii (2015) prepared 3D FEM in Strand7 assuming, linear, homogeneous, and elastic material properties, to analyse a dowl-jointed concrete pavement's response under vehicular loading, which was successfully validated with classical analytical solutions of shear and moment along the dowel.

Table 11 demonstrates selected research findings and methods used to analyse the pavement performance using FEA.

Table 11 Numerical Modelling in pavement design findings.

Research title	Year of publication	Numerical modelling method	Findings
Finite Element Analyses of Pavements (Duncan et al., 1968)	1968	The finite element method (USE software) was used to prepare Linear and Non-linear Pavement models.	1) Accurate analysis of the behaviour of pavement structures with linear material properties may be made using finite element analysis.
Three-Dimensional Dynamic Response Model for Rigid Pavements (Mallela andGeorge, 1994)	1994	Three-dimensional finite element program ABAQUS was constructed to analyse the dynamic loading	1) Static load deflections are more significant than the dynamic load-deflection result.
Simulation of Flexible Pavement Utilizing Fly Ash as Alternative Stabilizer (Adedeji, 2015)	2015	Finite Element Analysis software (ABAQUS) was used to develop the models.	1) 3D Finite Element is more efficient than 2D axisymmetric models.
Critical Pavement Response Analysis of Low-Volume Pavements Considering Non-linear Behaviour of Materials (Gupta et al., 2015)	2015	Finite Element (FE) analysis software (ANSYS) was used to develop the 3D model.	1) Pavement response obtained from the 3D FE analysis method for typical low-volume roads, using non-linear characteristics of unbound pavement materials, differed by 34 to 44% compared to the linear analysis method.
Comparative study on asphalt pavement rut based on analytical models and test data (Yang et al., 2020)	2018	Finite Element Analysis software; ABAQUS	1) Time- hardening creep models were developed in ABAQUS for rutting analysis, and the models were validated using the indoor rut test and actual engineering data. 2) For average temperature, the surface rut of the pavement model for a standard load (at 12:00 to 14:00 PM) was found to be 0.281mm, whereas for the 15 years of design life (i.e., 350 x 10^4 times) was found to be 12.71mm.
A comparison of implementation of linear and nonlinear constitutive models in numerical analysis of layered flexible pavement (Ghadimi andNikraz, 2017)	2016	Pavements modelled in ABAQUS (2D for validation purpose, and 3D for comparison between the models) using linear, K – θ (widely used nonlinear model which relates the resilient modulus to bulk stress) and Lade Nelson models (a nonlinear pavement model which relates the depends on both the deviatoric stress and mean normal stress).	1) Linear pavement models were developed in ABAQUS (2D) was validated against a pavement model using similar material properties and geometry in KENLAYER, and CIRCLY7.0. The surface deflection results obtained from all three software's were similar. 2) 3D linear pavement model was found to be stiffer (having lower surface deformation, horizontal strains at the bottom of surface course, and vertical stress and stain at top of subgrade) than Lade – Nelson (max. 45.23% and min. 30.95% difference in surface deflection result of the linear pavement model with respect to Lade - nelson), and K - θ pavement model (max. 22.51% and min. 16.07% difference in surface deflection result with respect to K-θ pavement model).
Structural response of an inverted pavement with stabilised base by numerical approach considering isotropic and anisotropic properties of unbound layers (Biswal et al., 2020)	2019	3D Finite Element modelling using COMSOL (a general-purpose finite element analysis software).	1) The finite element pavement model was developed and validated using linear elastic pavement analysis software, IIT PAVE. The pavement model in FEM and IIT PAVE had close results (with error of 20.20% for tensile strain at bottom of base course). 2) Subgrade anisotropy has a positive effect on the response of subgrade, i.e., rutting life increases with the increase of anisotropy of subgrade.

2.6 Concluding remarks

The literature shows both the positive and negative sides of recycled aggregates (RCA, RAP, and RG) in HMA, such as RCA being strong increases the Marshall stability of an asphalt mixture but is highly absorptive. RAP helps reducing the OBC of an asphalt mixture but reduces rutting resistance. And, RG having engineering properties similar to a sand, helps reducing the OBC of an asphalt mixture, but has shown to reduce the Marshall stability of an asphalt mixture.

There is limitation on the amount of recycled materials that can be used as an aggregate in a HMA mixture specified by several specifications all around the world. Additionally, there is only few research conducted on the performance of pavement materials consisting of a recycled materials in higher percentage.

The recycling industry has improved with time; therefore, the quality of the recycled materials could be assumed to have been improved compared to what they were a decade ago. This research analyses the feasibility of the recycled material aggregate in the asphalt mixture and compares it against conventional asphalt mixture using comprehensive lab experiments (on individual aggregates and asphalt mixture designs).

The literature review proves the Finite element pavement models assuming linear elastic materials properties have been validated for pavement responses. This supports the accurate analysis of the pavement model could be done using linear material properties using FEA software.

Analysis and comparison between the conventional and recycled aggregate asphalt mixtures through pavement thickness design and performance analysis of pavement models (using finite

element models) helps in finding a conclusion on the feasibility of using the recycled materials

as an aggregate in the HMA mixtures, in this research.

3 Materials and research methodology

3.1 Collection of Materials

Graded sand and dust (filler), along with one-sized aggregates of 7, 10, 14, and 20mm were used to prepare conventional asphalt mixture. For the case of recycled material mixtures, graded recycled material aggregates i.e., RCA, RAP, and sand size-RG were used to prepare three 10mm dense graded asphalt mixtures and three 20mm dense graded asphalt mixtures. For this research, type C320 bitumen was used which was also provided by Boral. The locations of borrowed aggregates are shown in Figure 3. As seen in this figure, RAP, RG, and natural aggregates were supplied by Boral Asphalt located at Deer Park, VIC. Graded Class 2 RCA was supplied by the Delta Group located at Sunshine, VIC. The collected materials were taken to Victoria University, Footscray Park Campus, for storage and lab testing.
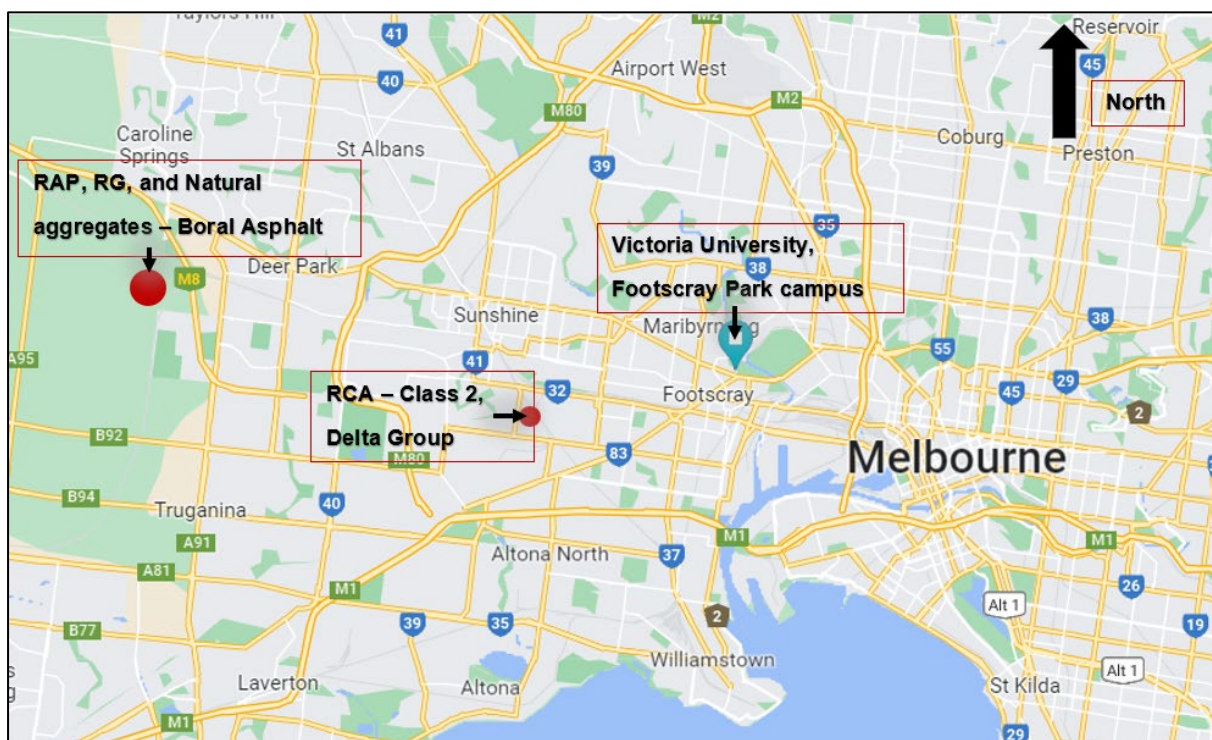
Figure 3 Collection sites of aggregates used in this project (Google, 2023).

The following steps were undertaken to collect the aggregate and bitumen required for this research:

1) Risk assessments were done each time for collecting aggregates from industry to university using the university's Ute,
2) Personal protective equipment were worn to ensure safety at site,
3) A whole box of large plastic bags, cable ties, and shovels were taken for aggregate collection purposes,
4) The plastic bags loaded with aggregate were brought to the Victoria University Footscray Park campus.

Figure 4 demonstrates the RAP aggregate piles at Deer Park, Victoria, Australia. Similarly, Figure 5 shows the pile of class 2 RCA, which belongs to Delta Group, located at Sunshine, Victoria, Australia. Figure 6 demonstrates images of some of the aggregates used in this research at their wet state.
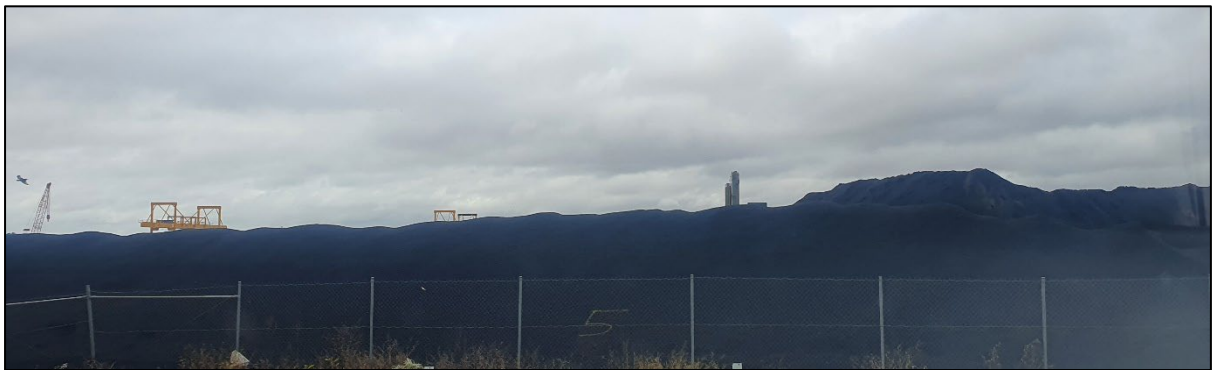
Figure 4 Pile of RAP, Boral Asphalt.

Figure 5 Pile of Class 2 RCA, Delta Group.

Figure 6 Images of the used aggregates in their wet state.

3.2 Raw materials and proposed asphalt mixtures

The RCA, RAP, and RG were the three types of recycled wastes selected in this research to form proposed blends. Selection of the percentage of each recycled aggregate in the asphalt mixture was systematic than arbitrary. In this regard, the upper and lower bands of the HMA gradation provided by VicRoads-RC500.01 (2021) were used as a guide. The properties of the individual aggregates will be presented in Chapter 4 of this thesis.

The binder used in this study was Grade C320 bitumen, which is typically suitable for medium to heavy asphalt applications and heavy-duty and hot climate seals. The typical viscosity at 60ºC and 135ºC of C320 bitumen are 320 and 0.5 Pa.s, respectively; similarly, the typical penetration at 25ºC and flashpoint is a minimum of 40 dmm, and a minimum of 250ºC respectively (Tahmoorian et al., 2018). Additionally, Tahmoorian et al. (2018) mentioned that the typical specific gravity of the C320 bitumen is 1.03 kg/m^3, and the softening point is 52ºC. Table 12 demonstrates the properties of C320 bitumen used in the asphalt mixtures in this research.

Table 12 Typical characteristics of C320 bitumen (Tahmoorian et al., 2018).

Properties	Units	Typical
Viscosity at 60ºC	Pa.s	320
Viscosity at 135ºC	Pa.s	0.5
Penetration at 25ºC	dmm	Min 40
Flashpoint	ºC	Min 250
Binder density @15ºC	kg/m3	Min 1000

Table 13 presents the composition of aggregates in each asphalt mixture considered in this research. In Table 13, as an example, in 10 RCA75, "10" and "75" refer to the maximum aggregate size of the mixture, and the percentage of RCA in the mixture, respectively. The maximum particle size of supplied RAP was 10mm, whereas RCA had a maximum particle size of 19mm. Therefore, RCA was sieved through a 9.5mm sieve for the preparation of the 10mm asphalt mixtures.

Table 13 Composition of aggregates in each asphalt mixture.

Asphalt mixture	Asphalt size (mm)	Aggregate composition
10NA	10	10mm NA,20%; 7mm NA,20%; Sand,25%; and 35% of dust
20NA	20	20mm NA,17%; 14mm NA,10%; 10mm NA,15%; 7mm NA,10%; Sand,25%; and 23 % of the dust
10RCA 75	10	75% of RCA, 15% of RAP, and 10% of RG
10RCA 65	10	65% of RCA, 25% of RAP, and 10% of RG
10RCA 55	10	55% of RCA, 35% of RAP, and 10% RG
20RCA 75	20	75% of RCA, 15% of RAP, and 10% of RG
20RCA 65	20	65% of RCA, 25% of RAP, and 10% of RG
20RCA 55	20	55% of RCA, 35% of RAP, and 10% RG

The maximum particle size of RAP was 10mm, whereas RCA had a maximum particle size of 19 mm. Therefore, for preparing the so-called 10mm mixtures, RCA was sieved through a 9.5 mm as can be seen in Figure 7. In this research, 20RCA 75, 20RCA 65, and 20RCA 55 indicate size 20 mixtures where the maximum particle size of RCA is 20mm, whereas 10RCA 75, 10RCA 65, and 10RCA 55 indicate size 10 mixture prepared.

Figure 7 RCA sieved through the 9.5 mm sieve.

3.3 Experimental procedures

3.3.1 Preparation of identical aggregate samples

Keeping the same particle size distribution (PSD) for each mixture type throughout the experimental phase plays a significant role in obtaining reliable test results. The quartering of aggregates helps achieve the required mass for specific preparation of each mixture while keeping the same PSD. Dust, sand, and RG were quartered by making each aggregate pile, flattening the sample into a circular shape and then quartering them into four equal parts. The quartering process using a sample splitter was applied for graded aggregates such as RCA and RAP. Prior to quartering process, three bags, each weighing approximately 20kg, of a graded aggregate were dried and mixed for quartering, in order to reduce errors in aggregates gradation. Plus, all aggregates were dried prior to the quartering process. After quartering the aggregates into smaller portions, they were stored in a plastic container with proper labels.

Figure 8 shows a sample splitter being used to split a significant portion of the recycled material sample into two equal portions of similar gradation in this research.

Figure 8 Aggregate quartering process using sample splitter.

3.3.2 Particle Size Distribution test

Two methods of PSD testing were adopted in this project which were dry and wet sieve analysis. Dry and wet sieve analyses were carried out as per the Australian standard AS_1141.11 (1996) and AS_1141.12 (2015), respectively. The mass required for the testing was selected as per the aggregate size, type and the PSD testing method. Aggregates such as 7, 10, 14, 20mm, RG, and RCA were undertaken for dry sieve analysis after drying the aggregate in an oven. However, the aggregates, such as dust, sand, and RAP, that had finer particles, were tested using the wet sieve analysis technique.

3.3.2.1 Dry sieve method

In this test, 300mm diameter sieves of size 37.5, 26.5, 19, 13.2, 9.5, 6.7, 4.75, 2.36, 1.18, 0.6, 0.3, 0.15, and 0.075mm were taken, and their empty masses were noted down. Then, the oven-dried aggregates at 105 - 110ºC for at least 24 hours were taken, and the mass was noted down for dry sieve analysis. Figure 9 illustrates the arrangement of the sieves and the mechanical

sieve shaker used in this research. At first, the empty sieves were arranged from 37.5 to 0.075mm (top to bottom); secondly, dried aggregates were poured on the top sieve, and then a mechanical sieve shaker was used to shake the sieve for 5 to 10 minutes. Finally, the weight of each sieve after the shaking process were noted down.

Figure 9 The set of sieves used for the determination of the PSD.

3.3.2.2 Wet sieve method

Similar to the dry sieve analysis method, all empty sieves were taken, and the mass were recorded. Sand and dust were dried at 105 – 110ºC, whereas RAP was dried at 60ºC for 2 days as RAP consists of binder coated around the aggregates, which could flow at 110ºC temperature, providing a misleading PSD result. Instead of the shaking process, water was used to help the aggregates flow through the sieves. Care was taken for the water not to flow above

the sieve. The water was slowly poured into the sieve consisting of the dry aggregate sample. Similarly, after using water to help aggregates pass through each sieve, aggregates retained on each sieve were then transferred onto separate containers of known empty mass and dried for 24 hours at 110ºC. Finally, the dry mass of retained particles on each sieve were recorded.

3.3.3 Particle density & water absorption tests

The particle density and water absorption test are necessary to understand the aggregates' water holding capacity and the mass required to achieve a particular volume. The mass required to achieve a particular volume is important in estimating the mass of the sample required for preparation of samples for the Marshall stability, IDT, and moisture sensitivity tests. The water absorption property of an aggregate can be an indication of the binder absorption, resistance to freezing & thawing, and resistance to ravelling and stripping properties of an asphalt mixture (Tahmoorian et al., 2017). The particle density and water absorption of coarse and fine aggregates were carried out as per AS_1141.6.1 (2000) and AS_1141.5 (2000), respectively. Those aggregates consisting of both coarse and fine aggregates at a significant amount, were evaluated by separating the coarse and fine particles and analysing their particle density and water absorption separately. Finally, the PSD test result of the aggregate, and separate particle density and water absorption test result of fine and coarse particles of the aggregate, were used to calculate particle density and water absorption of the aggregate (consisting of both coarse and fine particles). Since PSD is used when calculating the overall particle density and water absorption of the aggregates, these results can be considered to be dependent on the aggregate's gradation. Table 14 presents the equation used for the determination of the particle density and water absorption of the aggregates.

Table 14 Equations used for particle density and water absorption test.

Parameter	Coarse aggregates	Fine aggregates
Apparent particle density	$\dfrac{m1 \times \rho w}{m4 - W}$	$\dfrac{m1 \times \rho w}{m4 + m1 - m3}$
Particle density on a dry basis	$\dfrac{m1 \times \rho w}{m2 - W}$	$\dfrac{m1 \times \rho w}{m4 + m2 - m3}$
Particle density on a saturated surface dry basis	$\dfrac{m2 \times \rho w}{m2 - W}$	$\dfrac{m2 \times \rho w}{m4 + m2 - m3}$
Water absorption	$\dfrac{(m2 - m1) \times 100}{m1}$	$\dfrac{(m2 - m1) \times 100}{m1}$

In the equations of Table 14,

m1 = dry mass of the test portion, in grams

m2 = mass of the saturated surface-dry test portion, in grams

ρ_w = Density of water at test temperature, in grams per cubic centimetre

m3 = mass of the basket with water and the test portion, in grams

m4 = mass of the basket filled with water, in grams, and

W = weight of the aggregates test portion underwater.

3.3.4 Flakiness Index test

The flakiness index test provides information about the percentage of flaky particles in an aggregate. The presence of more than 35% flaky particles is restricted from being used in dense graded asphalt (DGA). The presence of flaky particles is known to result in less binder consumption but can cause low air voids (<4%) in the mixture which is not desirable

(Austroads-5.3.2, 2022). AS_1141.15 (1999) was used to conduct flakiness index testing on aggregates with at least 80% by mass retained on 4.75mm sieve. The aggregates with at least 80% by mass retained on 4.75mm sieve were RAP, RCA, and one-sized NA aggregates (7, 10, 14, and 20mm). A flakiness index gauge consists of openings with different sizes of holes for aggregates retained on different sieves. As shown in Figure 10, for each aggregate, the required mass of the sample according to the standard was taken and particles were separated based on their sizes by passing them through sieves, then the aggregate retained on different sieves was attempted to pass through a relevant thickness hole in the flakiness index gauge. The aggregate passing through the thickness gauge hole was considered a flaky particle. Finally, the flakiness index (FI) was calculated for an aggregate using Equation 1.

$$FI = \frac{\sum m2}{\sum m1} \times 100 \qquad\qquad \text{Equation 1}$$

where,

FI = Flakiness index of an aggregate

$\sum m2$ = Sum of masses of size fractions passing the slotted sieve, in grams

$\sum m1$ = Sum of masses of selected entire size fraction, in grams

Figure 10 Images showing a) aggregate separated based on particle size using sieves, and b) Flakiness Index gauge.

3.3.5 Marshall Mix Design

Marshall Mix Design method was used to evaluate the Optimum Binder Content (OBC) for each asphalt mixture. The laboratory experiment and calculations undertaken in order to get the OBC of an asphalt mixture following Marshall Mix Design are listed below:

1) Preparation of at least three test specimens at trial bitumen content having an interval of ± 0.5% bitumen content,

2) Maximum theoretical density testing,

3) Bulk density evaluation,

4) Marshall stability and flow analysis,

5) Air voids, VMA, and VFB calculation.

The above-mentioned procedures are explained in the following sections.

3.3.5.1 Test specimen preparation

The particle density test results were used to calculate the required dry mass of each aggregate for the required test specimens of height 63.5mm and 101.6mm in diameter. According to Vicroads-RC201.01 (2016), Marshall mix design requires a minimum of 12 test specimens for each asphalt mixture. For each asphalt mixture, a minimum of four trial bitumen content was selected at an interval of 0.5%. Each trial bitumen content had a minimum of three test specimens. Overall, 148 test specimens were prepared to find the OBC of eight different asphalt mixtures. Out of 148 test specimens, 90 were prepared for 10mm asphalt mixtures and 58 test specimens for 20mm asphalt mixtures.

The specimen preparation started with 10mm asphalt mixtures. For the natural aggregate mixture, 4.5, 5, 5.5 and 6% of bitumen content were selected. For 10RCA 75, and 10RCA 65, trial bitumen contents were selected from 4.5 to 7.5% at an interval of 0.5% to understand the test specimens' behaviour in achieving peak stability. The selection of the trial bitumen content

was changed as per the experience working with the recycled material mixture. For example, the trial bitumen content for 10RCA 55 was selected from 5.5 to 7% at an interval of 0.5%. Later with a 20mm asphalt mixture, the trial bitumen content range was selected based on the experience gained working with recycled asphalt mixture. Therefore, the number of test specimens prepared for 10mm asphalt mixture was larger than 20mm asphalt mixtures.

3.3.5.2 Maximum theoretical density of the asphalt mixture

AS_2891.7.1 (2004) was used to perform the maximum theoretical density of the asphalt mixture. The loose dry asphalt mixture was placed on top of a steel table until the mixture was cooled down. Once the loose asphalt mixture was cooled down, its dry weight was recorded. The dry aggregates were transferred to a container filled with 25ºC water, and their mass was noted. The aggregates in the container were covered with water up to 50 mm above the aggregate level. Figure 11 demonstrates one of the loose samples and the equipment setup used during the maximum theoretical density testing phase of this research.

Figure 11 Images showing a) a loose asphalt mixture sample b) maximum theoretical density testing equipment setup.

Additionally, a vacuum of about 600 mmHg was applied in the container to remove the air bubbles from the asphalt mixture. Following the air bubble removal from the container, the container's mass with the aggregate and water was measured using the weigh-in water setup. Finally, the maximum density of the asphalt mixtures was calculated using the formula mentioned in Equation 2.

$$G_{mm} = \frac{A}{A-C}$$
<div align="right">Equation 2</div>

Here,

G_{mm} = Theoretical maximum specific gravity of HMA,

A = Dry mass of the test portion, and

C = Submerged Mass of the test portion

3.3.5.3 Marshall compaction and extraction

AS_2891.5 (2004) was followed to conduct the compaction and extraction phase. Two ovens were used to get the aggregates and bitumen ready for mixing and compaction phase. The C320 bitumen was heated up to 150ºC for a minimum of 2 hours. Similarly, the aggregates, metal scoop, spatula, mixing container and Marshall moulds were heated up to 180ºC for a minimum of 2 hours. The temperature of the aggregate was tracked using a thermometer. After both bitumen and aggregate were heated up to their required temperatures, they were mixed in a mixing bowl using a laboratory asphalt mixer. The mixing phase was continued until 80% of the coarse aggregates were coated around by bitumen, i.e., generally about 1-2 minutes of mixing. Quickly after mixing, the mixture was cured for 15 minutes at 150 degrees Celsius before compaction to ensure all the heat was evenly distributed within the mixture and the temperature of the mixture is suitable for compaction. After the temperature check, the mixture was compacted with 50 blows on each side using an automatic Marshall impact compactor. The compacted test specimens were kept in the mould until reaching the room temperature and

were next extracted from the mould using a specimen extruder. Figure 12 demonstrates the laboratory asphalt mixer, Marshall impact compactor and specimen extruder used in this research.
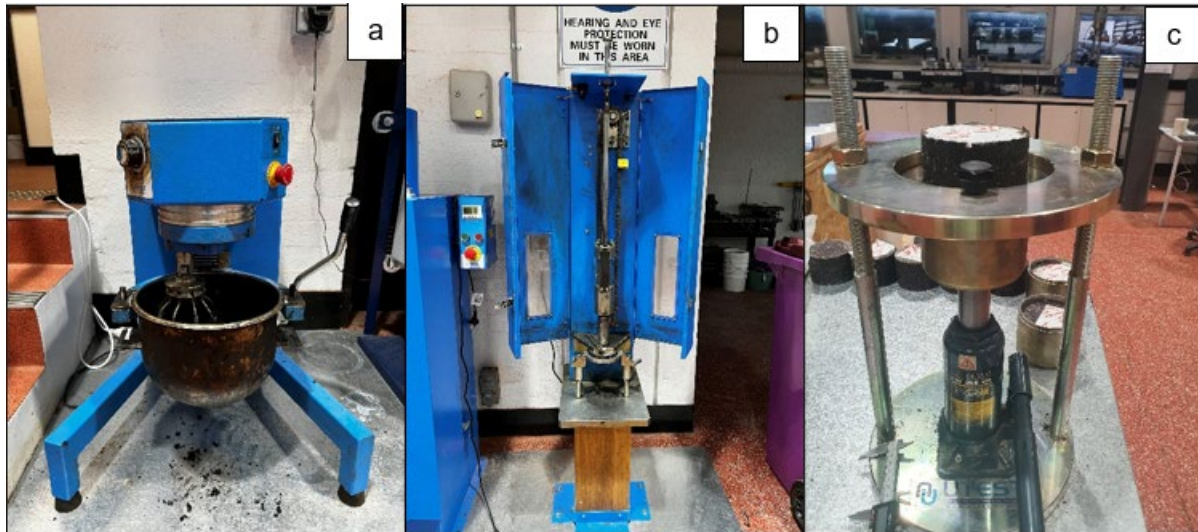
Figure 12 Images showing a) Laboratory asphalt mixer, b) Marshall impact compactor, and c) Specimen extruder.

3.3.5.4 Bulk density

The test specimen's bulk density was determined following the procedure mentioned in AS_2891.9.2 (2005). Firstly, the temperature of the water was measured using a thermometer. Secondly, the air-dried mass of the test specimen was recorded, followed by the immersion of the test specimen in water. Thirdly, after 5 minutes, the weight of the test specimen in water was recorded using a weigh-in water scale setup as can be seen in the Figure 13. Finally, the test specimen was removed from the water, the surface of the specimen was wiped using a damp towel to reach the surface-dry condition, and the mass was recorded.

Figure 13 Weigh-in-water balance used for bulk density testing.

The bulk density of the test specimen was calculated using Equation 3.

$$\rho_{bulk} = \frac{m1 - \rho w}{m3 - m2}$$ Equation 3

where,

ρ_{bulk} = bulk density of the test specimen, g/cm^3

ρ_w = density of water, g/cm^3

m1 = Air-dried Mass of the test specimen, g

m2 = mass in water, g

m3 = Saturated surface mass of the test specimen, g

3.3.5.5 Marshall stability and flow

AS_2891.5 (2004) testing method was followed to perform the Marshall stability and flow analysis. The automatic Marshall stability testing machine is shown in Figure 14. The equipment takes the height of the specimen as an input parameter and automatically applies the correction factors to display the stability and flow result of the test specimen.

Before the test, the specimens were conditioned using the alternative method mentioned in Asphalt-Institute (2014), which is by placing the specimens in a temperature oven at 60ºC for 2 hours. The alternative method of conditioning the sample was considered due to the delay in water bath equipment's delivery to the facility. The stability testing equipment has a loading rate of 50.8 mm/min. The Marshall stability value explains the maximum load a test specimen can take just before its failure. The flow of the test specimen is similarly used to understand the total vertical deformation when the maximum load is reached.

Figure 14 Image showing Marshall Stability testing equipment.

3.3.6 Indirect Tensile Modulus Test

An advanced equipment, named "AsphaltQube" was used to carry out the Indirect Tensile Modulus (IDT) testing, following AS_2891.13.1 (1995). The test parameters included the test temperature at 25ºC, 10% to 90% rise time at 40 ± 5 ms, pulse repetition period at 3000 ± 5

ms, and five conditioning pulses on the test specimen followed by five testing pulses. The equipment uses two LVDTs to test the horizontal deformation on the test specimen in response to the applied loading.

For IDT testing, 24 test specimens (3 test specimens for each asphalt mixture) were compacted at their respective OBC. The asphalt mixture compacted at their OBC was aimed for $5.0 \pm 0.5\%$ air voids, which is also the required air void content for the IDT testing, as mentioned in the code of practice for the registration of bituminous mix (VicRoads-RC500.01, 2021). The specimens were tested at three different temperatures, which were 21, 25, and 29°C. For conditioning of the samples, the test specimens were kept inside the environmental chamber of the equipment maintained at respective temperatures for a minimum of 4 hours. Immediately after conditioning, IDT test was conducted on the test specimen using AsphaltQube having the environmental chamber set to the respective temperature. Figure 15 demonstrates the IDT testing setup and a mounted test specimen.
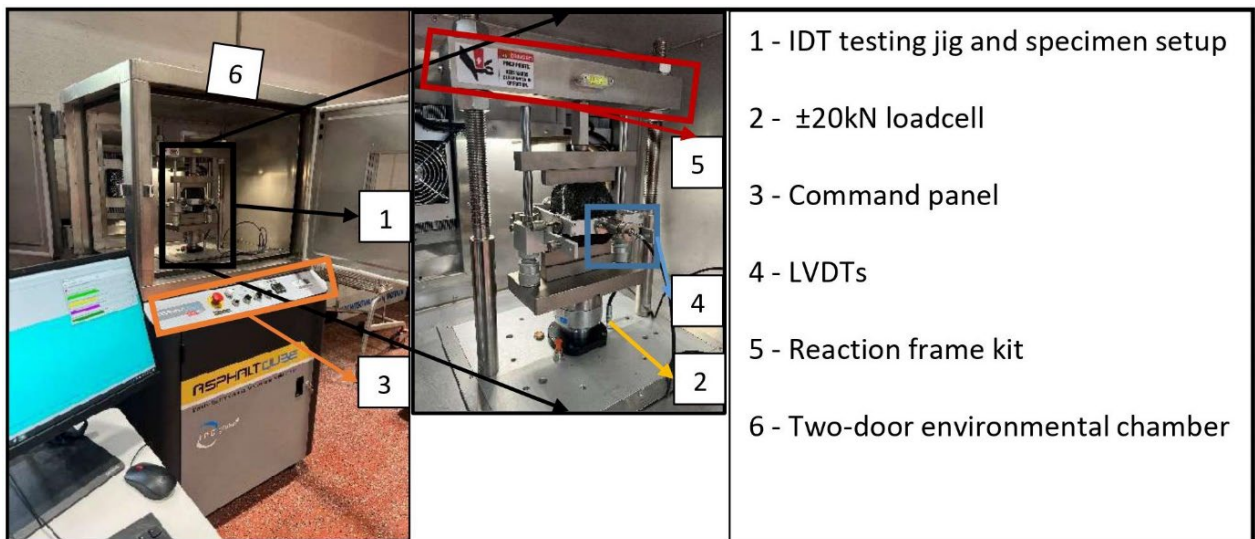
Figure 15 The modular testing machine and the IDT test setup.

The general testing procedure for the evaluation of IDT on each asphalt mixture at their respective OBC was:

1) Preparation of at least three test specimens at OBC,
2) Maximum theoretical density testing,
3) Conditioning of the specimen at specific temperatures,
4) IDT testing, and
5) Bulk density analysis.

3.3.7 Moisture Sensitivity

AGPT_T232-07 (2007) was used to carry out the moisture sensitivity test of each asphalt mixture at their respective OBC. For this, each mixture was compacted at its respective OBC using the Marshall compaction method to achieve an air void of $8 \pm 1\%$. Achieving an air void of $8 \pm 1\%$ for each asphalt mixture involves a hit-and-trial method during the compaction phase. A minimum of three test samples for each mixture were compacted using the Marshall compaction method with 50, 45, and 40 blows on each side. Following the compaction of three test specimens with different number of blows, separate graphs for each asphalt mixture were drawn for the number of blows versus air voids (%) of the test specimen to evaluate the number of blows required to achieve the air void of $8 \pm 1\%$. The maximum theoretical density of each asphalt mix had been calculated during the IDT test phase.

In total, 72 test specimens were compacted using the Marshall compaction method achieving 41 test specimens within the required range of air voids. Approximately 43 blows were required to achieve 7 - 9% air voids for size 10mm asphalt mixes. Similarly, 33 blows were required for size 20mm asphalt mixtures.

The general testing procedure for the evaluation of moisture sensitivity for each asphalt mixture included the following steps:

1) Compacting the test portions of each asphalt mixture at their respective OBC with 50, 45, 40, and 35 blows on each side,

2) Bulk density and air voids calculation on the compacted test specimens,

3) Calculation of the number of blows required to achieve and then prepare $8 \pm 1\%$ air voids for each asphalt mixture,

4) Dry subset specimens were maintained at 25 ± 1ºC for 2 hours $\pm$ 5 minutes prior to being tested.

5) For moisture conditioned subset specimens, partial saturation was reached by vacuuming the specimens at 600 ± 25 mm Hg for 10 minutes in vacuum desiccator consisting of 50 ± 5ºC water,

6) The specimens were made sure to reach partial saturation by checking the degree of saturation which should be between 55 to 80%.

7) The partial saturated specimens were then kept at 60ºC water bath for 24 ± 1 hours, followed by conditioning of the same wet specimens at 25ºC water bath for 2 hours $\pm$ 5 minutes before testing,

8) The rest of the two test specimens were immersed in 25ºC water for 30 minutes before running the ITS test on the specimens,

9) ITS test on specimens were carried out using the IDT jig in Marshall stability equipment where the maximum load applied to break the specimen were noted down,

10) Finally, using Equations 4 and 5, the Tensile Strength Ratio (TSR) was evaluated.

Figure 16 demonstrates the water bath used to condition the test specimens in moisture sensitivity testing. As can be seen, 9 wet subset specimens were able to be conditioned at a time.

Figure 16 Water bath with test specimens inside.

The ITS and TSR of the specimens were calculated using Equations 4 and 5, respectively.

$$ITS = \frac{2 \times P}{\pi \times H \times D} \text{ x } 10^6 \qquad\qquad \text{Equation 4}$$

where,

ITS = Indirect Tensile Strength of a test specimen

P = Maximum applied force indicated by the testing machine, kN

H = Specimen height, mm

D = Specimen diameter, mm

$$TSR = \frac{\text{ITS on conditioned test specimens}}{\text{ITS on unconditioned test specimens}} \text{ x } 100 \qquad\qquad \text{Equation 5}$$

where,

TSR = Tensile Strength Ratio of an asphalt mixture

3.4 Determination of the design modulus

Methodological steps provided in Austroads-Part2 (2017) were followed to convert the experimentally obtained resilient modulus results into the pavement design modulus. The weighted mean annual pavement temperature (WAMPT) was taken from Austroads specified values as per the selected site location, i.e., Werribee, Victoria, Australia, to be 24ºC. The field air void of the mixture was assumed to be 7%, and the traffic speed on the pavement was taken as 60 km/hr. The design modulus was obtained using Equations 6 (corrected based on in-service air voids), 7 (corrected based on field temperature) and 8 (corrected based on selected traffic speed).

1) $\dfrac{\text{Modulus at in-service airvoids}}{\text{Modulus at test airvoids}} = \dfrac{21 - \text{Air void at inservice}}{21 - \text{Air void at lab testing}}$ \qquad Equation 6

2) $\dfrac{\text{Field modulus at WMAPT}}{\text{Laboratory modulus at test temp (T)}} = e^{(-0.08(\text{WMAPT}-\text{T}))}$ \qquad Equation 7

3) $\dfrac{\text{Modulus at speed V}}{\text{Modulus at tested loading rate}} = 0.19\,\text{V}^{0.365}$ \qquad Equation 8

where, V = Traffic speed, WMAPT = in-service temperature, and T = IDT tested temperature at lab.

The design modulus can be used as an input parameter in pavement designing software such as CIRCLY7.0 for thickness design of flexible pavement.

3.5 Flexible Pavement Design

The methodology of the numerical modelling part of this research involved designing four flexible pavements using the experimentally obtained design modulus of asphalt mixtures. The designed flexible pavements were then simulated by modelling into two finite element analysis software: ABAQUS and Strand7. The use of two FEA software's helped increase the certainty of the result obtained by cross-comparison. Furthermore, comparing the ABAQUS and CIRCLY7.0 test results gave an insight on the result difference between outcomes of ABAQUS against a widely used pavement thickness design software, i.e., CIRLCY7.0. Based on the result differences, necessary recommendations have been made in the recommendations section to simulate the pavement for more realistic results in the future.

Designing a flexible pavement in CIRCLY7.0 requires traffic design data and structural layers data as input. The pavement designing procedure in CIRLCY7.0 typically involves the following steps:

1. Determination of input parameters, such as material properties, traffic loadings, and environmental conditions,
2. Selecting a trial pavement,
3. Analysing the pavement under truck axle loads determining allowable traffic,
4. Comparing this with the predicted design traffic over the design period, and
5. Finishing by accepting or rejecting the trial pavement.

The design inputs taken for this research in CIRCLY7.0 included, desired project reliability, subgrade CBR, capping layer CBR, material and performance criteria, and design traffic load as detailed in Tables 15 and 16.

Basically, CIRCLY7.0 takes traffic load distribution data, the design period of the pavement, and pavement structures as input parameters and carries out the analysis where the stress and

strain response at the critical locations of the pavement is calculated. Later, the performance criteria are applied and finally, the software calculates the cumulative damage factor (CDF). The fatigue criteria in CIRLCY7.0 uses Equation 9 for asphalt layer design purpose.

$$N = \frac{SF}{RF} \left(\frac{k}{\varepsilon}\right)^5$$ Equation 9

where,

N = Repetitions to failure,

SF (Shift Factor) = difference between in-service fatigue life and laboratory fatigue life (presumptive value = 6),

RF (Reliability Factor), which depends on the project reliability selected,

K = a parameter that depends on the stiffness, and

ε = unitless horizontal tensile strain at the underside of the layer

For the pavement not to fail during the design life, each layer needs to have a CDF value of less than 1. If CDF = 1, then the pavement is assumed to fail exactly at the targeted design life. If CDF is more than 1, the pavement is expected to fail before it reaches its design life. The total damage calculated by CIRCLY7.0 is the sum of damage calculated from strains caused by the traffic loading. Equation 2 demonstrates the determination of CDF by CIRCLY7.0 for pavement designing purposes.

$$CDF = \frac{n}{N}$$ Equation 10

where,

n is the actual number of repetitions of the load, and

N is the allowable repetitions of the response parameter that would cause failure.

In this research, asphalt mixtures were designed for light to medium level traffic. Therefore, a flexible pavement as a collector road with a 60 km/hr design speed was selected for the pavement design. A design period of 20 years was selected as suggested by VicRoads-RC500.22 (2018) and Austroads-Part2 (2017). The subgrade was assumed to be an expansive clay, where design CBR value of 2 was selected, as suggested in Table 5.4 of Austroads-Part2 (2017). Since the subgrade was assumed to be expansive clay, a capping layer with CBR 10 having a minimum 150mm depth was selected, as suggested by VicRoads-RC500.22 (2018). The project reliability for collector roads was chosen to be 90%, as suggested by Table 8.2 in VicRoads-RC500.22 (2018) and Table 7 in EDCM (2011) guidelines. CIRCLY7.0 has built-in traffic loading database for Australian roads. Upper range collector road's traffic data present in the CIRCLY7.0, was used for design purposes in this research.

The design moduli converted from the IDT test were used as material input parameters in the software for pavement design purposes. The subgrade, capping layer, subbase, and base course layer's thickness were kept constant for four flexible pavement designs to study the change in thickness of the asphalt mixtures based on their resilient modulus properties. Austroads mentions that the asphalt mixtures having less than 40mm thickness are not considered to provide any structural contribution (Austroads-Part2, 2017). Since this research aims to analyse the performance of both 10mm and 20mm asphalt mixtures, the thickness of both wearing and structural course layer were taken more than 40 mm. Table 15 presents the selected parameters that were taken as the traffic input for the upper-range collector roads from the EDCM guide (EDCM, 2011). In this table, AADT is the annual average daily traffic, N_{DT} is the design traffic in cumulative heavy vehicle axle group, HVAG is heavy vehicle axle group DESA is design number of equivalent standard axles of traffic loading and ESA is equivalent standard axles for the traffic load distribution.

Table 15 The traffic data adopted in this research.

Design traffic data	Value	Design Traffic data	Value
ESA/HVAG	0.656	%HV	8%
Project Reliability	90%	%HV's (HVPD)	560
Design speed	60 km/hr	Design period (years)	20
Traffic lanes	2	Growth Rate	2.5%
Direction Factor	0.5	Growth Factor	25.54
Lane Distribution	1	HVAGs per HV	2.35
AADT	7000	ESA per HVAG	0.50
N_{DT} (HVAG's)	6.1E+6	ESA per HV	1.18
DESA (ESA's)	3.1E+6	HVs (HVPD)	280

The proposed composition of structural layers and their properties in the four different flexible

pavement profiles are presented in Table 16.

Table 16 Flexible pavement layers designed using CIRCLY7.0.

NA pavement	RCA75 pavement	RCA65 pavement	RCA55 pavement
10 NA (Mr = 2,401 MPa)	10 RCA75 (Mr = 4,143 MPa)	10 RCA65 (Mr = 4,258 MPa)	10 RCA55 (Mr =5,884 MPa)
20 NA (Mr = 3,954 MPa)	20 RCA75 (Mr = 5,768 MPa)	20 RCA65 (Mr =6,999 MPa)	20 RCA55 (Mr =6,178 MPa)
Base (Mr = 210 MPa)	Base (Mr = 210 MPa)	Base (Mr = 210 MPa)	Base (Mr = 210 MPa)
Subbase (Mr = 150 MPa)	Subbase (Mr = 150 MPa)	Subbase (Mr = 150 MPa)	Subbase (Mr = 150 MPa)
Capping layer (CBR = 10)	Capping layer (CBR = 10)	Capping layer (CBR = 10)	Capping layer (CBR = 10)
Subgrade (CBR = 2)	Subgrade (CBR = 2)	Subgrade (CBR = 2)	Subgrade (CBR = 2)

The designed profiles were used for finite element analysis simulation to analyse the distress experienced by each layer under vehicular wheel loads.

3.6 Finite Element Analysis procedures

In this research the finite element modelling (FEM) software, ABAQUS and Strand7, were used to model and analyse the performance of the designed pavements. The design modulus for asphalt mixtures, resilient modulus for base and subbase layers, porosity and density were the fundamental properties defined for the simulation of the pavement. Since the non-linear properties were not defined in this simulation, the pavement models simulation could be considered as a linear analysis of the pavements.

For the ease of discussion, the pavement models with asphalt layers of 10NA and 20NA will be called "NA pavement". Other pavement models, depending on the proportion of recycled material in the wearing and structural layer, were named "RCA 75 pavement", "RCA 65 pavement", or "RCA 55 pavement".

Figure 17 demonstrates general steps undertaken in the numerical modelling part of this research to provide prediction of pavement's performance under static Single Axel Single Tyre (SAST) loading to draw conclusion and recommendations for future research.

```
┌─────────────────────────────────────────────────────────────────┐
│   Designing of four pavement profiles for a collector road       │
│   using CIRCLY7.0.                                               │
└─────────────────────────────────────────────────────────────────┘
                              ⇓
┌─────────────────────────────────────────────────────────────────┐
│   General analysis and comparison between CIRCLY7.0 and ABAQUS   │
│   for NA pavement under a SAST vehicle.                          │
└─────────────────────────────────────────────────────────────────┘
                              ⇓
┌─────────────────────────────────────────────────────────────────┐
│   Analysis of the pavement models in ABAQUS under static SAST    │
│   loading.                                                       │
└─────────────────────────────────────────────────────────────────┘
                              ⇓
┌─────────────────────────────────────────────────────────────────┐
│   Analysis of all pavement models in Strand7 under a static SAST │
│   loading.                                                       │
└─────────────────────────────────────────────────────────────────┘
                              ⇓
┌─────────────────────────────────────────────────────────────────┐
│   Comparison between Strand7 and ABAQUS results.                 │
└─────────────────────────────────────────────────────────────────┘
                              ⇓
┌─────────────────────────────────────────────────────────────────┐
│   Drawing conclusion on pavement's performance prediction based  │
│   on the result obtained.                                       │
└─────────────────────────────────────────────────────────────────┘
                              ⇓
┌─────────────────────────────────────────────────────────────────┐
│   Future recommendations on improving the FEA modelling.         │
└─────────────────────────────────────────────────────────────────┘
```

Figure 17 General steps undertaken for the FEM modelling part of this research.

3.6.1. Numerical Modelling using ABAQUS

The procedure adopted for modelling and simulating the pavement system and boundary conditions is shown in the flowchart of Figure 18. The preparation of a flexible pavement model in ABAQUS included modelling each pavement layer as a "part module" of required dimension (length, width and depth), specifying the material properties of the layers, assembling the drawn parts of a pavement and arranging according to the designed pavement profile, defining fully fixed interaction between each layers, defining boundary conditions to the model, partitioning the parts according to the load to be applied on the model, applying the static tyre

loading pressure at the top layer of the model, meshing model into finer elements for precise result, and finally submitting the model for analysis. Figure 18 shows the general steps carried out in the finite element part of this research in drawing and analysing all the pavement models.
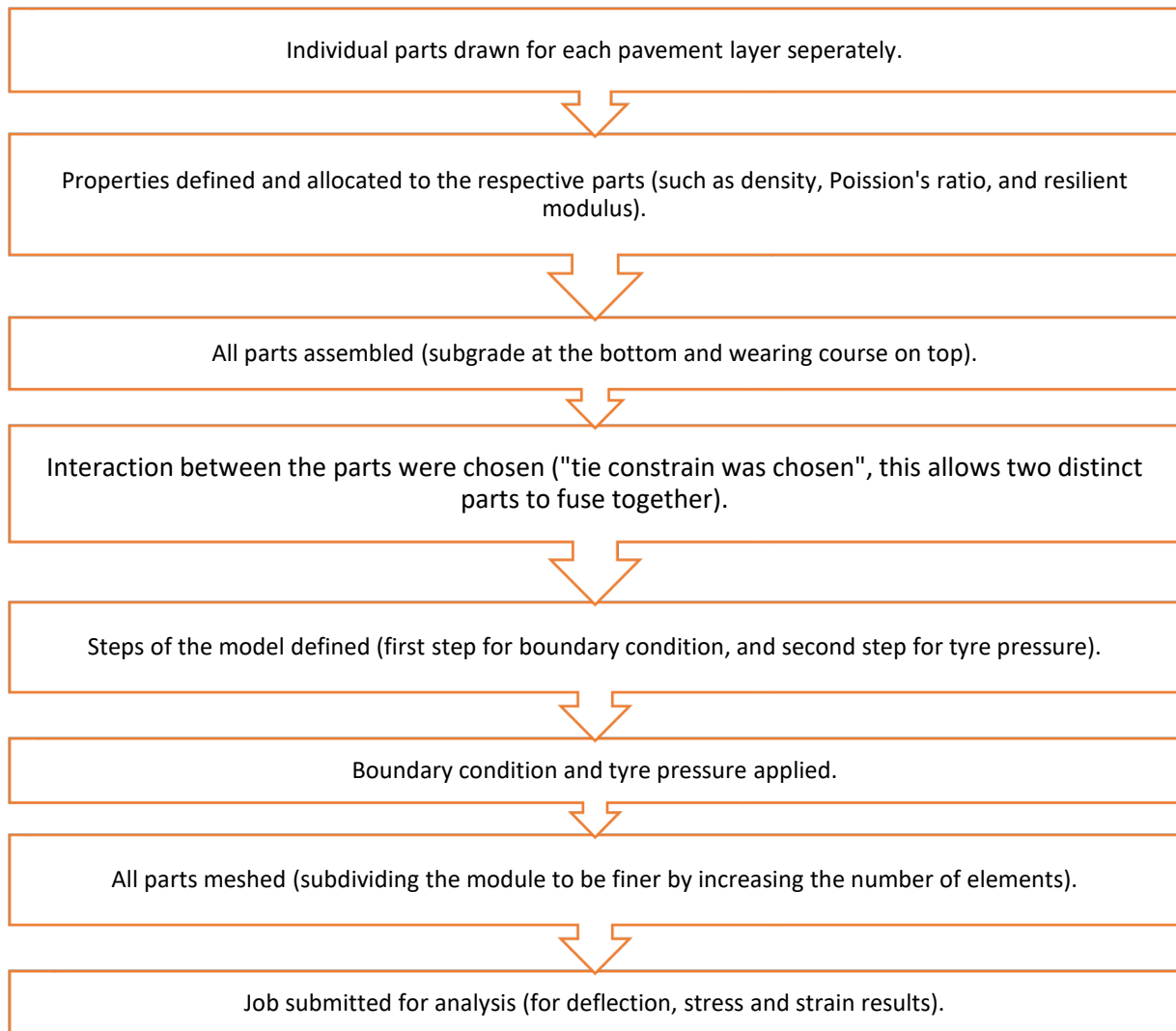
Figure 18 General steps preparing the pavement model for analysis in ABAQUS.

There were two types of loads that could be considered for a FEA: Single Axle Single Tyre (SAST) having 53 kN load (26.5kN load on each tyre) and Single Axle Double Tyre (SADT) having 80kN load (20kN load on each tyre) (Austroads-Part2, 2017). Both loads were applied in the NA pavement model to compare the deflection and stress-strain data. Comparatively,

SAST caused the pavement model to have increased deflection with increased tensile stress than when compared to SADT. Therefore, in this research, the worst-case scenario of loading, being SAST, was selected for the modelling and analysis purpose. Since all the pavement layers were assigned with linear elastic material properties, applying a single dynamic load was sufficient for the comparison of responses in the four pavement models. The Austroads-Part2 (2017) was followed, according to which the uniform pressure of 0.8MPa was distributed on a circular area of radius 102.4mm to define a SAST loading. The dynamic loading was applied at 60km/hr. Additionally, fixed restraints was applied at the bottom of the pavement model and symmetrical restraints on each of the vertical sides.

The standard lane width in Australia is 3.5 meters. In this simulation, a pavement was modelled to get the distresses below one vehicle tyre, as the distresses result below the other tyres would be identical. Therefore, only one tyre was used to model the pavement as it saved the time required for analysis. The flexible pavement of dimension 3000 x 3000 (mm) was drawn in the FEA software with its respective obtained thickness from CIRCLY7.0.

Meshing is an important step in the finite element analysis. A mesh validation was performed which enabled the identification of the mesh convergence for this particular finite element model. Whereby, the vertical displacement result was analysed to check the result differences with the increase in the mesh of the pavement model. For this, all four pavement models contained 165,902 nodes, and 130,592 linear hexahedral elements of type C3D8R. C3D8R is a linear brick element consisting of 8 nodes (ABAQUS, 2009). The increment in pavement model's mesh from 165,902 nodes to around 241,481 nodes resulted in less than 2% difference in maximum vertical displacement result. Furthermore, the analysis of the pavement model consisting of 165,902 nodes consumed half the amount of time compared to pavement model consisting of 241,481 nodes for job analysis. Therefore, meshing equivalent to 165,902 nodes

was done for all pavement models in ABAQUS, and the results were then exported into an excel sheet.

Finally, after the simulation of the SAST on the four pavement models, the vertical stress, vertical strain, horizontal strain, and vertical deflection data were recorded under the tyre pressure along the paths shown in Figures 19 and 20.
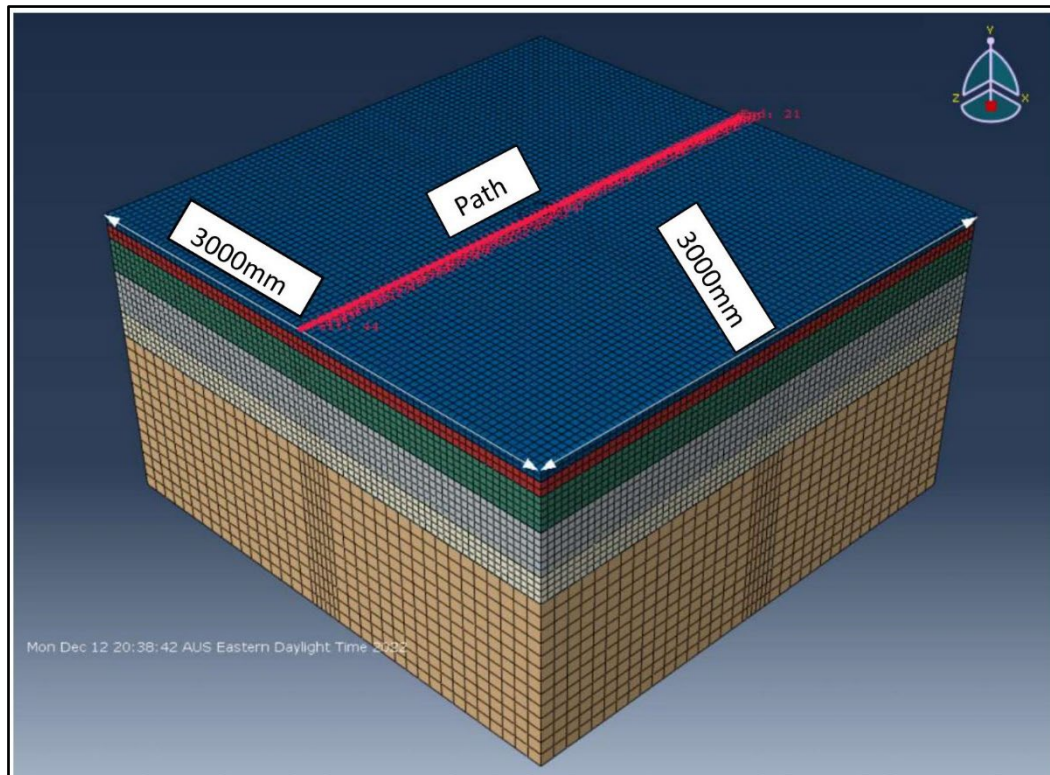
Figure 19 Finite element model showing the horizontal path along the pavement for the surface deflection analysis.

Figure 19 demonstrates the path along the pavement surface. This included all nodes selected to analyse the surface deflection due to SAST wheel loading in the four flexible pavements. The circular tyre pressure is applied at the midpoint of the top layer of the model.
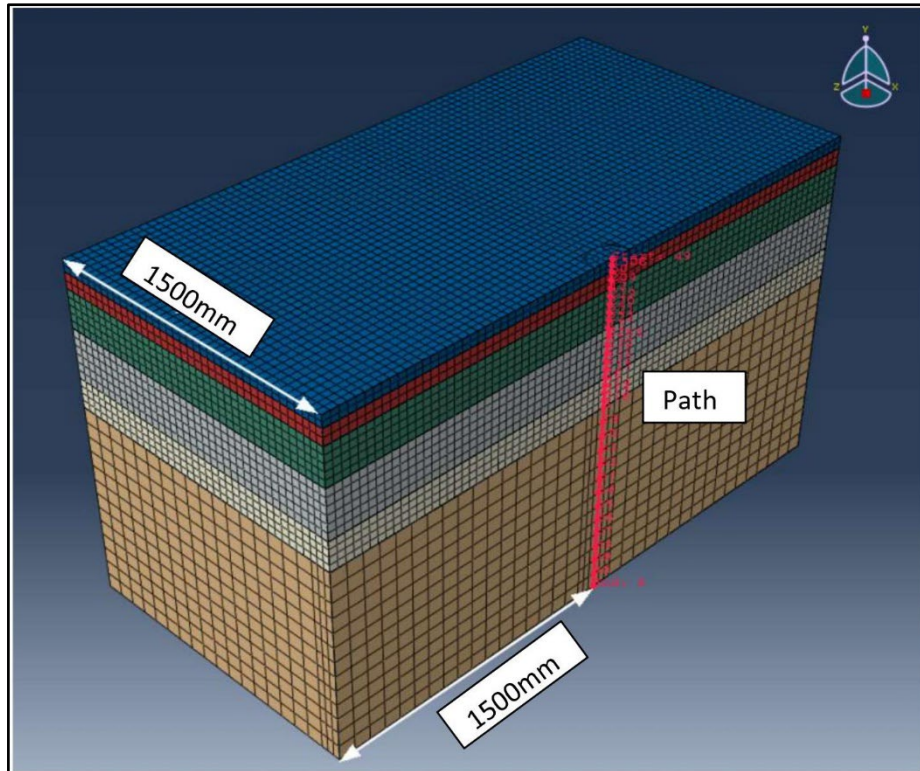
Figure 20 Image demonstrating the vertical path along the depth of the pavement for the stress and strain test results.

Figure 20 demonstrates the path along the depth of the pavement that was selected to analyse the displacements, vertical and horizontal stresses, and strain in the four flexible pavements.

3.6.2. Numerical Modelling using Strand7

The steps in drawing a pavement model in Strand7 was similar to ABAQUS, as indicated in Figure 17. The difference in the procedure in Strand7 than ABAQUS, was the method used to draw parts and meshing the pavement model. In Strand7, nodes were created at first using the "Create Node" function, then using the created nodes and the "Create Element" function, and the brick elements were created since, for the 3D model, the "Brick" element was recommended in Strand7 (Strand7, 2010). Additionally, while meshing the model, all the elements were subdivided onto "Hexa20" brick, which is a brick element with 20 nodes.

Since unlike Abaqus, modelling a circular load wasn't possible in Strand7, a 182 x 182 mm rectangular area was drawn for the tyre load to be applied on it to provide a loading area close to that of the circular area modelled in ABAQUS. The total area of the circular area having 102.4mm radius is 32,956mm^2, while the total area in the selected square is 33,124mm^2, which is very close to that of the circular area (0.5% difference).

Figure 21 demonstrates the NA pavement model in Strand7, consisting of tyre pressure, boundary conditions, layers, square area for tyre pressure, and meshing undertaken on the entire model.
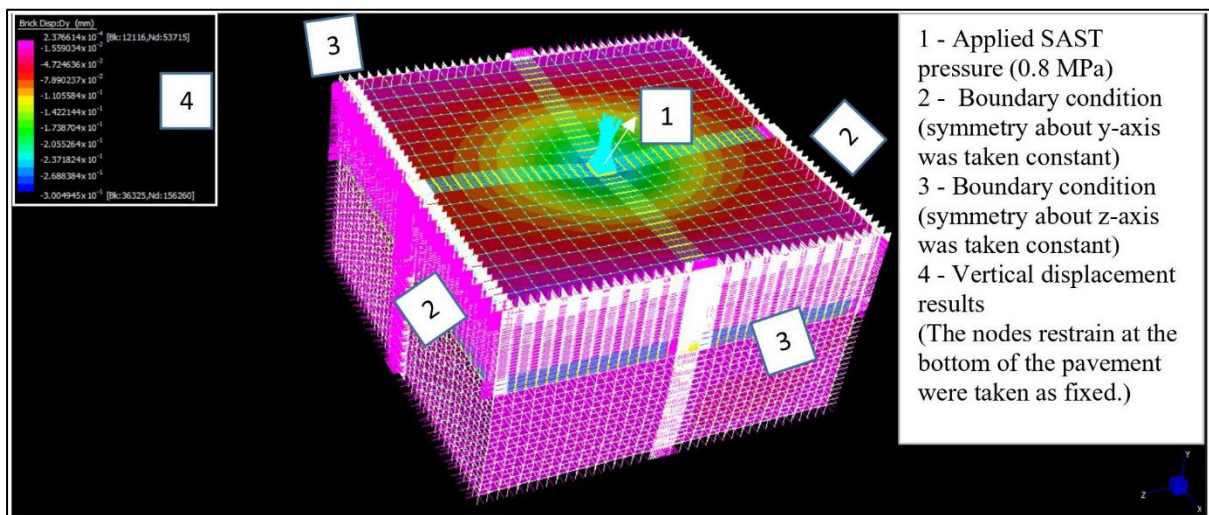
Figure 21 The NA pavement model in Strand7.

3.7 Occupational Health and Safety Risks

The geotechnical and pavement laboratory experiments involve several risk factors depending on the test being undertaken. OHS risk analysis and mitigation strategies help prevent any possible injuries or waste of materials. It increases the efficiency and productivity of the work being done. OHS risk management strategy increases productivity, reducing risk in the project; this supports research integrity in terms of the efficiency of the research project. Thus,

analysing the OHS risk before starting the task is a good research practice mentioned in Table 17 for this experimental research phase.

Table 17 OHS risk and management strategy.

Test	Testing equipment's	Risk/Hazard	Risk management strategy
Moisture content analysis	Oven, metal tray, aggregate samples, and a digital scale	• Possible inhaling of dust while working with aggregates • Possibility of getting electric shock or burning hand while using the oven	• Using a protective dusk mask while handling the recycled materials • Using gloves while working with a temperature oven
Aggregate sample preparation	Recycled material sample, oven, bucket, metal spoon	• Possible inhaling of dust • The dust can reach the eye and can cause an eye infection	• Mask and goggles should be worn while handling recycled materials aggregates.
Marshall compaction and stability testing	Marshall moulds, lubricants, compaction equipment, stability testing machine	• Injury because of the hot and heavy Marshall • Irritation of skin using lubricants • The ear can be damaged because of Marshall compaction noise • The oven heat can burn hand • Risk of getting an electric shock while handling electrical products.	• Safety boots should be working all the time to prevent injury from mould, base, and collar fall • Earmuffs should be used to prevent noise pollution • Gloves should be used while working with a temperature oven
Particle size distribution (PSD) and flakiness index	Sieves, scale, sieve shaker, containers and water spraying bottle	• Dust can reach eyes and cause an eye infection • Possible inhaling of dust	• Googles and gloves should be worn all the time to prevent any possible infection • Care must be taken while using a sieve shaker.

(There were no ethical approval required for this research)

66

4 Experimental results and discussions

4.1 Particle size distribution of raw aggregates

Figure 22 shows the particle size distribution (PSD) of the aggregates used in this research and Table 18 shows the maximum particle size (D_{max}) for each aggregate. Figure 22 also shows the presence of RCA finer than 0.075 mm due to the presence of non-hydrated cement, which can be considered as the filler in the recycled materials HMA mixtures. As can be noticed from Figure 22, the 20mm, 14mm, 10mm, and 7mm materials are one-sized aggregates, whereas RCA and RAP are graded aggregates.
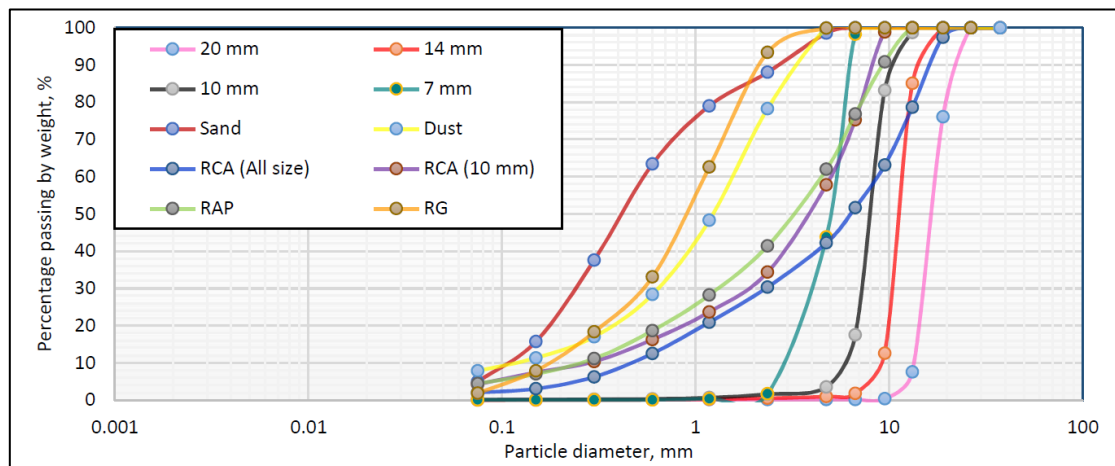
Figure 22 PSD result of the aggregates.

Table 18 Maximum particle size of the aggregates.

Aggregate	D_{max} (mm)	Aggregate	D_{max} (mm)
NA (20mm)	20	Dust	4.75
NA (14mm)	14	RCA (All size)	20
NA (10mm)	10	RCA (10mm)	9.5
NA (7mm)	7	RAP	9.5
Sand	4.75	RG	4.75

4.2 Water absorption, particle density, and flakiness index

Figure 23 demonstrates the apparent particle density and water absorption test results of all the aggregates, following AS_1141.5 (2000) and AS_1141.6.1 (2000) for fine and coarse particles respectively. Water absorption of RCA is higher than the rest of the aggregates indicating a greater potential for binder absorption. In contrast, RG and RAP generally show lower water absorption compared to natural aggregates. Figure 23 also shows that the particle densities of recycled material aggregates are generally lower than natural aggregates. A combination of RCA (material with higher absorption properties) with RAP, and RG (materials with lower absorption properties) was expected to consume a bitumen content not significantly higher than natural aggregates. The higher particle density for natural aggregates represents a higher amount of mass requirement to achieve a particular volume than the recycled material aggregate.

	20mm NA	14mm NA	10mm NA	7mm NA	Sand	Dust	RG	RCA	RAP
Water absorption (%)	2.31	2.81	3.77	3.25	0.57	1.23	2.27	7.68	2.65
Apparent particle density (g/cm3)	2.71	2.72	2.99	2.93	2.61	2.72	2.67	2.72	2.63
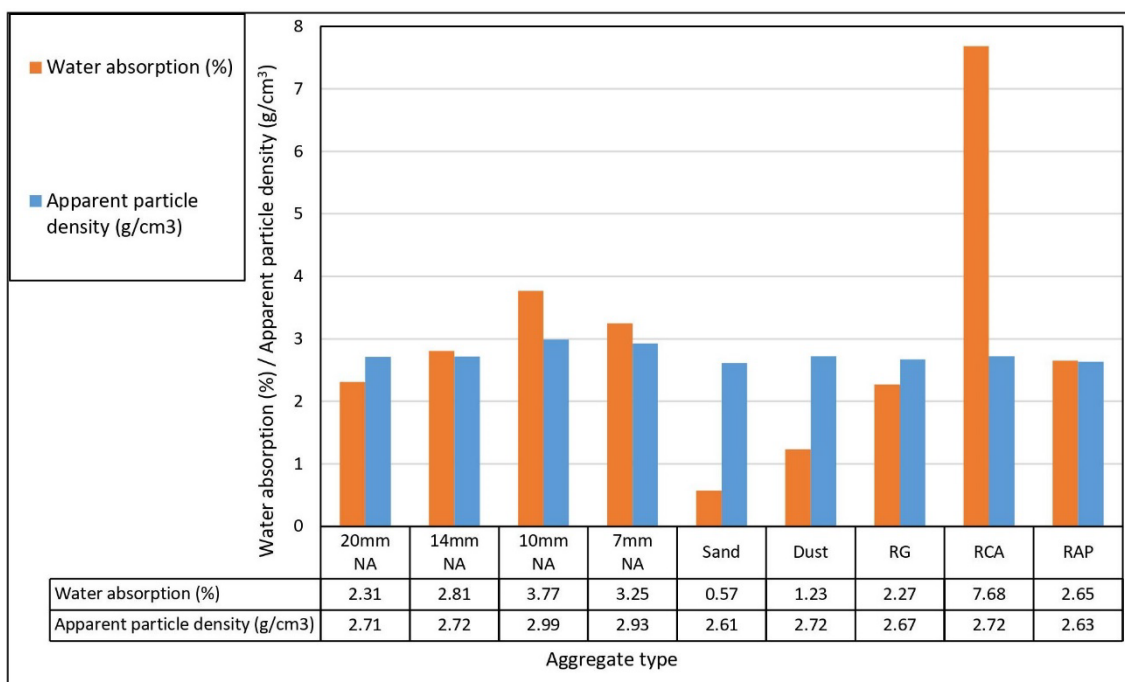
Figure 23. Apparent particle density and water absorption test result.

Figure 24 demonstrates the flakiness index test results for aggregates with 80% particle size larger than 4.75mm according to AS_1141.15 (1999). The result indicated that highest percentage of flaky particles belonged to the RCA. However, RCA particles that passed through a 9.8mm sieve had low flaky particles. The flakiness index result shows that the natural aggregates are of higher quality than the recycled material aggregates. However, the flakiness index of all aggregates was below 35%, which is the maximum limit stated by VicRoads standard document for Hot Mix Asphalt (VicRoads-Section407, 2014).
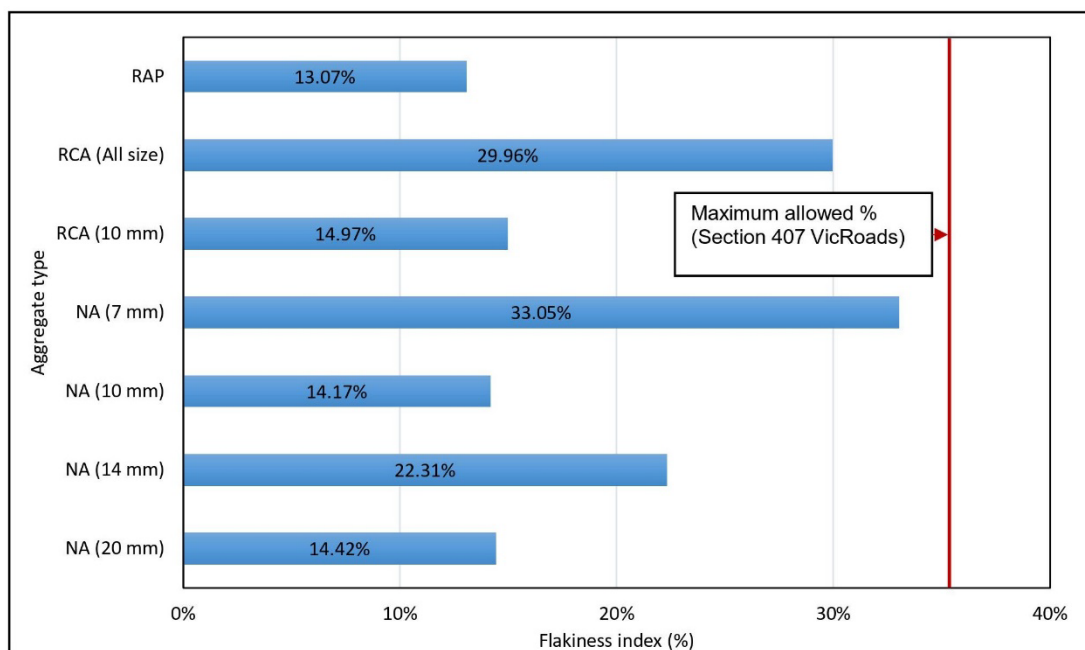
Figure 24. Flakiness index of the aggregates.

4.3 Gradation of 10mm and 20mm mixtures

The upper and lower limits were taken from the "VicRoads – Registration of Bituminous mix" technical note (VicRoads, 2021). As can be seen in Figure 25, the gradation of NA in both 10 and 20mm asphalt mixtures, was above the midpoint of upper and lower limits, indicating both the 10NA and 20NA to have finer gradation. The recycled material mixtures gradation for size 10mm were closer to the lower limit, indicating a coarser blend. However, the 20mm recycled

material mixtures had a gradation finer. In general, the gradation of all aggregate mixtures were within the tolerance limit for upper and lower limits, as specified in VicRoads-RC500.01 (2021).
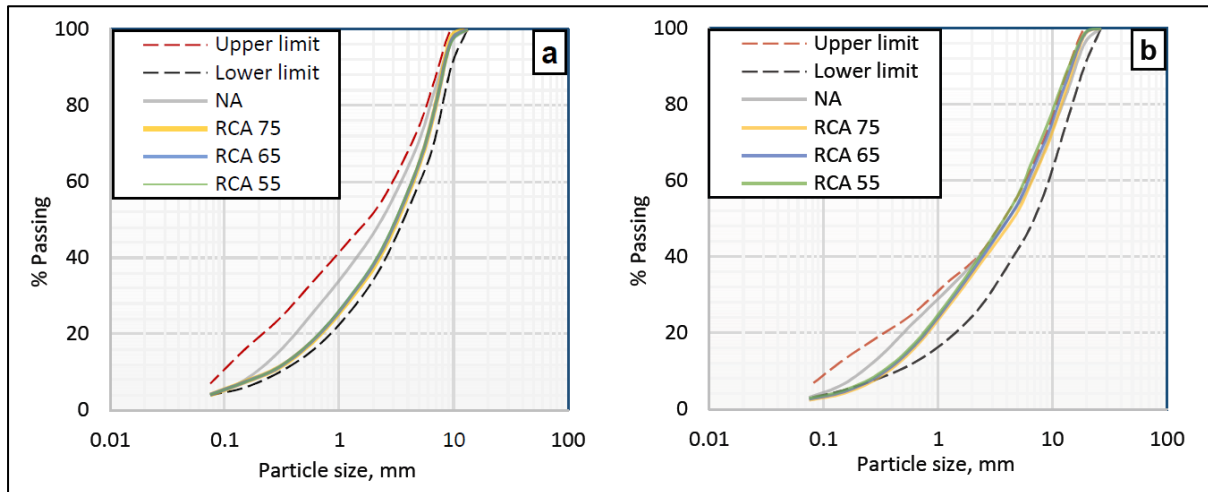
Figure 25 Aggregate gradations of a) 10mm, and b) 20mm mixtures.

4.4 Determination of the optimum binder content

The OBC of the mixtures was determined using the Marshall mix design method. According to VicRoads-RC500.01 (2021), the asphalt mix designed for light to medium traffic roads, i.e., type N for the wearing course and type SI for the structural course, must have 4.9 to 5.3% air voids. Thus, the bitumen content corresponding to air void of 5.0% was selected as the OBC of the mixture and other properties such as the voids in mineral aggregate (VMA), stability, flow, and voids filled with the bitumen (VFB) were checked against the recommended limits stipulated in VicRoads-RC500.01 (2021) and Asphalt-Institute (2014). For this, the above-mentioned properties were plotted against the bitumen content. An example of the Marshall charts obtained from the test results for the 10NA mixture is demonstrated in Figure 26. The Marshall charts for all other asphalt mixtures are presented in the appendix section of this thesis.
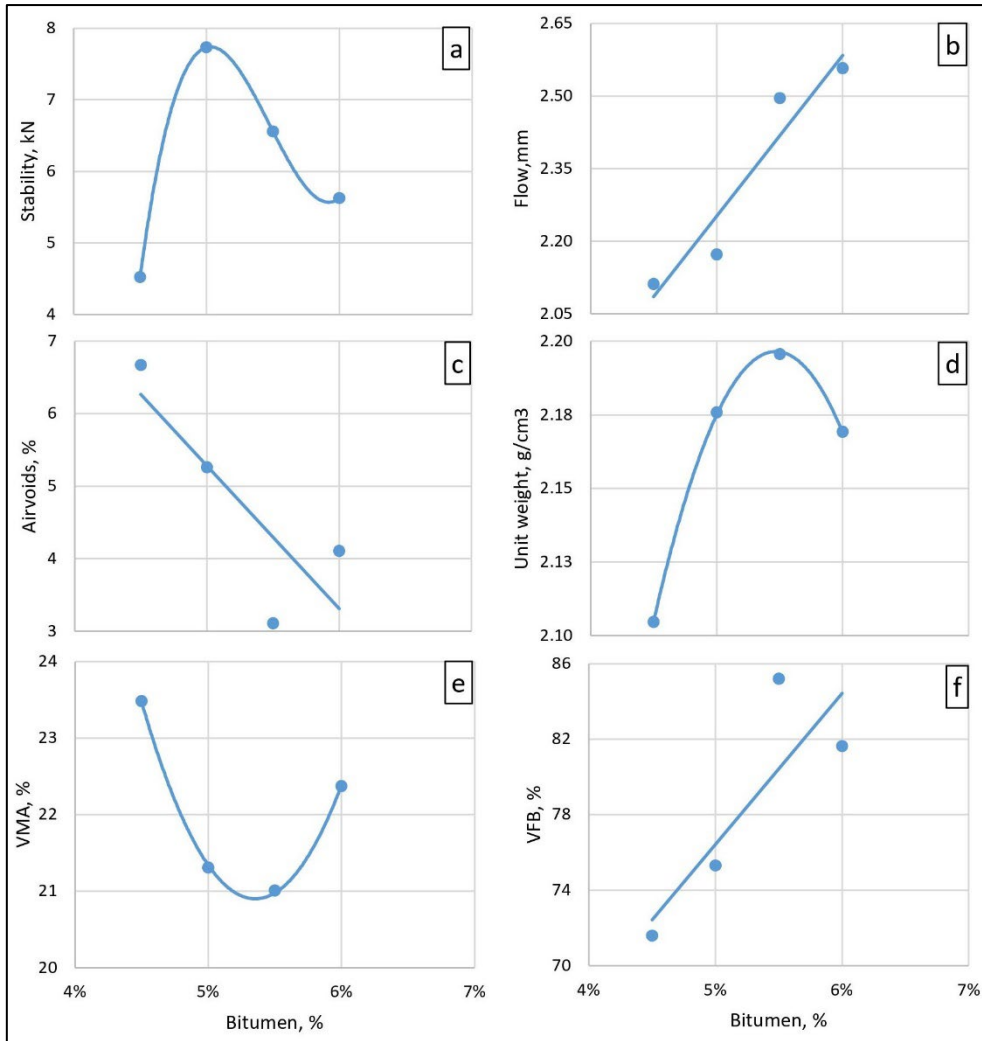
Figure 26 Example Marshall charts of 10NA mixture showing Bitumen content (%) vs a) Stability (kN), b) Flow (mm), c) Air voids (%), d) Unit weight (g/cm3), e) VMA (%), and f) VFB (%).

The voids in the mineral aggregate (VMA), voids filled with bitumen (VFB), Marshall stability, flow value, and unit weight at the respective OBC for all the eight asphalt mixtures were calculated and are demonstrated in Figures 27 (size 10mm) and 28 (size 20mm). Where available, these plots mention the maximum and minimum required values recommended by the VicRoads-RC500.01 (2021). Figures 27 and 28 reveal that NA asphalt mixtures have the least OBC followed by RCA 55, RCA 65, and RCA 75 in both 10mm and 20mm mixtures.
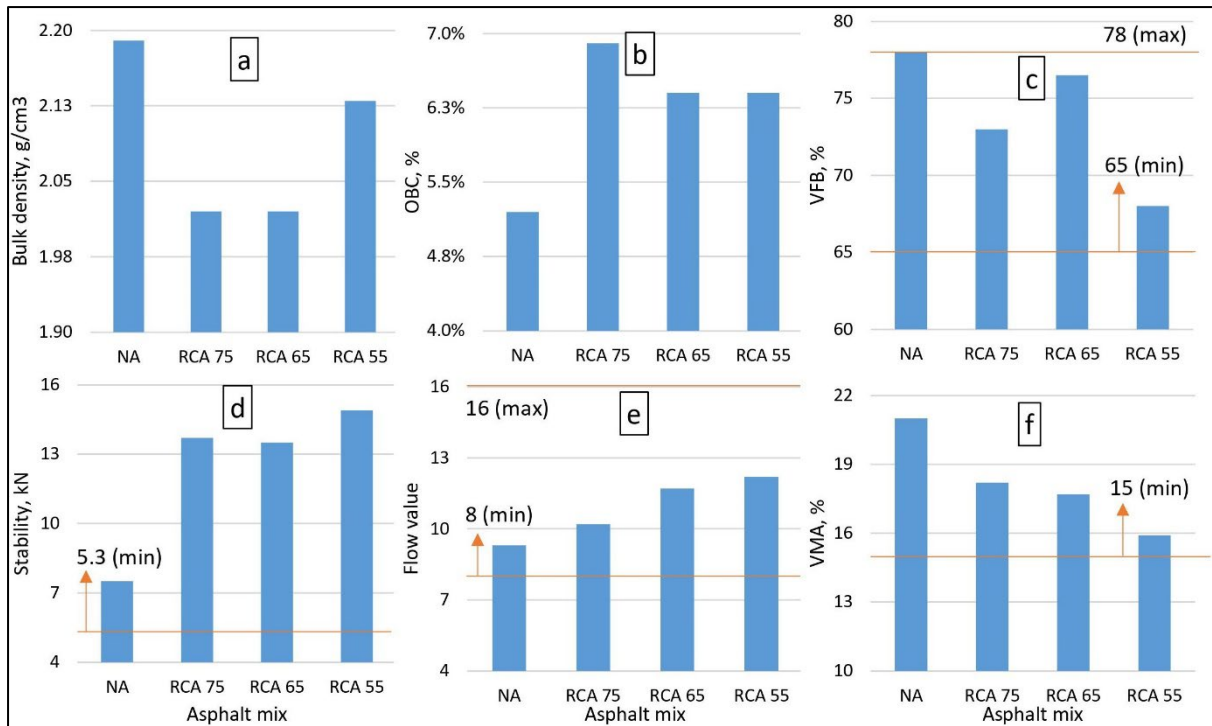
Figure 27 Comparison of a) Bulk density, g/cm^3 b) OBC, % c) VFB, % d) Stability, kN e) Flow value, and f) VMA, % of the 10mm mixtures.
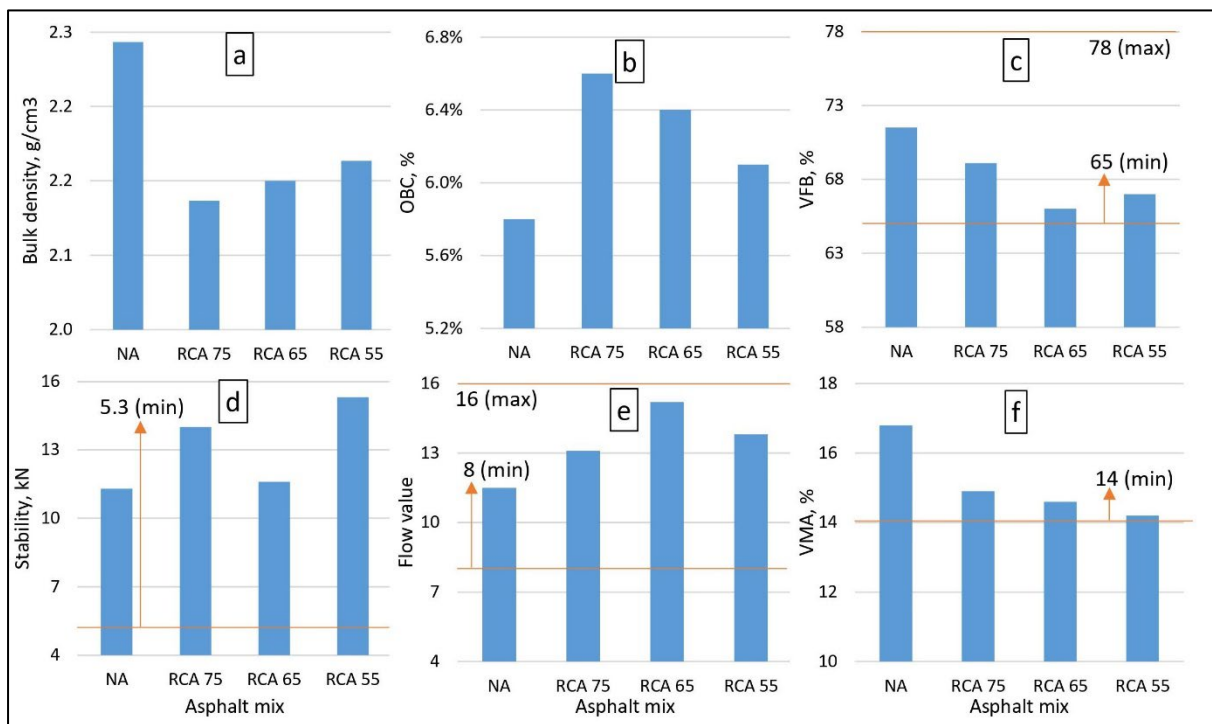
Figure 28 Comparison of a) Bulk density, g/cm^3 b) OBC, % c) VFB, % d) Stability, kN e) Flow value, and f) VMA, % of the 20mm mixtures.

VMA refers to the void space between the aggregate particles in a compacted specimen. Bruce A. Chadbourn (1999) during his research, proved that an increase in finer particles decreases the VMA in the asphalt mixture. The VMA results observed in this research reveals the reduction of VMA with the simultaneous addition of RAP and reduction of RCA. This indicates that the asphalt mixture is getting finer with simultaneous reduction of RCA and addition of RAP in both 10 and 20mm asphalt mixtures. Following the observed trends in Part f of Figures 27 and 28, it could be predicted that simultaneous reduction of RCA and addition of RAP beyond 55% and 35% would eventually reach a point where the VMA requirements would not be met. Eventually, it could be estimated that simultaneous reduction of RCA and addition of RAP in the mixture below 20RCA 50 will not satisfy the VMA and asphalt mixtures gradation criteria.

The only variable differentiating the 10mm and 20mm recycled material mixtures is the particle size of RCA. The water absorption test result indicates that the absorbing capacity of coarse RCA (>4.75mm) was lower than fine RCA (<4.75 mm). Additionally, the bitumen required to coat around the coarser particles is less than finer particles due to the lower specific surface area of the coarser aggregates. Visual inspection of the aggregates showed that the 10mm RCA had more round-shaped particles than the 20mm RCA with angular particles. Furthermore, the flakiness index test result shows that the flakiness index of the 10mm and 20mm RCA are 15% and 30%, respectively. Flaky particles in an asphalt mixture could result in a more compacted mixture, possibly due to breakage under compaction. These particles, however, have lower stiffness which can compromise the mechanical strength of the mixture. The aggregate shape, water absorption, and flakiness index difference between two different recycled material mixtures resulted in lower OBCs for the 20mm recycled material mixture than those of 10mm mixtures, while the stability test result remains quite similar.

The stability of an asphalt mixture is directly proportional to the friction between particles and cohesion. The inter-particle friction depends on the surface roughness, inter-granular contact pressure, binder content, aggregate gradation, and angularity. The cohesion depends on the aggregate gradation and aggregate density (Austroads-Part2, 2017). Figures 27 and 28 also show that the Marshall stability of recycled aggregate mixtures' is greater than that of NA mixtures. The higher stability value indicates that a mixture has a higher resistance to distortion, displacement, rutting, and shearing stresses. It is generally expected to achieve a higher stability in a coarser mixture. However, Figures 27 and 28 show no significant difference in stability test results between 10 and 20mm recycled material mixture. This could be attributed to the higher flakiness index of 20mm mixtures compared to the 10mm mixtures.

The flow value of a test specimen is the indication of the maximum vertical displacement reached during the loading up to the maximum load. The flow value is recommended to be between 8 and 16 (Asphalt-Institute, 2014). All asphalt mixtures had flow values within the limit specified. In the 10mm mixtures, the flow value was the lowest for NA, followed by RCA 75, RCA 65, and RCA 55. In the 20mm mixtures, again, the flow value was the lowest for NA, followed by RCA 75, RCA 55, and RCA 65. ASTM_D6927-15 (2015) mentions that when the flow value is above the upper limit (Flow value of 16, for 10 and 20mm mixtures), the mix is considered too plastic or unstable, and when the flow value is lower than the lower limit (Flow value of 8, for 10 and 20mm mixtures), it is considered too brittle. Hence, based on the flow value results, recycled material mixes are expected to be less brittle and more plastic than NA mixtures.

VFB represents the percentage of the voids filled with an effective bitumen in an asphalt mixture. It has a limit range between 65 to 78% for 10 and 20mm asphalt mixtures, respectively (Asphalt-Institute, 2014). AGPT04B-14 (2014) mentions that at lower VFB value, around 60%, the mixture becomes "dry", lack cohesion, exhibit lower durability, and fatigue

resistance, while, at higher VFB, around 85% or more, the mixture can become unstable and susceptible to rutting. Figures 27 and 28 show that for both sizes of asphalt mixtures, the NA asphalt mixtures had a higher VFB than the recycled material asphalt mixtures. Similarly, 20RCA 65 had the lowest VFB followed by 20RCA 55, 10RCA 55, 20RCA 75, 20NA, 10RCA 75, 10RCA 65, and 10NA. 10NA had a VFB of 78%. Therefore, based on the VFB test result, the recycled material mixtures are predicted to be less susceptible to rutting.

The bulk density of NA mixtures was higher than recycled material mixtures. Within the simultaneous fall in RCA content and rise of RAP in the asphalt mixture, the bulk density of the asphalt mixture at their respective OBC is observed to be increasing.

4.5 Indirect Tensile Modulus test

The Indirect Tensile Modulus (IDT) test was performed at temperatures of 21, 25, and 29ºC to observe the rate of stiffness change of all asphalt mixtures with variations in the temperature. The same test specimens for each asphalt mixture were used for non-destructive IDT test first at 25°C, then 21°C, and finally 29°C. Figure 29 illustrates the resilient moduli of the mixtures at these temperatures. While the resilient modulus generally decreases with the increase in the temperature, the trends demonstrated in Figure 29 reveal a more significant decrease in resilient modulus from 25 to 29ºC than from 21 to 25ºC.
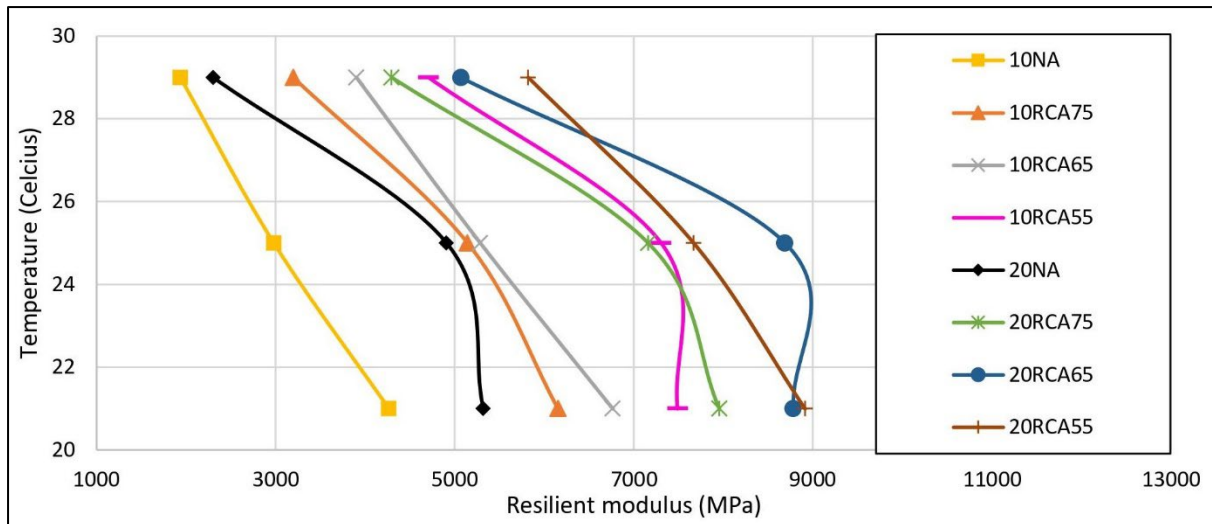
Figure 29 The IDT test results of all eight mixtures at their respective OBC.

Results presented in Table 19 reveal that the recycled aggregate mixtures are generally stiffer than the conventional HMA mixtures. The stiffness of the 10mm HMA increases with the simultaneous reduction of RCA and increase in RAP in the mixture. This pattern in the stiffness change might be because of the gradation, which gets finer with the reduction of RCA in the mixture. However, the 20mm HMA's resilient modulus increased and then decreased with the regular reduction of RCA.

Table 19 IDT test result of the asphalt mixtures at 25ºC (MPa).

Asphalt mix	Size 10mm	Size 20mm
NA	2,979	4,907
RCA 75	5,142	7,159
RCA 65	5,284	8,686
RCA 55	7,303	7,667

4.6 Moisture sensitivity

The moisture sensitivity test was carried out on all the 10 and 20mm mixtures. Table 20 demonstrates the Tensile Strength Ratio (TSR) of the mixtures compacted using the Marshall compaction method.

Table 20 Tensile Strength Ratio of the mixtures.

TSR	Size 10mm	Size 20mm
NA	78.3%	67.8%
RCA 75	82.4%	92.8%
RCA 65	75.0%	88.9%
RCA 55	84.4%	82.0%
Minimum specified TSR (VicRoads-RC500.01, 2021)	80.0%	80.0%

Asphalt-Institute (2014) mentions that some agencies accept a TSR value of 70% or greater based on their experience. All asphalt mixtures, except for 10NA, 20NA, and 10RCA 65, were within the TSR limit specified in VicRoads's code of practice, "Registration of Bituminous Mix Designs", as can be seen in Table 19.

Figure 30 demonstrates that all asphalt mixtures, except for 10NA and 10RCA 75, satisfy the minimum wet tensile strength criteria specified in VicRoads standards (VicRoads-RC500.22, 2018).
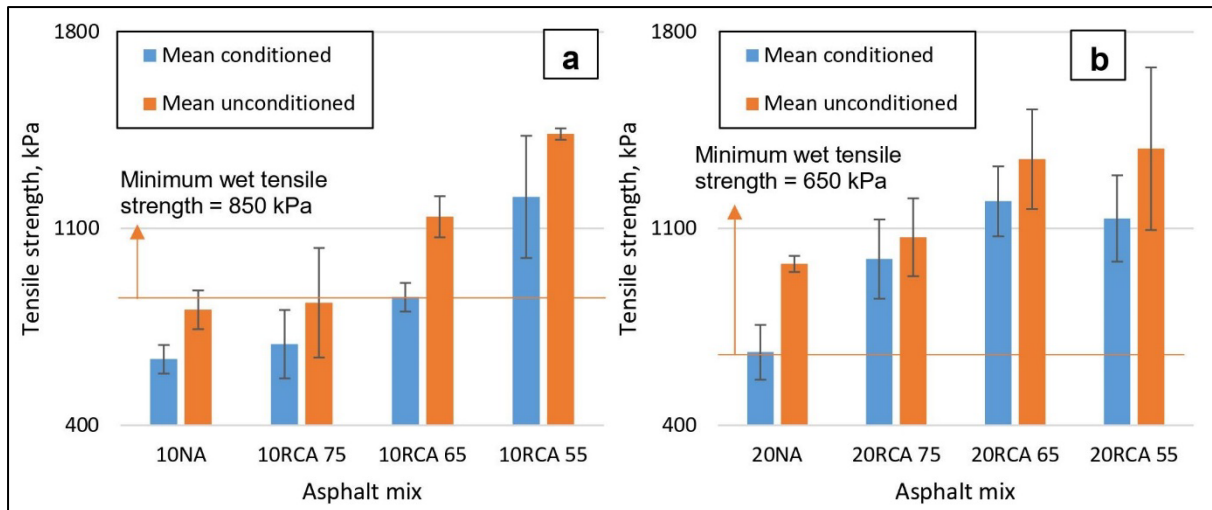
Figure 30 Dry and wet tensile strength of a) 10mm, and b) 20mm asphalt mixtures.

Based on the results presented in Figure 30, with the decrease in RCA content in the mixture, the minimum wet tensile strength is observed to be increasing. However, the minimum wet tensile strength of 20RCA 65 was slightly higher than 20RCA 55.

Comparing the recycled and natural aggregate asphalt mixtures in terms of the tensile strength ratio, 10RCA 75 and 10RCA 55 exhibited better results than 10NA. While amongst all the 20mm asphalt mixtures, all recycled material asphalt mixtures exhibited higher TSR than the 20mm NA specimens. In terms of minimum wet tensile strength, all recycled material mixtures showed greater wet tensile strength values than natural aggregate specimens.

5 Numerical Modelling

5.1 Translation of the IDT results into design input

Austroads Guide to Pavement Technology Part 2 procedures were used to convert the IDT test result into the design modulus of all the mixtures. The site location for converting the lab tested resilient to design modulus was selected to be Werribee in Melbourne, with a traffic speed of 60 km/hr. The design moduli presented in Table 21 were used to design the pavement thickness and run a numerical model simulation to analyse the response of the flexible pavements.

Table 21 Determined design modulus based on Melbourne's climate and traffic speed of 60 km/hr.

Mixture	IDT (MPa) at 25ºC	Design modulus (MPa)
10NA	2,979	2,401
10RCA 75	5,142	4,143
10RCA 65	5,284	4,258
10RCA 55	7,303	5,884
20NA	4,907	3,954
20RCA 75	7,159	5,768
20RCA 65	8,686	6,999
20RCA 55	7,667	6,178

5.2 Pavement Design using CIRCLY7.0

The IDT results converted into the design modulus values were used in the CIRCLY7.0 software for the pavement thickness design. Figure 31 demonstrates the thickness of the pavement layers for four scenarios, in which the subgrade, capping layer, subbase, base, and wearing course layers are kept the same, and only the structural course is different. The

thickness of the designed flexible pavement is the highest for the conventional asphalt (NA), followed by RCA75 and RCA65, and finally RCA55 pavement, for the same ground condition and same design traffic. The designed thickness for surface course was rounded up to nearest 5mm. The total pavement layer thickness designed using CIRCLY7.0 for NA, RCA75, RCA65, and RCA55 pavement was 600, 585, 585, and 580 mm, respectively. The IDT test results showed that the reduction in RCA content generally increases the stiffness of the mixture. Therefore, the thickness of the pavement was reduced with the decrease in the RCA content.
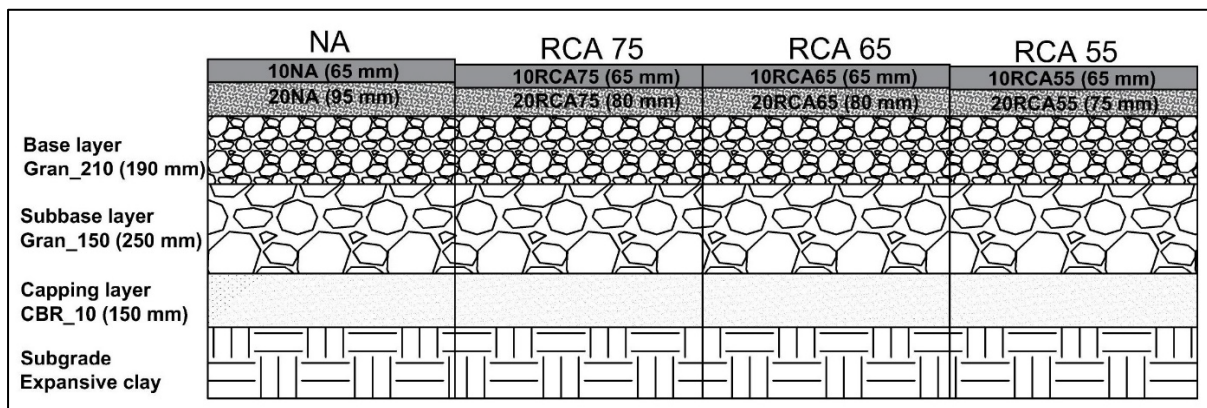
Figure 31 Designed flexible pavements for the same ground and traffic conditions, using different asphalt mixtures in the structural and wearing course.

Table 22 demonstrates the CDF value calculated by CIRCLY7.0 for the respective layers. CIRCLY7.0 doesn't provide CDF result when a layer has only compressive strains, therefore RCA65 pavement's wearing course layer is missing CDF value in Table 22. As can be seen, the CDF value is close to 1 for HMA–20mm, where, the highest CDF can be seen for RCA75, followed by NA, RCA55, and RCA65 pavement. According to CDF result, the fatigue performance of RCA65 pavement looks better than RCA55 pavement. Similarly, looking at the CDF on capping layer and subgrade, rutting failure in subgrade can be expected to be high for NA pavement, followed by RCA75, RCA65 and RCA55 pavement. It should be noted that

the differences in the CDF values is partially due to the rounding of software outputs for practical reasons.

Table 22 Values of CDF calculated by CIRCLY7.0.

Pavement model	NA	RCA75	RCA65	RCA55
HMA layer – 10mm	3.86E-11	5.90E-09		2.80E-06
HMA layer – 20mm	9.75E-01	9.94E-01	8.50E-01	8.89E-01
Base layer	-	-	-	-
Subbase layer	-	-	-	-
Capping layer	8.62E-05	6.56E-05	5.39E-05	5.24E-05
Subgrade	8.41E-03	6.93E-03	6.04E-03	5.72E-03

5.3 Comparison of stress-strain behaviour in CIRCLY7.0 vs ABAQUS

Before comparing the results of the two FEA software's, ABAQUS and Strand7, surface deflection, stress, and strain components were cross-checked by comparing outcomes of CIRCLY7.0 with those obtained from ABAQUS for the NA pavement model. The difference between the pavement model in the ABAQUS and CIRCLY7.0 was the layer model type. In ABAQUS, all layers were taken as an isotropic layer with properties such as density, resilient modulus, and poison ratio. However, CIRCLY7.0 assumes the surface course layers (both wearing and structural layers) to be an isotropic layer, whereas the rest of the layers are adopted as an anisotropic elastic layer (Pavement_Science, 2022a). The anisotropy model provides a closer fit to observed surface deflection blows, that is narrower, deeper and increase in compressive strain at the top of the subgrade (Pavement_Science, 2022b).

In the general analysis step of CIRCLY7.0, the number of loadings was kept at 1, to be consistent with the loading condition in ABAQUS. The tyre pressure on the pavement model in CIRCLY7.0 used the same circular area of radius 102.4mm.

Figure 32 demonstrates the vertical stress, or stress yy, as can be seen in Figure 20, from the top to the bottom layer of the NA pavement in both ABAQUS and CIRCLY7.0, to be quite similar. The thickness of the surface course layer of NA pavement is 160mm, and as seen in the chart, the pressure transferred from the surface layer to the base course layer of the pavement is lower in ABAQUS than in CIRCLY7.0. 600mm is the top of the subgrade layer, and this layer is experiencing the same amount of pressure in both ABAQUS and CIRCLY7.0.
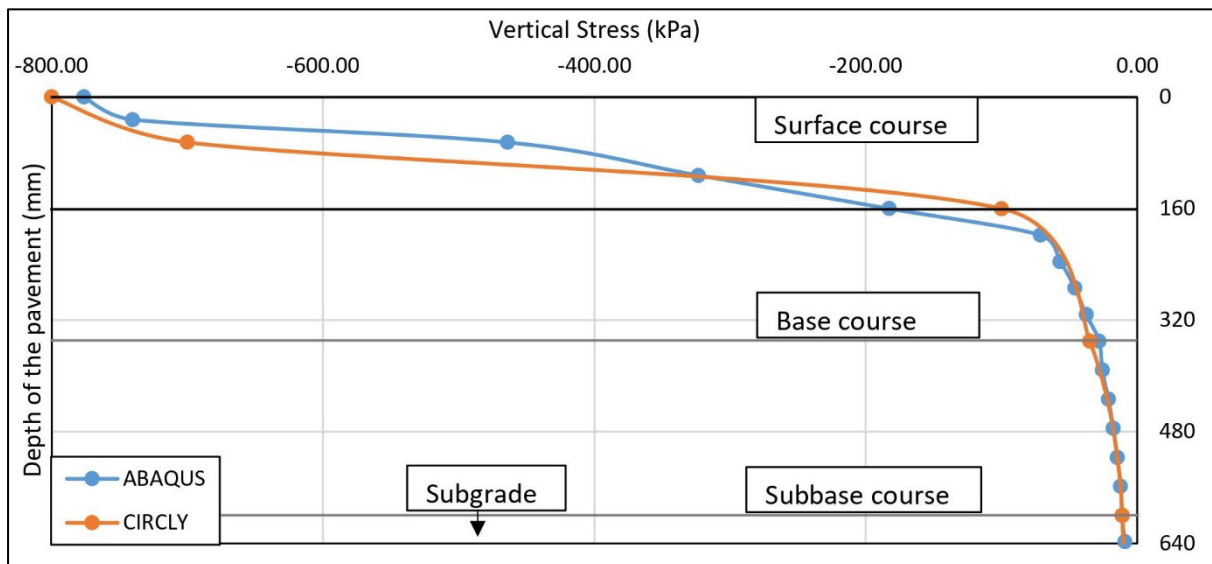
Figure 32 Comparison of vertical stress along the pavement depth in CIRCLY7.0 and ABAQUS as a result of a circular vehicle tyre load with a radius of 102.4mm.

Figure 33 demonstrates the difference in the vertical displacement, or displacement yy, result between ABAQUS and CIRCLY7.0. The results demonstrate a difference of around 0.34mm displacement along the pavement depth between the two software. Based on the result in Figure

33, the deflection in ABAQUS under similar tyre loading and traffic conditions is 52.30% lower than CIRCLY7.0.
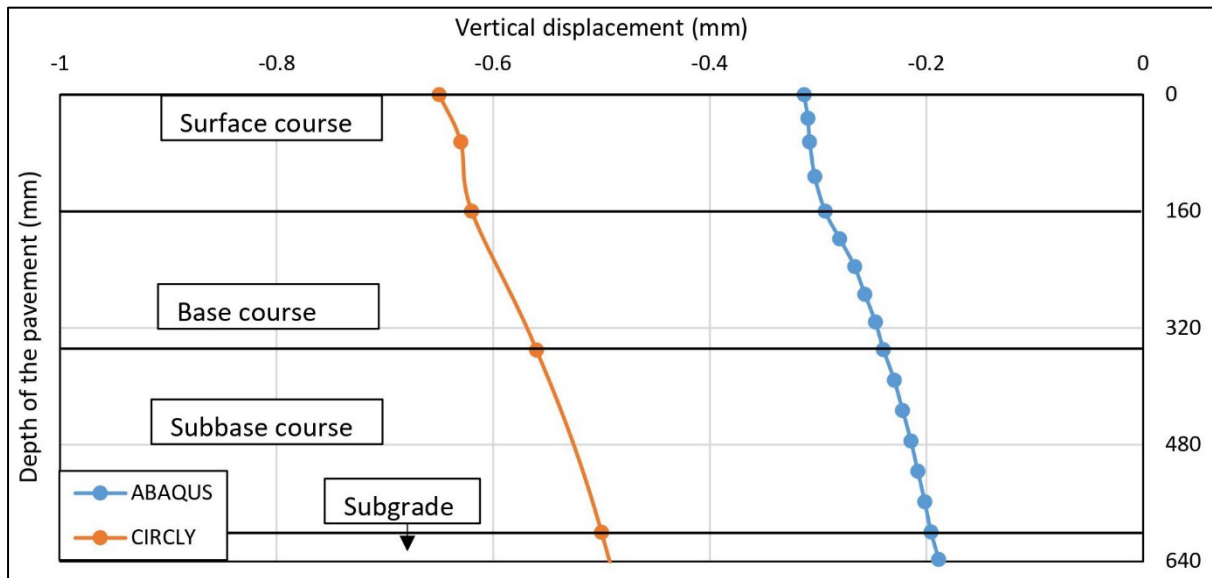
Figure 33 Vertical displacement comparison between CIRCLY7.0 and ABAQUS.

Table 23 provides the result of critical strains and deflections observed in ABAQUS and CIRCLY7.0 analysis. The analysis result in ABAQUS with respect to CIRCLY7.0 results shows a difference in surface deflection and vertical microstrain at the bottom of the HMA to be 52.30 and 66.85%, respectively. Figure 33 demonstrates the trend of the vertical displacement of ABAQUS being similar to that of CIRCLY7.0. This significant difference in the ABAQUS result were taken into account, and therefore, the pavement model results obtained from ABAQUS were only used to compare the four pavement models, not to predict the actual case scenario. Knowing that conventional asphalt has provided reliable performance for decades, exhibiting a better performance of the recycled material mixtures through ABAQUS analysis can indicate a better real-life performance. Overall, variances between the stress, strains and displacements attained through ABAQUS and CIRCLY are attributed to material and boundary condition assumptions in CIRCLY (Gillett, 2011).

83

Table 23 Comparison of distresses at a critical location in ABAQUS and CIRCLY7.0 simulations.

Pavement models	NA in ABAQUS	NA in CIRLCY7.0	Difference in ABAQUS with respect to CIRCLY7.0 (%)
Vertical microstrain on top of the subgrade	-177.88	- 210.00	15.29
Vertical microstrain at the bottom of the HMA layer	-165.71	- 500.00	66.85
Deflection of pavement surface (mm)	-0.31	-0.65	52.30
Horizontal microstrain at the bottom of the HMA layer	2	190.00	42.65

The horizontal and vertical microstrain comparison chart between ABAQUS and CIRCLY7.0 has been shown in Figures 48 and 49, provided in the Appendix section of this thesis.

5.4 Results of analysis by ABAQUS

The four designed pavement profiles were modelled in ABAQUS with the same loading conditions. The results of the surface deflection and stress-strain response of the pavement under a single axle single tyre (SAST) wheel loading are presented in this section. Surface deflection result, horizontal microstrain, vertical microstrain, and vertical displacement test results for four designed flexible pavements are presented in Figures 34, 35, 36, and 37, respectively.

The surface deflection results for four pavements in ABAQUS are demonstrated in Figure 34. In Figure 34, the surface distance along the pavement is reflected on the x-axis, and the vertical displacement due to the SAST wheel loading is on the y–axis. Evidently, the pavement with HMA made of natural aggregates has higher surface deflection, whereas the pavement having RCA55 in its surface course exhibits the lowest surface deflection. This comparison supports

the finding that pavement made using RCA55 has the high resistance to rutting compared to other pavements.
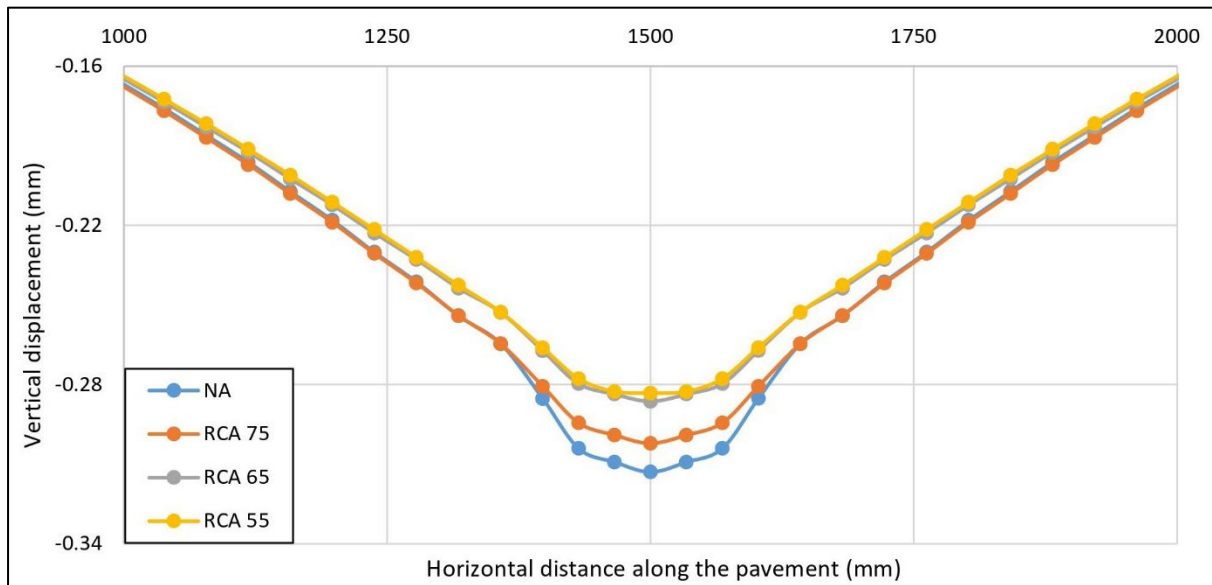
Figure 34 Surface vertical displacement under similar vehicular wheel loading.

Figure 35 demonstrates the pavement's horizontal strain, or strain xx, response under SAST loads in ABAQUS. In Figure 35, the horizontal strain on the surface is lowest for NA pavement, followed by RCA75, RCA65, and RCA55 pavement. At the location, just below the surface course, the horizontal tensile strain is the lowest for RCA65 pavement, followed by RCA55, RCA75, and NA pavement. As mentioned in Table 1, the horizontal tensile strain parameter is used to predict fatigue failure in the HMA. Therefore, Figure 35 indicates that the fatigue resistance is highest for RCA65 pavement, followed by RCA55, RCA75 and NA pavement.
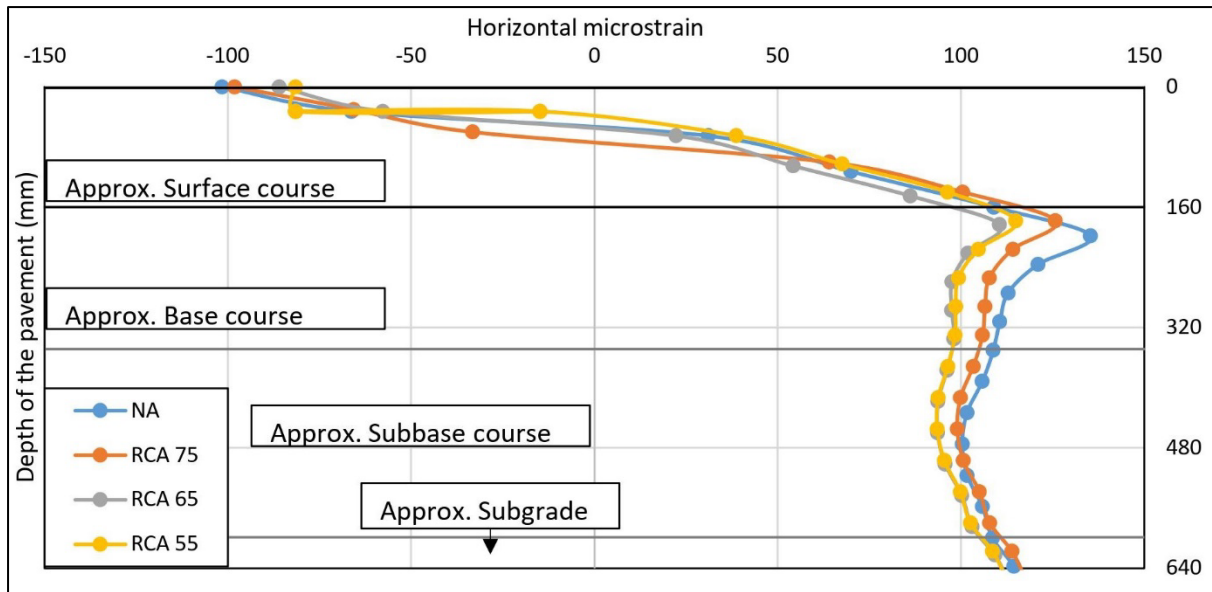
Figure 35 Horizontal micro strains along the depth of the pavement.

Figure 36 demonstrates the vertical compressive strain, or strain yy, where the result is highest at the surface for NA pavement, followed by RCA65, RCA75 and RCA55 pavement models. As mentioned in Table 1, vertical compressive strains in the top of intermediate layer and top of subgrade are used to predict rutting failure in the base or subbase, and in the subgrade, respectively. Figure 36 demonstrates, the vertical compressive strain is lowest for RCA55 pavement followed by RCA75, RCA65, and NA pavement at the surface. At the bottom of HMA layer, the vertical compressive strain is lowest for RCA65, followed by RCA55, RCA75, and NA pavements. Finally, at top of the subgrade layer, RCA55 pavement is performing better than RCA65 pavement.
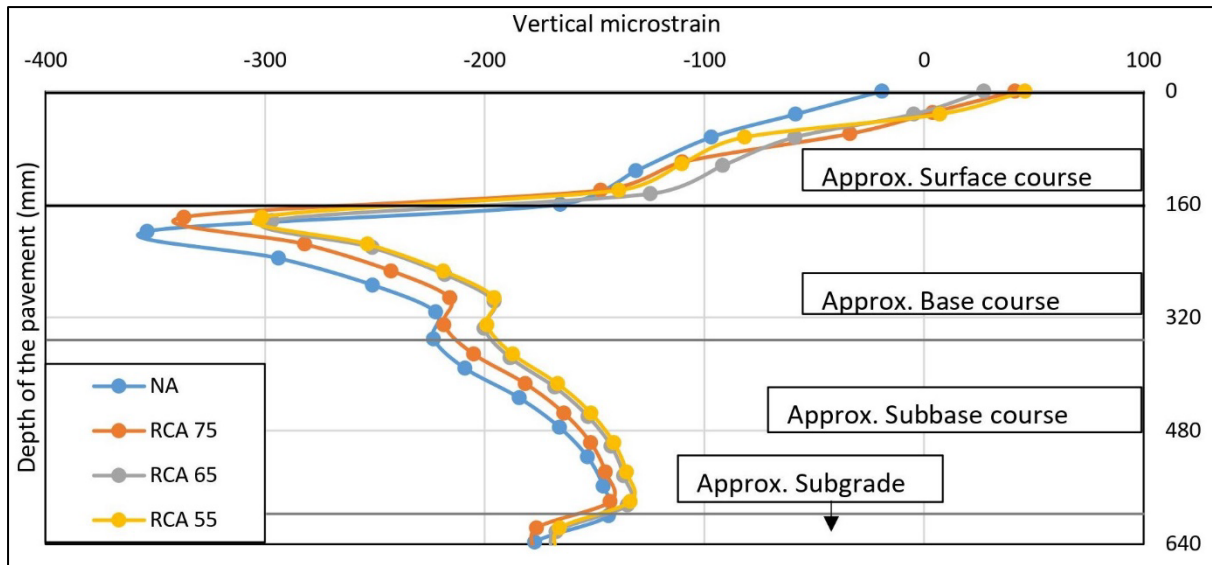
Figure 36 Vertical microstrains along the depth of the pavement.

Figure 37 demonstrates the vertical displacement, or displacement yy, along the depth of the pavement as a result of a SAST loading. The vertical displacement experienced by all the layers is highest for NA pavement, followed by RCA75, RCA65, and RCA55 pavement. With stiffer asphalt mixture in the pavement, the vertical displacement along the whole depth of the pavement is observed to be lower.
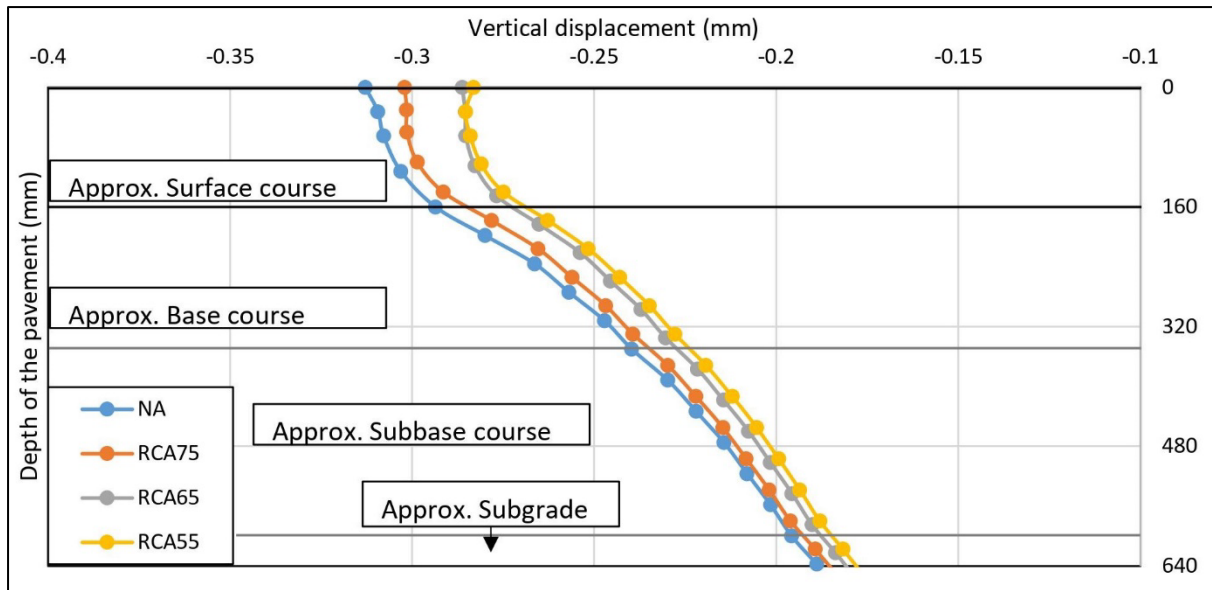
Figure 37 Vertical displacement along the depth of the pavement.

Table 24 demonstrates selected simulation results for displacement and strains along the depth of the pavement. Results shows that the surface deflection and vertical micro strain at the top of the subgrade (an indication of rutting performance) are the least, therefore, the resistant to rutting is higher for RCA55 pavement, followed by RCA65, RCA75, and NA pavement. Vertical and horizontal micro strains (an indication of fatigue performance) at the bottom of the HMA layer are the least, therefore, the fatigue resistant is higher for RCA65 pavement, followed by RCA55, RCA75, and NA pavement.

Table 24 Distresses at some critical locations of four pavements.

Pavement models	NA	RCA75	RCA65	RCA55
Vertical microstrain on top of the subgrade	-177.88	-176.90	-167.72	-166.12
Vertical microstrain at the bottom of the HMA layer	-165.71	-147.21	-124.62	-139.03
Horizontal microstrain at the bottom of HMA	108.96	100.44	86.13	96.32
Deflection of pavement surface (mm)	-0.31	-0.30	-0.29	-0.28

5.5 Result of analysis by Strand7

For the comparison and cross-checking of the pavement modelled in ABAQUS, the vertical displacement results of the nodes were checked along the surface and depth of the pavement model with Strand7.

Figure 38 demonstrates the surface deflection along the y–axis for all pavement models in Strand7. The peak vertical downward displacement at the pavement's surface was found out to be 0.301mm for NA pavement. Comparatively for the same NA pavement model, the maximum downward displacement along the wheel path was 0.313mm for ABAQUS. Between ABAQUS and Strand7, the vertical surface displacement result difference for NA, RCA75, RCA65, and RCA55 pavement was found to be 3.2, 6.6, 6.9, and 17.8%, where ABAQUS projected higher surface deflection than Strand7 for all pavement models.
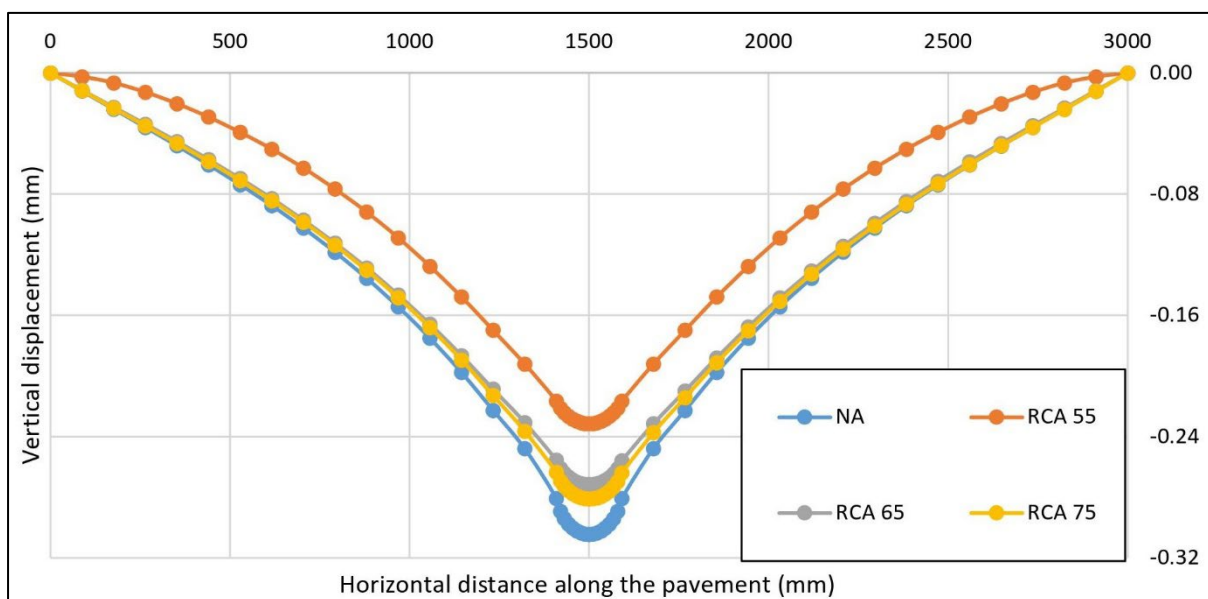
Figure 38 Vertical displacement along the pavement surface in Strand7.

Figure 38 demonstrated the lower vertical displacement, or displacement yy, along the depth of the pavement model in Strand7 compared to ABAQUS. Figures 39 indicates that the

pavement models in Strand7 had less vertical displacement compared to ABAQUS. The minor difference in the vertical displacement results between the two software's could be because of the difference in the shape of the loading area. The shape of the applied tyre pressure area in ABAQUS and Strand7, was different, i.e., a circular load was applied in ABAQUS, whereas a square-shaped load of a similar area was defined in Strand7. The slight difference in displacement result could also have been impacted by the choice of element type used for modelling. Strand7 used Hexa20 element, whereas ABAQUS used C3D8R. This indicates that the brick element adopted by Strand7 had higher nodes, and the brick in ABAQUS had lower nodes. For NA pavement, Strand7 model contained 168,628 nodes, while ABAQUS model had 165,902 nodes. The focus of this research, regarding the meshing of the pavement model, was to match the number of nodes in both ABAQUS and Strand7. Based on the NA pavement result, noting the type of element and number of nodes present in both software's, it could be mentioned that the pavement model's in ABAQUS had higher meshing done compared to Strand7. This resulted in greater displacement result for ABAQUS model which may be more realistic.
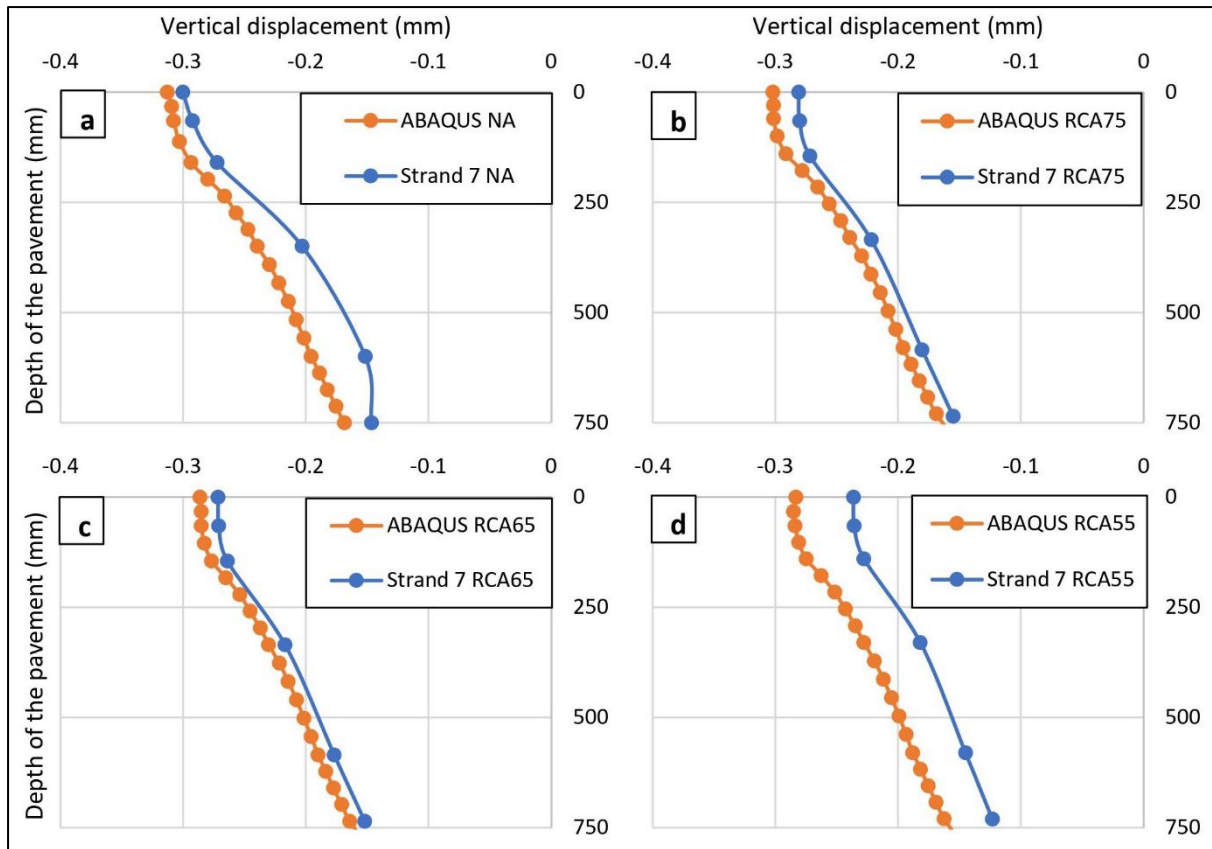
Figure 39 Vertical displacement along the depth of the pavement result in ABAQUS and Strand7.

To understand whether the pavement is having less vertical displacement because of the resistance of the pressure due to the element type selected or lower pressure experienced by the selected square tyre pressure loading area, the pressure experienced by all the layers in Strand7 were studied and displayed in Figure 40. Figure 40 shows the vertical stress throughout the pavement depth. Despite of different shape of the loading area used for defining the SAST pressure, the vertical stress flow through the pavement depth in both Strand7 and ABAQUS are quite similar. The vertical stress experienced by subbase, capping layer, and subgrade layers of all pavement profile are the same in both software's.
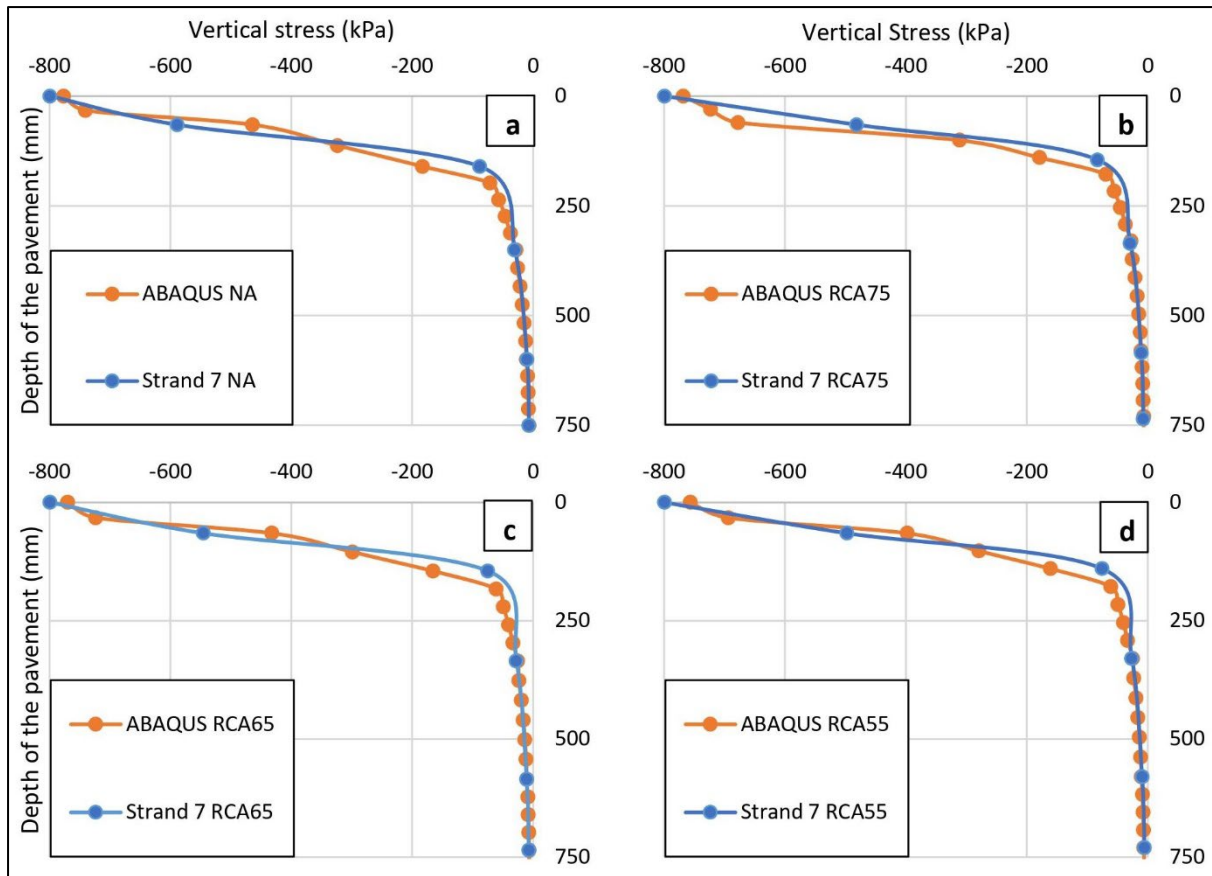
Figure 40 Vertical stress along the depth of the pavement for a) NA, b) RCA75, c) RCA65, and d) RCA55 pavement models in both ABAQUS and Strand7.

The analysis results could be more realistic in both FEA software's by adding more non-linear properties and increasing the cycle of a load equivalent to the number of load repetitions for the entire design life of the pavement. Although, due to the software limitations, the deformations cannot be converted to real-life results, comparing the four pavement profiles, both software's showed that recycled material pavements exhibit more resistance to rutting and fatigue failures than conventional NA pavement. This satisfied the main aim of this project that was providing evidence on better or at least acceptable performance of recycled material HMA compared to the conventional HMA.

6 Conclusions and recommendations

6.1 Experimental program

In this research, the suitability of the recycled aggregates, namely recycled concrete aggregates (RCA), reclaimed asphalt pavement (RAP) and recycled glass (RG), were investigated for their influence on the material properties of HMA. The experimental laboratory findings are summarised as follows:

- While the water absorption of RCA was increased when compared to natural aggregates, RAP and RG had decreased water absorption potential compared to the natural aggregates. Thus, mixture of RCA, RAP and RG in appropriate proportions were expected to result in an optimum binder content (OBC) that was not significantly higher than that of conventional asphalt.

- The particle densities of recycled materials were lower than natural aggregates, potentially resulting in lower bulk density of compacted asphalt specimens made of recycled aggregates.

- The flakiness test result showed that the natural aggregates are of higher quality than the recycled aggregates. Nevertheless, the flakiness index of all recycled aggregates met the requirements of the VicRoads specifications.

Next, three mixtures with different proportions of recycled aggregates were proposed in two different sizes of 10 and 20mm (total of 6 mixtures made of recycled materials). Benchmark mixtures made of natural aggregates were also prepared for both 10 and 20mm aggregate sizes. Findings based on the experimental investigations on the asphalt mixtures are summarised below:

- Natural aggregate mixtures had the least OBC compared to recycled material mixtures. Amongst the 20mm recycled material mixtures, 20RCA 55 had the least OBC followed by 20RCA 65 and 20RCA 75. For the 10mm recycled material mixtures, both 10RCA 55 and 10 RCA65 had the same OBC which was lower than 10 RCA 75. The 10mm and 20mm recycled material mixtures require 1.2 to 1.7%, and 0.3 to 0.8% more bitumen, respectively, compared to conventional asphalt.

- The Marshall stability of the recycled material mixtures were 80 to 99% higher than the conventional asphalt mixtures for 10mm, and up to 35% for 20mm asphalt mix.

- The flow values of recycled material mixtures were 9 to 31% higher than the conventional asphalt mixtures for 10mm, and 15 to 34% higher for 20mm asphalt mixtures.

- Asphalt mixtures made of recycled aggregates demonstrated increased resistance to moisture damage compared to conventional asphalt mixtures, possibly due to unhydrated cement in the RCA that contributes to the binding of the mixture over time when submerged in water. This is particularly important in wet climates where the wearing course is prone to environmental damage due to precipitation.

- The indirect tensile modulus of asphalt mixtures made of recycled aggregates was 72 to 145% higher than the conventional mixture for 10mm, and 45 to 75% greater for the 20mm asphalt mixtures.

- Considering the wet tensile strength criteria, the Tensile Strength Ratio (TSR) criteria, and subsequent resistance to water damage, greater Marshall stability and higher resilient modulus, 10RCA55, containing 55% RCA, 35% RAP and 10% RG was found to be the superior mixture in the 10mm asphalt mixtures of this research. Under the aforementioned criteria, for the 20mm mixtures, the 20RCA 55 followed by 20RCA 65 were the recommended mixtures.

- The properties of the 10RCA 55 and all 20mm recycled material asphalt mixtures were within the requirements specified in VicRoads-RC500.01 (2021) and can hence, be considered in the design and construction of flexible pavements.

This research followed an industry-focused approach to investigate the possibility of maximising the proportion of recycled aggregates in the production of HMA. This evidence-based promotion of recycled materials in HMA is the most effective step, to date, towards encouraging the use of sustainable construction materials and approaches.

6.2 FEM modelling

The engineering properties and FEA pavement model comparison of the mixtures allowed comparing the natural aggregate with recycled material asphalt mixtures. Below are some conclusions made based on the CIRCLY7.0, Strand7, and ABAQUS test results on pavement models:

- The designed thickness was highest for NA pavement, followed by RCA 75, RCA 65, and RCA 55 pavement for the same design conditions.

- RCA 65 pavement had the highest resistance to fatigue failure, followed by RCA 55, RCA 75, and NA pavement. This concluding statement is supported by the CDF result from CIRCLY7.0 and horizontal tensile strain below the HMA layer obtained from ABAQUS.

- Based on both ABAQUS and Strand7 results, RCA 55 pavement, followed by RCA 65, RCA 75, and NA pavement, were found to have higher resistance to rutting.

- The linear elastic layers considered in this research are less accurate; therefore, it is only best to compare the four pavements of this research and not to predict the actual stress and strain in the layers.

- The surface deflection in CIRCLY7.0 was higher than the ABAQUS. This indicates ABAQUS linear properties assigned to the pavement layers should not be used to predict the actual case scenario.

6.3 Recommendations for future research

The properties of the recycled material aggregate mixtures were within the requirements specified in VicRoads (2021), except for 10RCA 70.5 and 10RCA 65. The 10RCA 55 and all 20mm recycled material asphalt mixtures satisfied the criteria and hence were recommended to be used in the pavement layers. However, additional research is recommended to be undertaken in future on the use of 100% recycled material aggregates in an asphalt mixture.

Some recommendations which might help in more realistic simulation and comparison between the pavements in the future are presented below:

1) A non-linear analysis of the pavement models with creep and viscoelastic properties for the appropriate layers would make the model more realistic.

2) Using C3D20R instead of C3D8R elements in ABAQUS (same cubical shape element but instead of 8, they have 20 nodes in an element) could provide a more accurate result.

6.4 Publications

Mechanical Characteristics and Durability of HMA made of recycled aggregates (Submitted)

Performance analysis of HMA made of recycled aggregates using FEM (under preparation)

7 Reference

ABAQUS. (2009). *ABAQUS/Standard User's Manual*. Retrieved from http://130.149.89.49:2080/v6.14/books/usb/default.htm

Adedeji, J. A. (2015). Simulation of Flexible Pavement utilising fly ash as alternative stabilizer. 104. Retrieved from https://core.ac.uk/download/pdf/222967447.pdf

AGPT04B-14. (2014). Guide to Pavement Technology Part 4B: Asphalt. In (pp. 139): Austroads Ltd.

AGPT_T232-07. (2007). Stripping potential of asphalt - Tensile strength ratio. In.

Ai Jen Lim, Y. C., Daniel Dias-da-Costa, Amirali Ebrahimi Ghadi, Ali Abbas. (2020). *Recycled materials in roads and pavements*. Retrieved from https://lgnsw.org.au/common/Uploaded%20files/PDF/Technical_Review_Recycled_ Materials_in_Roads-Pavements.pdf

Al-Qadi, I. L., Aurangzeb, Q., Carpenter, S. H., Pine, W. J., & Trepanier, J. (2012). *Impact of high RAP contents on structural and performance properties of asphalt mixtures* (0197-9191). Retrieved from

Alhassan, H., Yunusa, G., & Sanusi, D. (2018). Potential of glass cullet as aggregate in hot mix asphalt. *Nigerian Journal of Technology, 37*(2), 338-345. Retrieved from https://www.ajol.info/index.php/njt/article/view/174964

Allan, P. (2019). *Assessment of Australian recycling infrastructure-Glass packaging update*. Retrieved from https://www.agriculture.gov.au/sites/default/files/documents/assessment-australian-recycling-infrastructure-glass-packaging.pdf

Anne-Marie. (2021). Positivist/Post-posotivist Perspectives: Quantative Research Methods. Retrieved from

https://vucollaborate.vu.edu.au/d2l/le/content/1004141/Home?itemIdentifier=D2L.LE.Content.ContentObject.ModuleCO-6202978

Arulrajah, A., Jegatheesan, P., Disfani, M., & Bo, M. (2013). Geotechnical and Geo-environmental Properties of Recycled Construction and Demolition Materials in Pavement Subbase Applications. *Journal of Materials in Civil Engineering, 25*, 1077-1088. doi:10.1061/(ASCE)MT.1943-5533.0000652

Arulrajah, A., Piratheepan, J., Ali, M., & Bo, M. (2012). Geotechnical properties of recycled concrete aggregate in pavement sub-base applications. *Geotechnical Testing Journal, 35*(5), 743-751.

AS_1141.5. (2000). Method for sampling and testing aggregates. In *Method 5: Particle density and water absorption of fine aggregates*.

AS_1141.6.1. (2000). Methods for sampling and testing aggregates. In *Method 6.1: Particle density and water absorption of coarse aggregates - Weighing-in-water method*.

AS_1141.11. (1996). Methods for sampling and testing aggregates. In *Method 11: Particle size distribution by sieving*.

AS_1141.12. (2015). Methods for sampling and testing aggregates. In *Method 12: Materials finer than 75 micrometer in aggregates (by washing)*.

AS_1141.15. (1999). Methods for sampling and testing aggregates. In *Method 15: Flakiness index*.

AS_2891.5. (2004). Methods of sampling and testing asphalt. In *Method 5: Determination of stability and flow - Marshall procedure*.

AS_2891.7.1. (2004). Methods of sampling and testing asphalt. In *Method 7.1: Determination of maximum density of asphalt - Water displacement method* (pp. 5).

AS_2891.9.2. (2005). Methods of sampling and testing asphalt. In *Method 9.2: Determination of bulk density of compacted asphalt - Presaturation method*.

AS_2891.13.1. (1995). Methods of sampling and testing asphalt. In *Method 13.1: Determination of the resilient modulus of asphalt - Indirect tensile method.*

Asphalt-Institute. (2014). MS-2 Asphalt Mix Design Methods. Retrieved from https://www.researchgate.net/profile/Yasir_Jebur/post/what_are_the_limits_of_thickn esses_of_asphalt_wearing_or_surface_binder_layer_base_materials_asphalt_base_an d_the_full_depth_asphalt_layer/attachment/5c13e9eccfe4a76455091d0d/AS:7037938 55483904@1544808939808/download/Asphalt-Institute-MS2-7th-Edition-Asphalt-Institute-Mix-Design.pdf

ASTM_D6927-15. (2015). Standard Test Method for Marshall Stability and Flow of Asphalt Mixtures. In.

Austroads-5.3.2. (2022). 5.3.2 Flakiness Index. Retrieved from https://austroads.com.au/publications/pavement/agpt04k/design-method/aggregate-size-and-shape/flakiness-index

Austroads-Part2. (2017). Guide to Pavement technology part 2 : Pavement structural design. Retrieved from https://austroads.com.au/publications/pavement/agpt02/media/AGPT02-17_Guide_to_Pavement_Technology_Part_2_Pavement_Structural_Design.pdf

Bhusal, S., Li, X., & Wen, H. (2011). Evaluation of effects of recycled concrete aggregate on volumetrics of hot-mix asphalt. *Transportation research record, 2205*(1), 36-39. Retrieved from https://journals.sagepub.com/doi/epdf/10.3141/2205-05

Biswal, D. R., Chandra Sahoo, U., & Ranjan Dash, S. (2020). Structural response of an inverted pavement with stabilised base by numerical approach considering isotropic and anisotropic properties of unbound layers. *Road Materials and Pavement Design, 21*(8), 2160-2179.

Blayi, R. A., Sherwani, A. F. H., Ibrahim, H. H., Faraj, R. H., & Daraei, A. (2020). Strength improvement of expansive soil by utilizing waste glass powder. *Case Studies in Construction Materials, 13*, e00427.

Board, G. S. (2021). The mining of sand, a non-renewable resource. Retrieved from https://www.greenfacts.org/en/sand-extraction/l-2/index.htm

Bruce A. Chadbourn, E. L. S., Jr., Benita L. Crow, Samantha Spindler. (1999). The Effect of Voids in Mineral Aggregate (VMA) on Hot-Mix Asphalt Pavements. 125. Retrieved from https://www.odot.org/materials/asph_tchnl_info/HMA_VMA_RPT.pdf

Cho, Y.-H., Yun, T., Kim, I. T., & Choi, N. R. (2011). The application of recycled concrete aggregate (RCA) for hot mix asphalt (HMA) base layer aggregate. *KSCE Journal of Civil Engineering, 15*(3), 473-478. Retrieved from https://link.springer.com/content/pdf/10.1007/s12205-011-1155-3.pdf

Creswell, J. W. C. J. D. (2018). *Research Design - Qualitative, Quantitative, and Mixed Methods Approaches* (Fifth Edition ed.).

Debnath, A. (2018). Flexible pavement - Highway Engineering. 23. Retrieved from https://vucollaborate.vu.edu.au/d2l/le/content/192165/viewContent/2672739/View

Disfani, M., Arulrajah, A., Bo, M., & Hankour, R. (2011). Recycled crushed glass in road work applications. *Waste Management, 31*(11), 2341-2351.

Duncan, J. M., Monismith, C. L., & Wilson, E. L. (1968). Finite element analysis of pavements. *Highway Research Record, 228*(18-33), 157-158.

EDCM. (2011). *Engineering Design and Construction Manual* Retrieved from Melbourne:

Ghadimi, B., & Nikraz, H. (2017). A comparison of implementation of linear and nonlinear constitutive models in numerical analysis of layered flexible pavement. *Road Materials and Pavement Design, 18*(3), 550-572.

Gillett, S. D. (2011). *Accuracy in Mechanistic Pavement Design Consequent upon Unbound Material Testing.* (Doctor of Philosophy). University of Nottingham,

Google. (2023). Google maps. Retrieved from https://www.google.com.au/maps

Gupta, A., Kumar, P., & Rastogi, R. (2015). Critical pavement response analysis of low-volume pavements considering nonlinear behavior of materials. *Transportation research record, 2474*(1), 3-11.

Hall, M. (2020). 6 things you need to know about sand mining. Retrieved from https://www.mining-technology.com/features/six-things-sand-mining/

Huang, Y. H. (2003). *Pavement Analysis and Design* (Second Edition ed.): Pearson.

Hughes, C. S. (1990). Feasibility of using recycled glass in asphalt. Retrieved from https://rosap.ntl.bts.gov/view/dot/19246

Hyder-consulting. (2011). Construction and Demolition Waste Status Report. Retrieved from https://www.awe.gov.au/sites/default/files/documents/construction-waste.pdf

Interactive, P. (2021). Flexible Pavement Mechanistic Models. Retrieved from https://pavementinteractive.org/reference-desk/design/structural-design/flexible-pavement-mechanistic-models/

Joe Pickin, P. R., Jenny Trinh, Bill Grant. (2018). National Waste Report 2018. Retrieved from https://www.awe.gov.au/sites/default/files/documents/national-waste-report-2018.pdf

Khayat, K. H., & Sadati, S. (2020). *High-volume recycled materials for sustainable pavement construction.* Retrieved from

Kieran Sharp, A. G. (2009). GUIDE TO PAVEMENT TECHNOLOGY - Part 1: introduction to Pavement Technology. Retrieved from https://austroads.com.au/publications/pavement/agpt01

Lachance-Tremblay, É., Vaillancourt, M., & Perraton, D. (2016). Evaluation of the impact of recycled glass on asphalt mixture performances. *Road Materials and Pavement Design,*

17(3), 600-618. Retrieved from https://www.tandfonline.com/doi/full/10.1080/14680629.2015.1103778

Ma, F., Sha, A., Lin, R., Huang, Y., & Wang, C. (2016). Greenhouse Gas Emissions from Asphalt Pavement Construction: A Case Study in China. *International journal of environmental research and public health, 13*(3), 351. doi:10.3390/ijerph13030351

Mallela, J., & George, K. (1994). Three-dimensional dynamic response model for rigid pavements. *Transportation Research Record, 1448*, 92-99.

Pavement_Science. (2022a). *CIRCLY 7.0*. Retrieved from https://ops.pavement-science.com.au/full-list-circly-files/download-info/circly-5-0-a-powerful-tool-for-pavement-design/

Pavement_Science. (2022b). *CIRCLY Workshop*. Retrieved from

Plati, C. (2019). Sustainability factors in pavement materials, design, and preservation strategies: A literature review. *Construction and Building Materials, 211*, 539-555.

Programme, U. N. E. (2014). *United Nations Environment Programme (2014) Sand, Rarer than One Thinks: UNEP Global Environmental Alert Service (GEAS)*. Retrieved from https://wedocs.unep.org/handle/20.500.11822/8665

Sanchez-Cotte, E. H., Fuentes, L., Martinez-Arguelles, G., Rondón Quintana, H. A., Walubita, L. F., & Cantero-Durango, J. M. (2020). Influence of recycled concrete aggregates from different sources in hot mix asphalt design. *Construction and Building Materials, 259*, 120427. doi:https://doi.org/10.1016/j.conbuildmat.2020.120427

Scott, G. (2021). The Difference Between Linear and Nonlinear Finite Element Analysis (FEA). Retrieved from https://control.com/technical-articles/the-difference-between-linear-and-nonlinear-finite-element-analysis-fea/

Sii, H. B. P. (2015). *Three-dimensional finite element analysis of concrete pavement on weak foundation.* (PhD Doctorate Thesis (PhD Doctorate)). Griffith University, Retrieved from http://hdl.handle.net/10072/366517

SIMULIA. (2011). *Abaqus 6.11 - Theory manual*. Retrieved from http://130.149.89.49:2080/v6.11/pdf_books/THEORY.pdf

Strand7. (2010). *Using Strand7 - Intorduction to the Strand7 Finite Element Analysis System*. Retrieved from

Su, K., Hachiya, Y., & Maekawa, R. (2009). Study on recycled asphalt concrete for use in surface course in airport pavement. *Resources, Conservation and Recycling, 54*(1), 37-44. doi:https://doi.org/10.1016/j.resconrec.2009.06.003

Su, N., & Chen, J. (2002). Engineering properties of asphalt concrete made with recycled glass. *Resources, Conservation and Recycling, 35*(4), 259-274. Retrieved from https://www.sciencedirect.com/science/article/pii/S0921344902000071

T.F. Fwa , W. O. T. (2006). The Handbook of Highway Engineering - Highway Material. Retrieved from https://www.academia.edu/31489704/the_handbook_of_highway_engineering_pdf

Tahmoorian, F., Samali, B., Tam, V. W., & Yeaman, J. (2017). Evaluation of mechanical properties of recycled material for utilization in asphalt mixtures. *Applied Sciences, 7*(8), 763.

Tahmoorian, F., Samali, B., Yeaman, J., & Crabb, R. (2018). The use of glass to optimize bitumen absorption of hot mix asphalt containing recycled construction aggregates. *Materials, 11*(7), 1053.

Vicky. (2020). Road Pavement: Purpose, Types & Components.

Vicroads-RC201.01. (2016). Design of Asphalt Mixes (Marshall Method). 4. Retrieved from https://www.vicroads.vic.gov.au/-/media/files/technical-documents-new/test-methods/test-method-rc-20101--design-of-asphalt-mixes-marshall-method.ashx

VicRoads-RC500.01. (2021). Registration of Bituminous Mix Designs. 10. Retrieved from https://www.transport.tas.gov.au/__data/assets/pdf_file/0004/298120/Code_of_Practic e_RC_50001_Registration_of_Bituminous_Mix_Designs_July_2001.pdf

VicRoads-RC500.22. (2018). Selection and Design of Pavements and Surfacings (RC 500.22). Retrieved from https://www.vicroads.vic.gov.au/-/media/files/technical-documents-new/codes-of-practice-rc500/code-of-practice-rc-50022-selection-and-design-of-pavement-and-surfacings-december-2018.ashx

VicRoads-Section407. (2014). Hot Mix Asphalt. Retrieved from https://view.officeapps.live.com/op/view.aspx?src=http%3A%2F%2Fwebapps.vicroa ds.vic.gov.au%2FVRNE%2Fcsdspeci.nsf%2Fwebscdocs%2F1775DC9756592F32C A257DA4001D4C6D%2F%24File%2FSec407.doc&wdOrigin=BROWSELINK

VicRoads. (2021). Registration of Bituminous Mix Designs. Retrieved from https://www.transport.tas.gov.au/__data/assets/pdf_file/0004/298120/Code_of_Practic e_RC_50001_Registration_of_Bituminous_Mix_Designs_July_2001.pdf

Wiedmann, T. O., Schandl, H., Lenzen, M., Moran, D., Suh, S., West, J., & Kanemoto, K. (2015). The material footprint of nations. *Proceedings of the National Academy of Sciences, 112*(20), 6271-6276. doi:10.1073/pnas.1220362110

Yaghoubi, E., Ahadi, M. R., Alijanpour Sheshpoli, M., & Jahanian Pahlevanloo, H. (2013). Evaluating the performance of hot mix asphalt with reclaimed asphalt pavement and heavy vacuum slops as rejuvenator. *International Journal of Transportation Engineering, 1*(2), 115-124.

Yaghoubi, E., Sudarsanan, N., & Arulrajah, A. (2021). Stress-strain response analysis of demolition wastes as aggregate base course of pavements. *Transportation Geotechnics, 30*, 100599.

Yang, L., Hu, Y., & Zhang, H. (2020). Comparative study on asphalt pavement rut based on analytical models and test data. *International Journal of Pavement Engineering, 21*(6), 781-795.

8 Appendix

This appendix presents the Marshall method plots for 7 mixtures. The plots of 10NA asphalt mixture were presented in Chapter 4. Additionally, the figures of vertical and horizontal microstrains comparison between CIRCLY7.0 and ABAQUS are included in this appendix section.
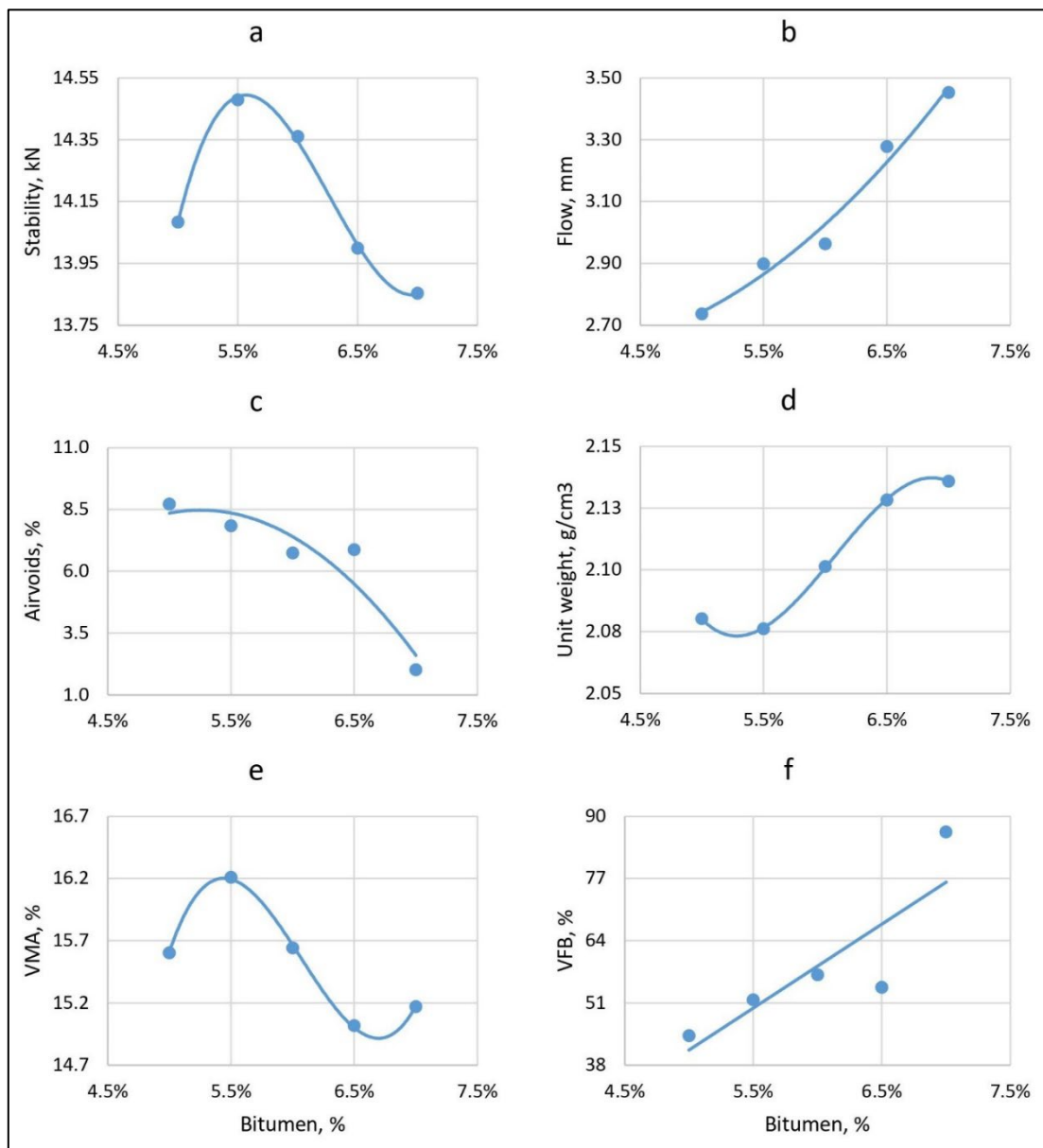
Figure 41 Marshall charts of 10RCA 75 mixture showing Bitumen (%) vs a) Stability (kN), b) Flow (mm), c) Air voids (%), d) Unit weight (g/cm3), e) VMA (%), and f) VFB (%).
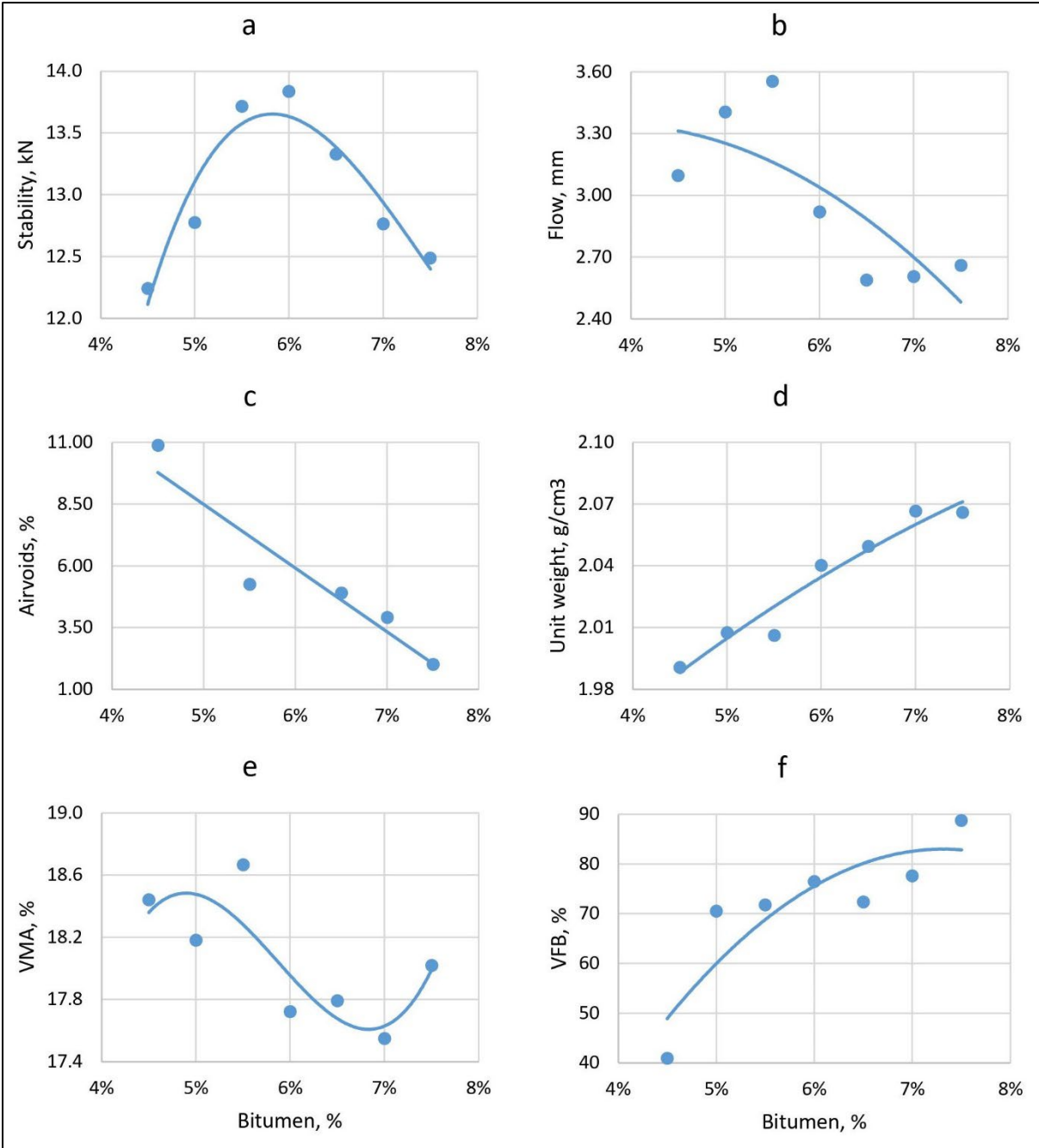
Figure 42 Marshall charts of 10RCA 65 mixture showing Bitumen (%) vs a) Stability (kN), b) Flow (mm), c) Air voids (%), d) Unit weight (g/cm3), e) VMA (%), and f) VFB (%).
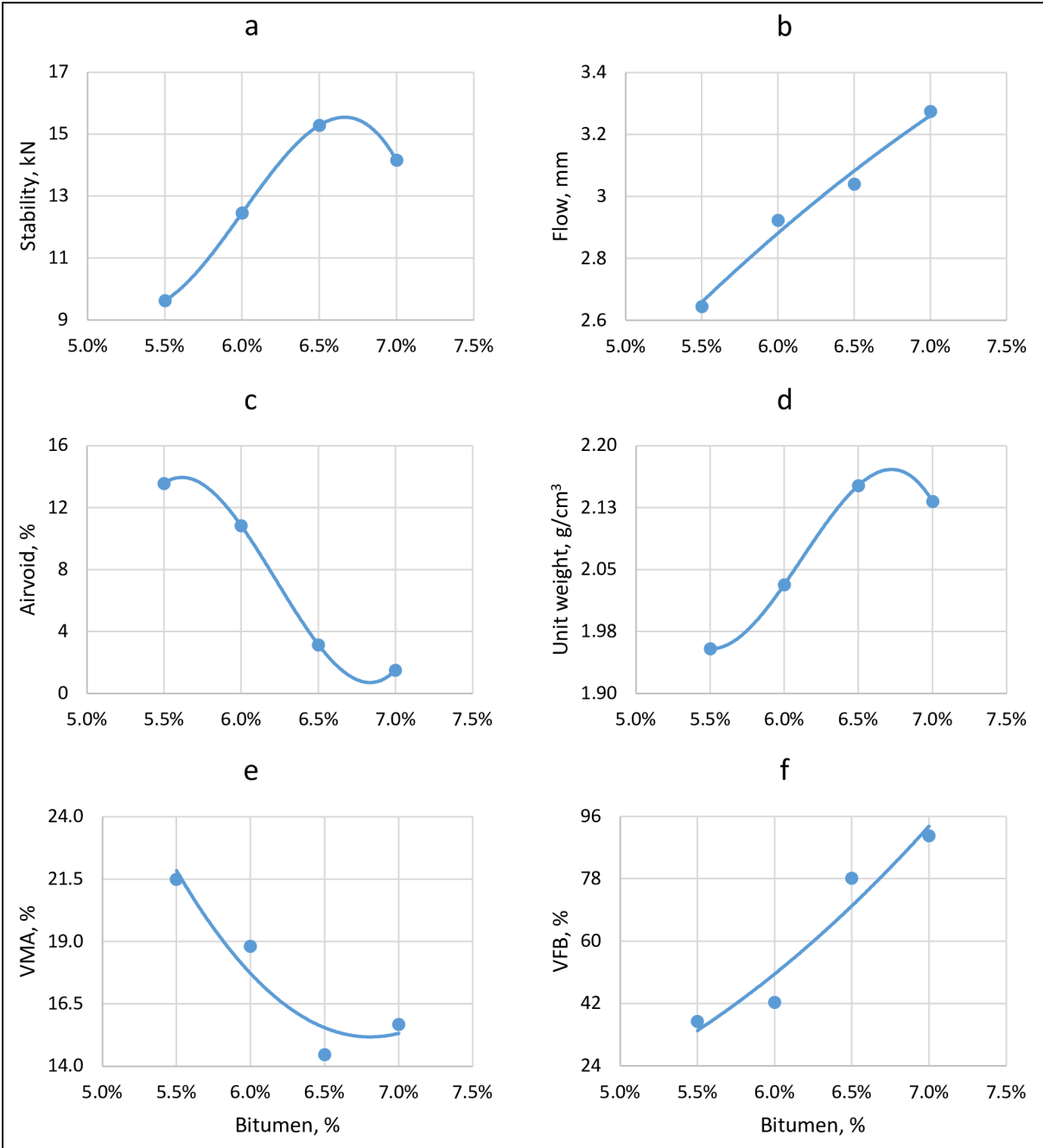
Figure 43 Marshall charts of 10RCA 55 mixture showing Bitumen (%) vs a) Stability (kN), b) Flow (mm), c) Air voids (%), d) Unit weight (g/cm3), e) VMA (%), and f) VFB (%).
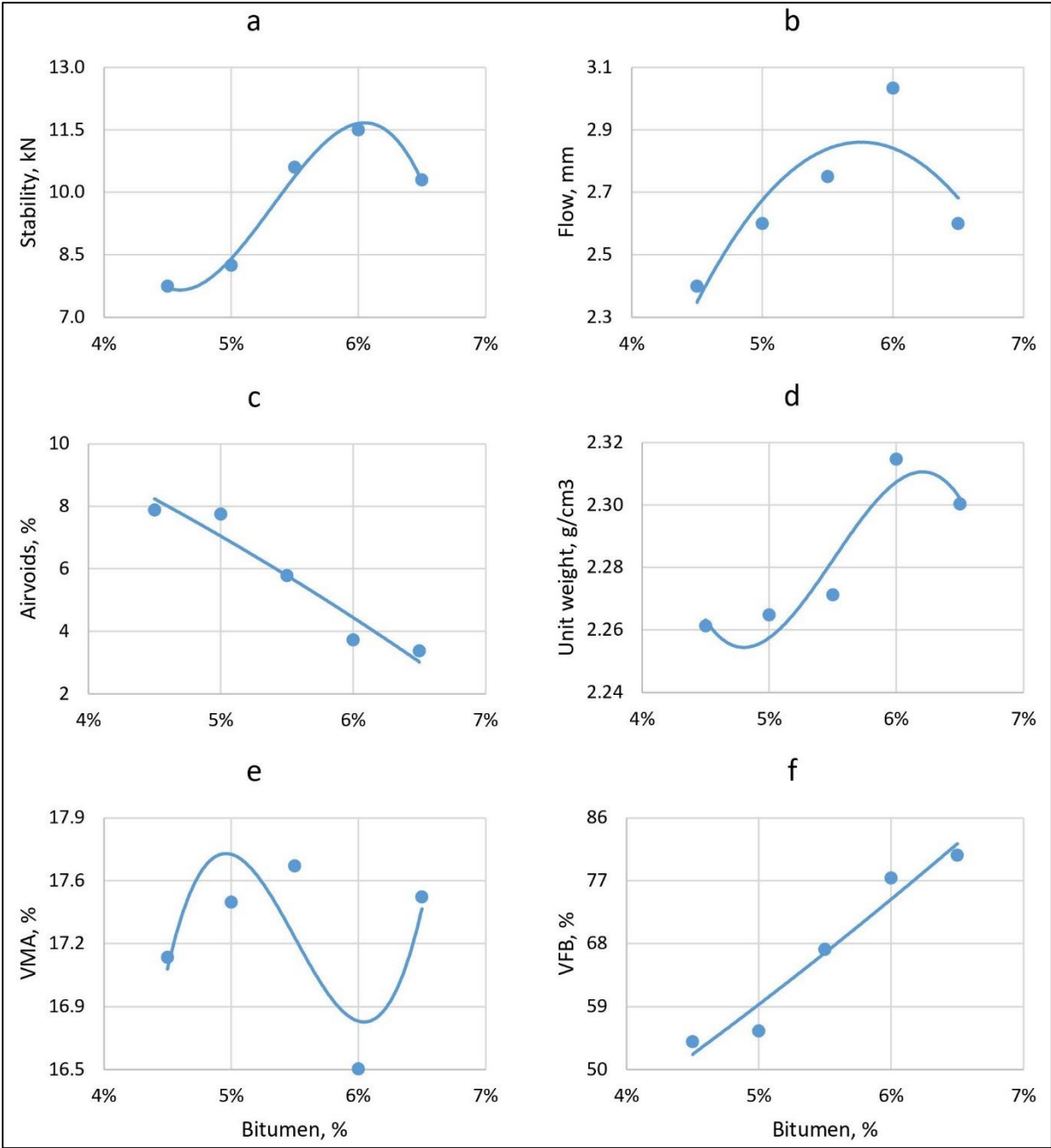
Figure 44 Marshall charts of 20NA mixture showing Bitumen (%) vs a) Stability (kN), b) Flow (mm), c) Air voids (%), d) Unit weight (g/cm3), e) VMA (%), and f) VFB (%).
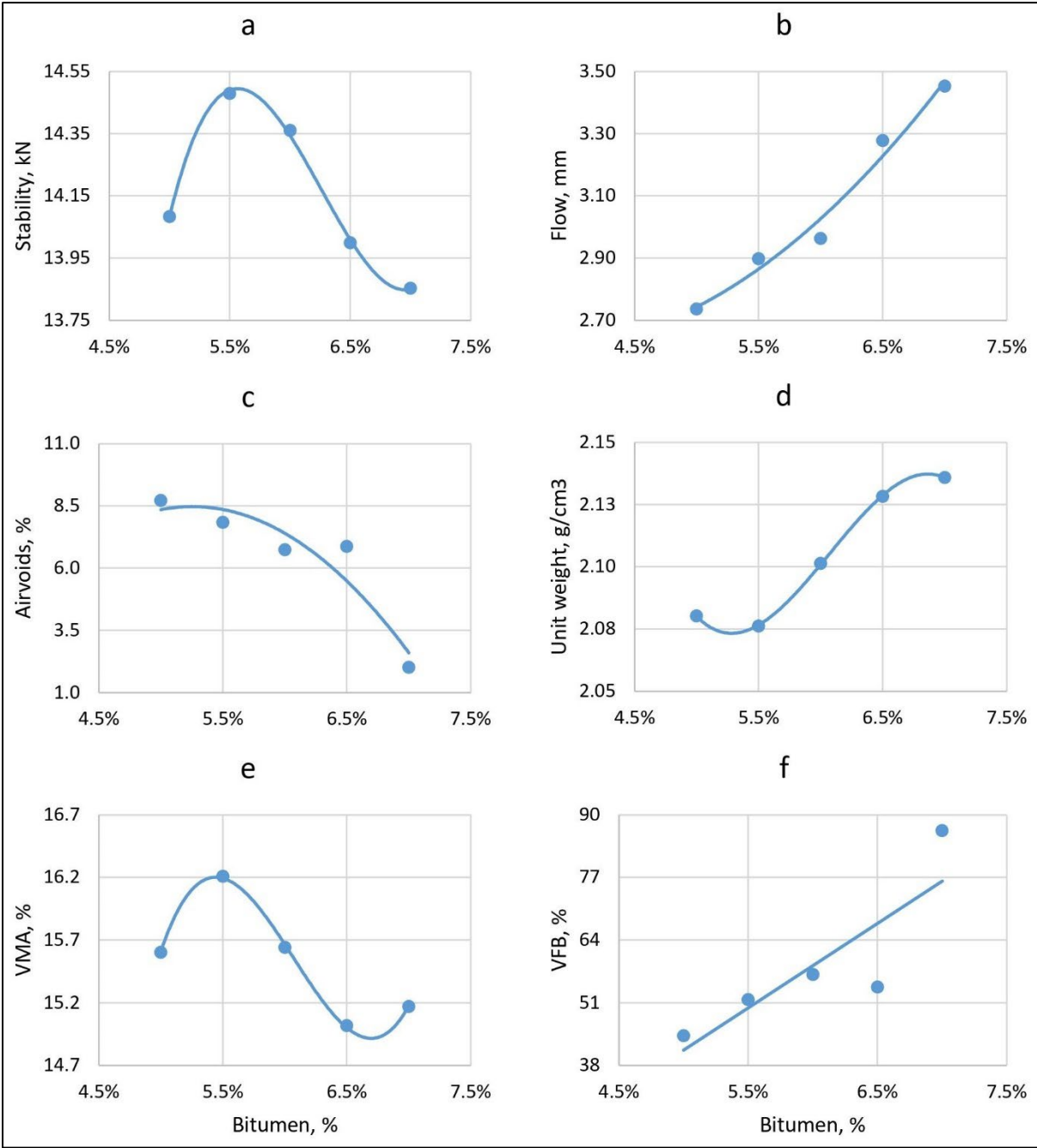
Figure 45 Marshall charts of 20RCA 75 mixture showing Bitumen (%) vs a) Stability (kN), b) Flow (mm), c) Air voids (%), d) Unit weight (g/cm3), e) VMA (%), and f) VFB (%).
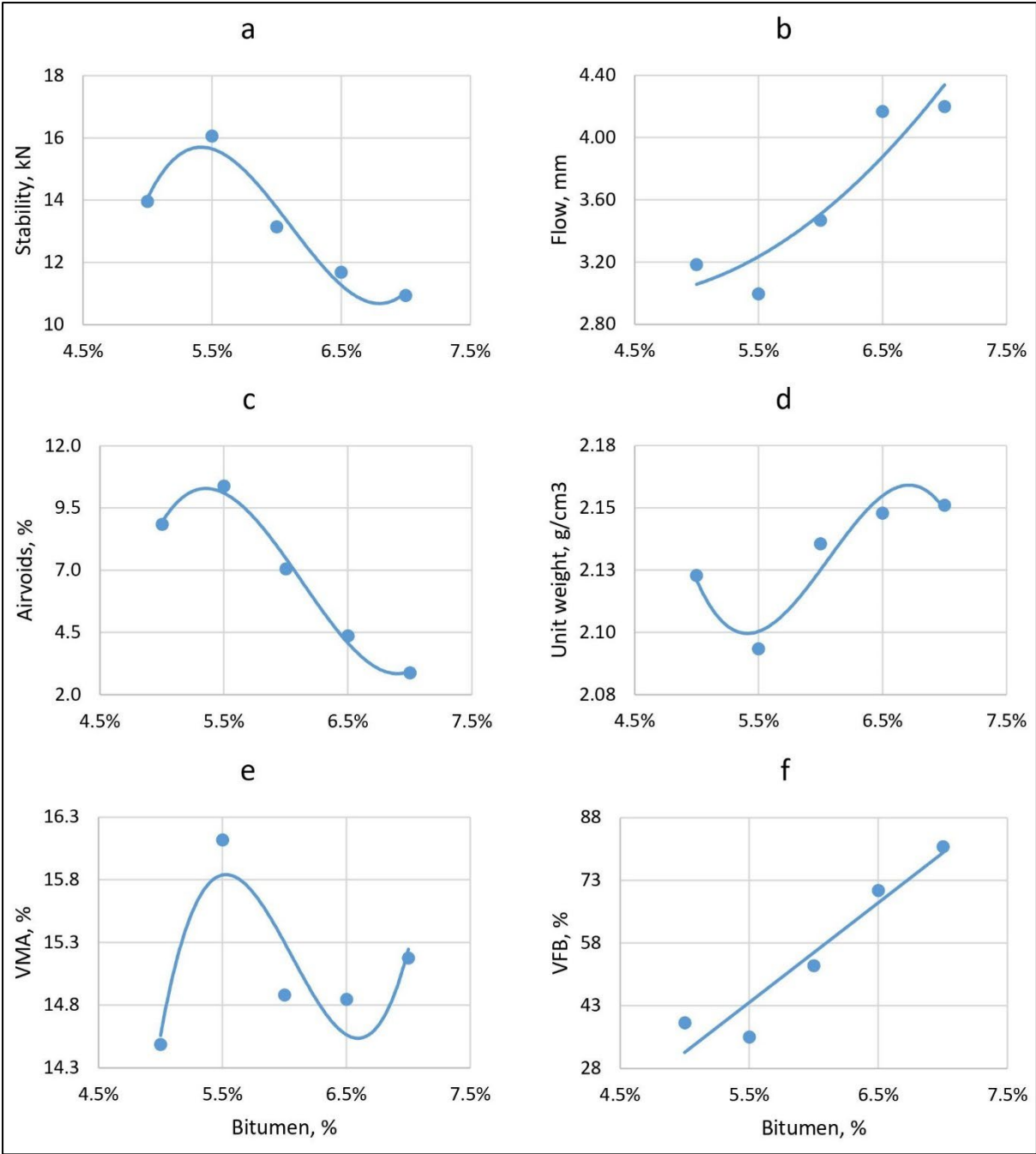
Figure 46 Marshall charts of 20RCA 65 mixture showing Bitumen (%) vs a) Stability (kN), b) Flow (mm), c) Air voids (%), d) Unit weight (g/cm3), e) VMA (%), and f) VFB (%).
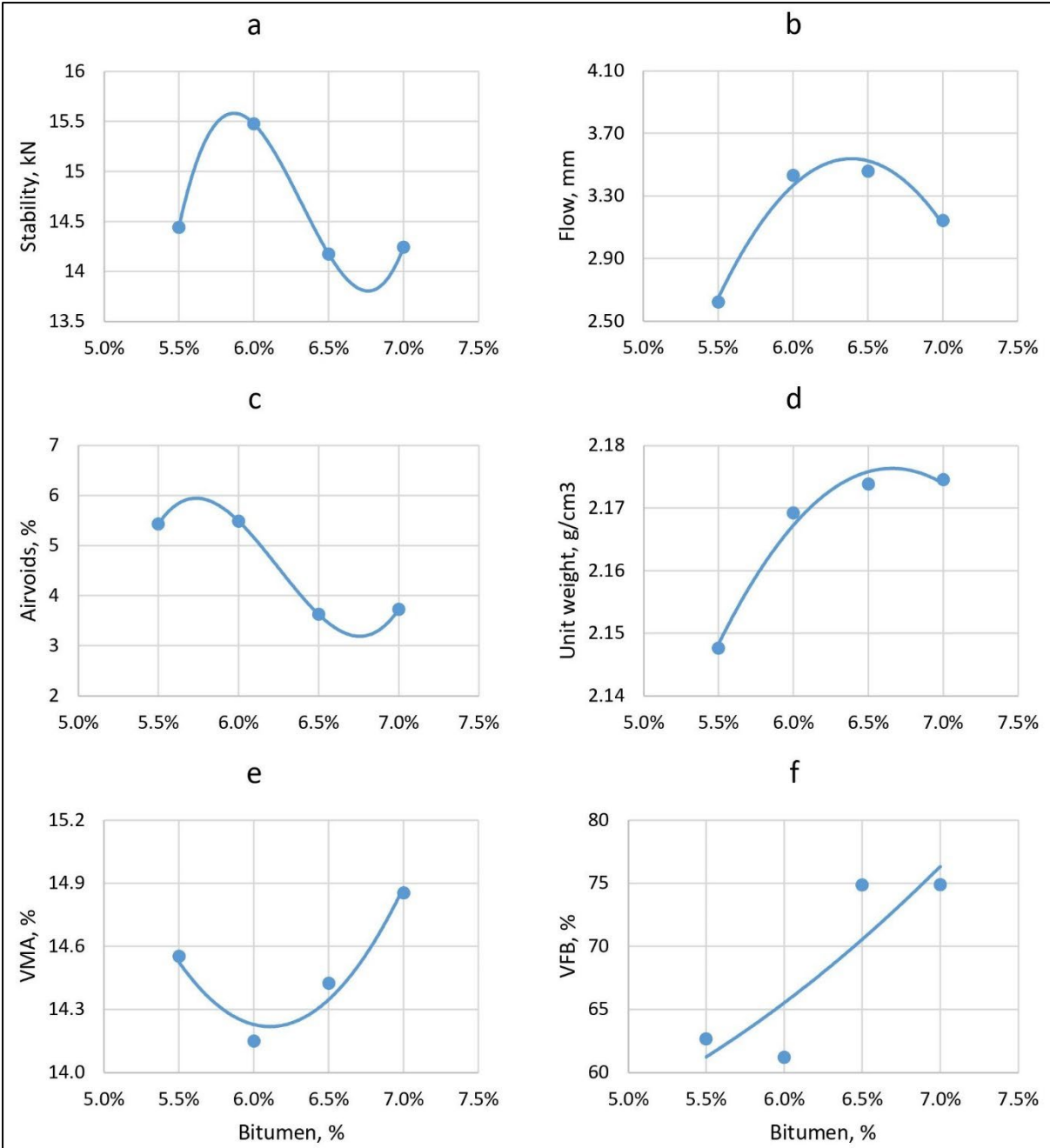
Figure 47 Marshall charts of 20RCA 55 mixture showing Bitumen (%) vs a) Stability (kN), b) Flow (mm), c) Air voids (%), d) Unit weight (g/cm3), e) VMA (%), and f) VFB (%).
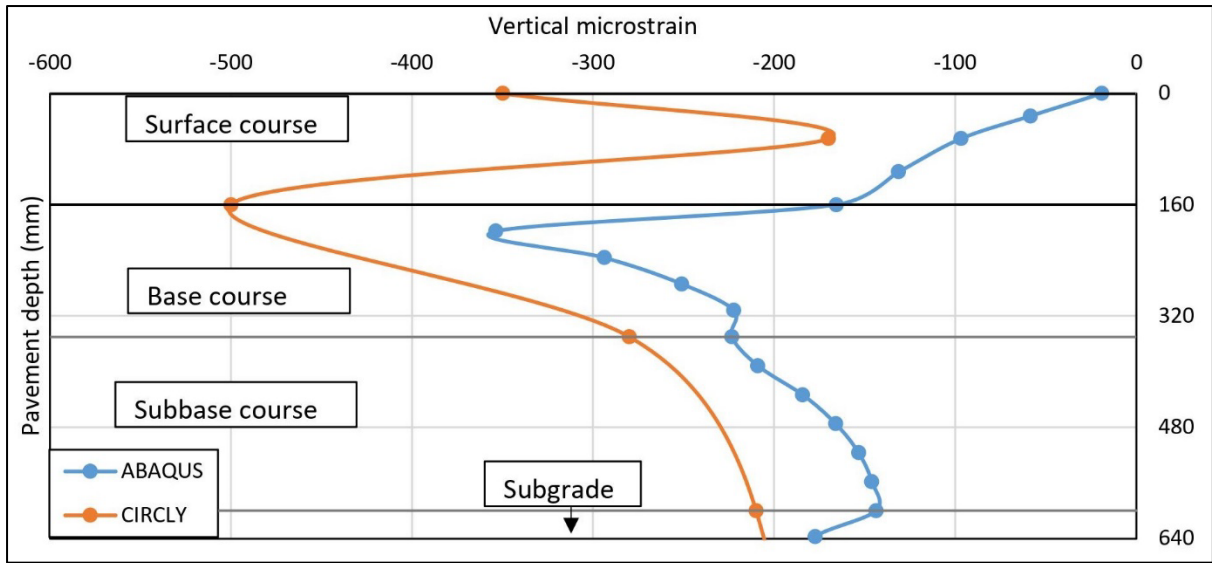
Figure 48 Vertical microstrain comparison between CIRCLY7.0 and ABAQUS.
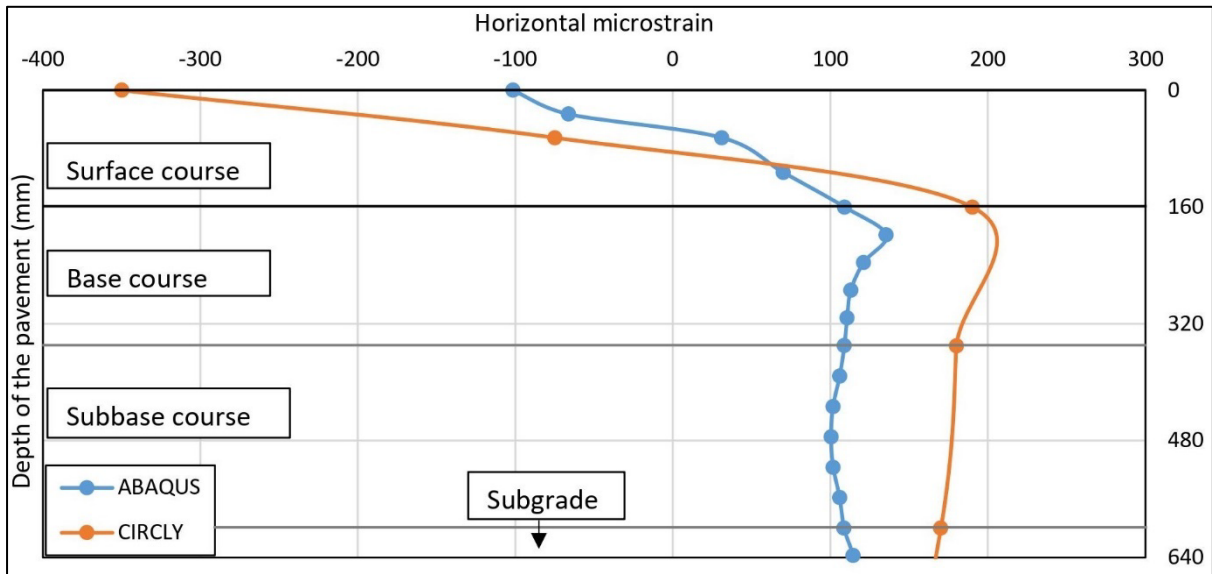
Figure 49 Horizontal microstrain comparison between CIRCLY7.0 and ABAQUS.